(2)

DOT/FAA/CT-88/33

FAA Technical Center
Atlantic City International Airport
N.J. 08405

Boeing 727-100 Test Project (High Energy Radiated Field Tests)

T. Crowther, et al.

Scientech, Incorporated
Idaho Falls, Idaho

July 1989

Final Report

U.S. Department of Transportation
Federal Aviation Administration

NOTICE

This document is disseminated under the sponsorship of the U. S. Department of Transportation in the interest of information exchange. The United States Government assumes no liability for the contents or use thereof.

The United States Government does not endorse products or manufacturers. Trade or manufacturers' names appear herein solely because they are considered essential to the objective of this report.

Technical Report Documentation Page

1. Report No.	2. Government Accession No.	3. Recipient's Catalog No.
DOT/FAA/CT-88/33		

4. Title and Subtitle	5. Report Date
BOEING 727-100 TEST PROJECT (High Energy Radiated Field Test)	July 1989
	6. Performing Organization Code
	8. Performing Organization Report No.
7. Author(s) T. Crowther, L.J. Ybarrondo, N. Skousen and M. Hintze	
9. Performing Organization Name and Address SCIENTECH Inc. 1680 Foote Dr. Idaho Falls, ID 83403-1406	10. Work Unit No. (TRAIS)
	11. Contract or Grant No. DTFA03-88-A-00027
12. Sponsoring Agency Name and Address U.S. Department of Transportation Federal Aviation Administration Technical Center Atlantic City International Airport, NJ 08405	13. Type of Report and Period Covered Final December 1985 - January 1986
	14. Sponsoring Agency Code ACD-230

15. Supplementary Notes

Program Manager: Michael Glynn
FAA Technical Center

16. Abstract

This document is the final report of a radio frequency (RF) coupling test on a BOEING 727-100 commercial aircraft. The objective of the test was to measure the coupling, or penetration, of RF signals in a BOEING 727-100 in the frequency range of 1.0 MHz to 6.0 GHz. The RF field levels generated inside the airplane during flight are probably not a health hazard with respect to passengers and crew because exposure time to high intensity RF fields is of short duration. However, this project has demonstrated that RF energy can couple into aircraft compartments and onto electrical wiring. The extent to which existing RF sources can impose unwanted electrical signals or voltages on critical aircraft components during a flyby are shown in the report.

17. Key Words	18. Distribution Statement
Electro-Magnetic Radiation Transfer Factor Path-Loss	Document is available to the public through the National Technical Information Service, Springfield, Virginia 22161

19. Security Classif. (of this report)	20. Security Classif. (of this page)	21. No. of Pages	22. Price
Unclassified	Unclassified	147	

Form DOT F 1700.7 (8-72) Reproduction of completed page authorized

PREFACE

This document is the final report of a radio frequency (RF) coupling test on a government owned BOEING 727-100 commercial aircraft. The objective of the test was to measure the coupling, or penetration, of RF signals in a BOEING 727-100 for the frequency range of 1.0 MHz to 6.0 GHz. The RF field levels generated inside the airplane during flight are probably not a health hazard with respect to passengers and crew because exposure time to high intensity RF fields is of short duration. However, this project has demonstrated that RF energy can couple into aircraft compartments and onto electrical wiring. The extent to which existing RF sources can impose unwanted electrical signals or voltages on critical aircraft components, during a flyby, are shown in the report.

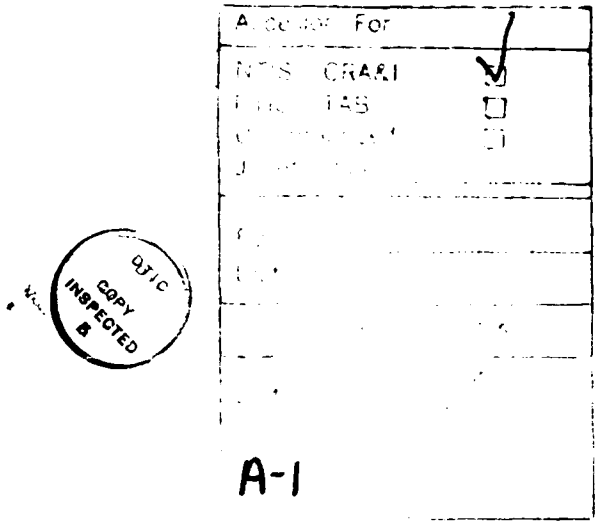

TABLE OF CONTENTS

TABLE OF CONTENTS

LIST OF FIGURES

LIST OF FIGURES

LIST OF FIGURES

LIST OF TABLES

ACRONYMS

AF	Antenna Factor
ANSI	American National Standards Institute
APU	Auxiliary Power Unit
BX	Box
DAS	Data Acquisition System
dB	Decibels
DC	Direct Current
EMC	Electromagnetic Compatibility
EMI	Electromagnetic Interference
EMP	Electromagnetic Pulse
ENG	Engine
EXC	Exciter
FAA	Federal Aviation Administration
GHz	Gigahertz (one billion cycles per second)
HF	High Frequency
Hz	Hertz
IBM	International Business Machines
IEEE	Institute of Electrical and Electronic Engineers
IGN	Ignition
IND	Indicator
LH	Left Hand
MHz	Megahertz (one million cycles per second)
NRS	National Resource Specialist
RF	Radio Frequency
RFI	Radio Frequency Interference
RH	Right Hand
SW	Switch
TF	Transfer Factor
UHF	Ultra High Frequency
VHF	Very High Frequency

EXECUTIVE SUMMARY

This document is the final report of a radio frequency (RF) coupling test on a BOEING 727-100 commercial aircraft. The objective of the test was to measure the coupling, or penetration, of RF signals in a BOEING 727-100 in the frequency range of 1.0 MHz to 6.0 GHz. The project was conducted in six steps:

1. A literature search of related work was conducted. Sources used were the aircraft manufacturers, U. S. Government, and the private sector.

2. A visual inspection was made of various types of aircraft built since the 1950's. The objective was to note if upgrades, made to the aircraft since they were manufactured, included equipment inherently soft with respect to RF, such as microprocessors or other subsystems.

3. Subsystems in commercial aircraft were examined to determine RF interference susceptibility.

4. Measurements were made within various compartments of the BOEING Model 727-100 to determine internal field strength as a function of external RF fields.

5. Induced voltages, on internal airplane wiring, were measured while the 727-100 was subjected to external RF energy.

6. The potential hazard from Radio Frequency (RF) penetration, to the critical subsystems of the aircraft and to the health of the people on-board, was analyzed.

The following summarizes the main conclusions of this project:

1. RF energy was typically attenuated by 25dB (reduced by a factor of 300) between the outside and the inside of the aircraft (path-loss);

2. Externally induced voltage, on internal aircraft wiring, was measured and analyzed. A transfer factor (TF) relationship for external fields to internal wire voltage was derived. The following is an equation for induced voltage as a function of external field strength (see appendix F for a detailed derivation of the equation):

$$V_w \text{ (wire voltage)} = \frac{\text{V/M (field strength)}}{10^{TF/20}}$$

An example is shown in the following figure that the RF fields which have been measured by the FAA around various airports can induce voltages of considerable magnitude on aircraft internal wiring.

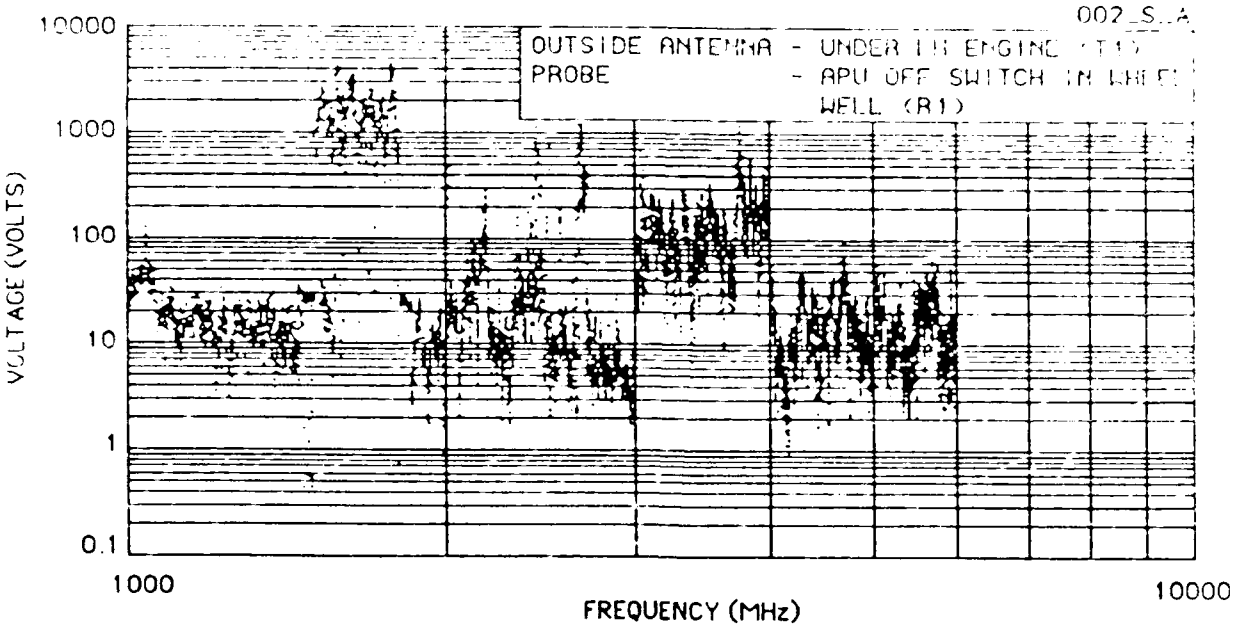

AN EXAMPLE OF INDUCED VOLTAGE ON INTERNAL WIRING DUE TO EXTERNAL RF FIELDS

Combining the transfer factor "values" presented in this report (see section 7) with the FAA "Predicted Maximum Field Strength Levels" (see appendix G) may induce significant and potentially disrupting, or damaging voltages on aircraft internal wiring and equipment.

The RF field levels generated inside the airplane during flight are probably not a health hazard with respect to passengers and crew because exposure time to high intensity RF fields is of short duration.

In conclusion, this project has pointed out that RF energy can couple into aircraft compartments and onto electrical wiring. The extent to which existing RF sources can impose unwanted electrical signals or voltages on critical aircraft components during a flyby are shown in the report. It is significant to note that some of the induced voltage plots in this report display large EMF potentials on internal aircraft wiring. Modern electrical and electronic systems may not withstand these potentials without disruption or damage.

1 INTRODUCTION

This report presents the results of a BOEING 727-100 RF TEST PROJECT. The objective of this test was to measure RF penetration of an aircraft.

This project included literature searches, visual inspections and subsystem analysis of BOEING 727s and several other aircraft. Field measurements and data analysis of RF energy penetration and affects on the subject BOEING 727-100 were the main objectives of this project.

The report is divided into nine sections and seven appendices. The scope of the BOEING 727-100 RF TEST PROJECT is outlined in Section 2. The approach to performing this work is outlined in Section 3. Open literature were reviewed for background material on subjects closely related to this project as noted in Section 4. Conclusions were verified both through visual inspection (Section 5) of several aircraft types and models and thorough discussions with experts from the Federal Aviation Administration (FAA). Section 6 contains a description of the field tests conducted to determine RF energy penetration. These tests were conducted at low level RF energy to prevent damage to the FAA owned and operated BOEING 727-100 test aircraft. Test methodologies and RF data analysis techniques are discussed in Section 7. The mechanisms whereby RF energy enters an aircraft are assumed to be linear over the levels in question and therefore can be extrapolated to high RF energy levels. Section 8 summarizes the results of the project. Conclusions are presented in section 9. Appendix A lists a matrix of possible tests, which was prepared and used for guidance in the selection of the final tests. Appendix B contains a detailed list of test equipment and computer software used in the data analysis. Appendix C contains a set of selected and labeled photographs of the test equipment or setups along with various views of the aircraft and components. Appendix E contains a detailed presentation of the Transfer factors derived from the test data. Appendix E presents a complete set of available test data.

A derivation of induced voltage on internal wiring as a function of field strength incident upon the external surface of the aircraft is presented in appendix F. Appendix G presents predicted maximum peak field strength levels at several international airport environments.

2 SCOPE OF WORK

The work scope was to study the affects of RF energy penetration on certain BOEING 727s and other similar aircraft, and to conduct a field test of RF energy penetration on the subject FAA BOEING 727-100.

2.1 PROGRAM OBJECTIVE

The objective of the BOEING 727-100 RF TEST PROJECT was to determine the susceptibility of a BOEING 727-100 and similar aircraft to Radio Frequency Interference (RFI).

2.2 WORK EFFORT

The five steps of the project work effort were:

1. A literature search was made of RFI affects on aircraft, with respect to aircraft manufacturers, the U. S. Government, and others in the private sector.

2. A visual inspection was conducted of various aircraft built since the 1950's to determine if changes have been made, since manufacture, which might include susceptible systems such as add-on microprocessor subsystems.

3. A study was made of the subsystems in commercial aircraft to determine which are most susceptible to RFI.

4. Measurements were made on a BOEING Model 727-100 to determine the internal field strength and induced RF signals on typical airplane wiring produced by external RF fields.

5. An analysis was performed of some of the hazards RF penetration may cause to the critical subsystems of the aircraft and to the health of the people on-board the aircraft

3 APPROACH TO THE PROBLEM

3.1 LITERATURE SEARCH AND REVIEW

Perform a literature search of previous work done in this field by aircraft manufacturers, by the U. S. Government, and by the private sector.

3.2 VISUAL INSPECTION

Make a visual inspection of various types of aircraft built since the 1950's to determine if changes have been made to the aircraft since they were manufactured which might include microprocessor based subsystems.

3.3 SUBSYSTEM SUSCEPTIBILITY STUDY

Review aircraft operation, maintenance, design manuals and drawings to determine which subsystems in commercial aircraft are most likely to be susceptible to RFI.

3.4 FIELD TESTS

Perform field measurements on a BOEING 727-100 to determine outside RF penetration and the levels of induced RF signals on some of the critical wiring inside the aircraft. These measurements can be done at low RF energy levels and extrapolated linearly to high energy RF levels.

Analyze the data from the field measurements to determine the hazards RF penetration may cause to critical subsystems and to the health of the people on-board the aircraft. Then calculate the RF power levels that might penetrate the aircraft with enough energy to disrupt or even damage aircraft subsystems. And finally determine if there are any high energy RF sources (i.e., radar installations) that might disrupt or damage subsystems if the aircraft flies near the RF source.

4 LITERATURE SEARCH AND REVIEW

4.1 TECHNICAL ARTICLE SEARCH AND REVIEW

Technical articles were searched and reviewed for information regarding Electromagnetic Pulse (EMP), Electromagnetic Compatibility (EMC), lightning, and RF interference to aircraft, electronic equipment, and electronic components.

4.1.1 Open Literature Review

A library of several hundred technical articles from the open literature on the subject of Electromagnetic Compatibility (EMC) is maintained at SCIENTECH, Inc. and Eyring Research Institute, a subcontractor on this project. This library was reviewed in its entirety for articles that provided information helpful to BOEING 727-100 RF TEST PROJECT.

This literature search revealed articles on electronic component failure thresholds due to electromagnetic energy, articles on effects on aircraft due to lightning, commercial test procedures for RFI and EMC measurements, and even a review of the problems with US commercial aircraft operations.

4.2 AIRCRAFT OPERATIONS MANUALS, MAINTENANCE MANUALS, AND DESIGN DRAWINGS REVIEW

Operations manuals, maintenance manuals and design drawings of various aircraft types were reviewed to determine the classes of aircraft and the subsystems that would be critical to causing an aircraft to become inoperable.

4.2.1 Assessment of Aircraft Susceptibility to High Energy RF Fields

Commercial aircraft were categorized into three design types and their susceptibility to high energy RF fields was assessed. The three classes are:

Class 1: Commercial aircraft designed in the 1950's and built in the 1960's (such as the C141 and 707).

Class 2: Commercial aircraft designed in the 1960's and built in the 1970's (such as the 727, 737, 747, DC-8, DC-10, L1011).

Class 3: Commercial aircraft designed in the 1980's which are just now being built (such as the 757, 767, and the European A-320 Airbus).

4.2.1.1 Class 1 Aircraft Susceptibility to RFI

RFI problems exist in this class. Design notes on drawings indicate that changes were made to systems to overcome RFI. A C141 was inspected by the BOEING 727-100 RF TEST PROJECT team at Robbins Air Force Base in

Georgia and maintenance people there reported RFI problems. A good example is that the exciter cables had to be shielded to prevent RFI from interfering with starting the aircraft engines and to prevent other equipment from being interfered with when the engines were being started.

Many types of navigation equipment have been added to this class of equipment. The added navigation equipment has evolved from vacuum tube to the latest microprocessor controlled technology. This class of equipment is a mixture of the old, later, and latest types of electronic equipment. It has been reported that the latest navigational equipment has interfered with and been interfered with by many of the other aircraft subsystems, which has caused many modifications to be made to the aircraft to reduce the RFI problem.

This class of aircraft therefore is known to have RFI problems and may be susceptible to high energy RF fields.

4.2.1.2 Class 2 Aircraft Susceptibility to RFI

Efforts were made in the design of Class 2 aircraft to deliberately reduce the susceptibility to RFI. Specific mention of some of these efforts are noted on the design drawings. However, the latest microprocessor navigational equipment has also been added to Class 2 aircraft; and equipment modifications similar to those made in Class 1 aircraft had to be made to reduce new RFI problems. For the most part, Class 2 aircraft are designed to use relay logic controls which should be relatively immune to RFI. However, there are some semiconductors in critical areas of the aircraft subsystems. Plastics were used in Class 2 aircraft design as contact separators in relays, as hermetic seals on switches, and as insulation on wires. Plastic covered wires break down almost instantaneously in the presence of high energy RF fields in the laboratory, causing sparks and short circuits. Consequently, Class 2 aircraft may be susceptible to high energy RF fields.

4.2.1.3 Class 3 Aircraft Susceptibility to RFI

Class 3 aircraft have had strict design requirements to prevent RFI because of the extensive use of microprocessor control systems that do not have cable or hydraulic manual backup systems. The microprocessor control systems are known to be susceptible to RFI; however, the design limits, even with design safety factors, seldom are tested beyond one to ten volts per meter field strength. Malfunctions of systems when flying over radar facilities have been reported by pilots.

Class 3 aircraft are also using more and more lightweight composite (graphite and plastic) materials in place of aluminum. The composite materials provide less shielding against RFI than aluminum, thus making the aircraft more susceptible to RFI penetration. Therefore, Class 3 aircraft may be susceptible to high energy RF fields.

4.2.2 Conclusions of Aircraft Susceptibility to High Energy Fields

It must be stated at the outset that environmentally sealed aircraft made of aluminum with very small window openings are reasonably well protected against RFI, let alone being susceptible to the point of rendering the aircraft inoperable. In addition, the older aircraft (Class 1) are made with mostly mechanical systems (cables and pulleys or hydraulics and valves) to control every subsystem on the aircraft that is critical to maintaining flight. There are very few electronic subsystems; most of them are transducer systems for measuring rather than controlling fuel levels, position of valves, etc. However, these systems are not well protected against RFI.

As discussed, navigational equipment was added to this class of aircraft. The navigational systems are more electronic in nature and therefore are probably more susceptible to high levels of RF energy. However, the navigation systems are not critical for continued safe flight and landing even though the navigational systems are probably more easily disrupted by RF energy.

Class 2 aircraft designs are in some ways less and in other ways more susceptible to RFI than the older Class 1 aircraft designs.

The latest aircraft designs (Class 3) may be susceptible to RFI than the older Class 1 and 2 aircraft designs.

Even though an aircraft is to some degree susceptible to RF energy it is well protected by being environmentally sealed for the most part by a metal covering. The remaining question is what are the specific subsystems that might be affected by RFI.

4.2.3 Review and Classification of Critical Systems and Wiring Susceptible to RFI

For Class 3 airplanes, a preliminary hazard assessment of these systems is usually conducted by the airframe manufacturer and presented to the FAA for approval. This process identifies the critical systems installed in a particular airplane model. These systems are then analyzed and tested to determine their failure modes and susceptibility to RFI.

It is generally believed by experts in the electromagnetic compatibility field that the primary means by which RFI disrupts airborne electronic/electrical equipment operation is through the coupling path provided by the electrical wiring. The coupling of radiated energy through the equipment enclosure, which is generally made of aluminum (although with apertures), is believed to be relatively minor because the electromagnetic fields internal to the airplane are already attenuated by the airplane structure.

Electrical wiring is located throughout the airplane and depending upon its location, will be exposed to different levels of RFI for transmitters external to the airplane. Wiring may be installed in the following locations:

- Completely enclosed in a compartment without apertures such as the avionics bay;

- Enclosed within the pressurized fuselage but with apertures provided by cockpit and passenger windows and door seals;

- Outside the pressurized fuselage but in areas with limited apertures such as fuel quantity sensors in the fuel tanks;

- Outside the pressurized fuselage with some protection from external sources such as engine mounted wiring enclosed by the engine cowlings;

- In locations with little or no structural shielding such as in wheel wells or on landing gear struts.

5 VISUAL INSPECTION

The BOEING 727-100 RF TEST PROJECT team interviewed FAA personnel, physically inspected several aircraft in detail, and briefly inspected many other aircraft to verify consistency among and between aircraft models and manufacturers. The results of these interviews and inspections are summarized in the following sections.

5.1 C141 AT ROBBINS AIR FORCE BASE (CLASS 1 DESIGN AIRCRAFT)

The on-site inspection team found several interesting things about a C141. It was noted that the air intake system on the Auxiliary Power Unit (APU) had a motor operated cover with an electric position sensor. If this cover was closed the APU would automatically shut down. The position sensor switch was visible from the outside of the aircraft and possibly susceptible to RF energy causing the switch to fail and to shut down the APU.

5.2 BOEING-727-100 OWNED AND OPERATED BY THE FAA

Several days were spent inspecting in detail a B-727-100 at an FAA facility.

5.3 OPERATING AIRCRAFT INSPECTION

With the aid of a maintenance supervisor three model B-727-100 aircraft and five model B-737 aircraft were briefly inspected while in operation at a major airport. It was verified that the susceptible subsystems listed in Section 4.2.3. had not appreciably changed for each of these aircraft.

There were variations in components between the aircraft depending on the model and the year they were built, but the components performed the same functions. The reviewed aircraft varied in manufacturing date from the 1960's to the 1980's.

5.4 FAA EXPERT INTERVIEW

The FAA National Resource Specialist (NRS) in aircraft electrical/electronic systems was interviewed primarily to provide information on the Class 3 type of aircraft design. In these interviews it was confirmed that Class 3 aircraft design is probably more susceptible to RF energy and is the subject of present Electromagnetic Interference/Radio Frequency Interference/Electromagnetic Compatibility work by the FAA.

The Class 3 designs were so called "fly-by-wire" designs which means that engine controls, flight controls, etc. are controlled by signals through wires and do not have mechanical cable and pulley back-up systems. Therefore, there are more subsystems critical to causing the aircraft to become inoperable if failures occur in addition to each subsystem being more susceptible to RFI.

6 FIELD TESTS

The logarithmic ratio of RF power (in dB) in the air inside of the aircraft to the RF power in the air outside of the aircraft (in dB) will be called the RF path-loss of the aircraft. It is also of interest to determine the level of RF energy that is coupled onto the wiring of the aircraft. The logarithm of the ratio of RF power on a wire of the aircraft to the RF power in the air outside of the aircraft will be a type of RF transfer factor.

To measure these transfer relationships without causing damage to an operating aircraft, the measurements have to be made at low RF energy levels. Assuming that the transfer relations are linear with respect to energy level, the high energy transfer relationships should remain the same from low energy levels to high energy levels.

The transfer factors were measured over the frequency range of 1 MHz to 2.5 GHz on a predetermined number of wires and in a predetermined set of locations inside an aircraft. The test points are detailed in a test matrix (see section 6.2 and appendix A). The measurements were taken using a data acquisition system designed for this test.

6.1 PHYSICAL DESCRIPTION OF FIELD TESTS

A commercial B-727-100 aircraft owned and operated by the FAA was subjected to low level RF fields and the RF transfer factors were determined. The tests were conducted using a data acquisition system. The locations where measurements were taken is shown in graphical form in relation to the aircraft in figure 6.1.1.

The field tests data acquisition system is composed of an RF transmitter transmitting energy to a set of transmit antennas over the frequency range of 1 MHz to 2.5 GHz. A set of receiver antennas measure the RF power in the air both outside and inside of the aircraft. A spectrum analyzer records the information from the receive antennas and from probes connected to wires in the aircraft. The transmit and receive operations are controlled and recorded by a computer control system.

The impedances of the circuits connected to the wires of the aircraft were measured by a network analyzer and also recorded by the computer control system.

The points inside and outside of the aircraft and the wires where measurements were made were determined in advance as a test matrix (see tables 6.2.1 and 6.2.2 for reduced test matrix and appendix A for full test matrix).

The field tests were performed at an FAA facility. The field tests were made over a period of eleven days in December of 1986.

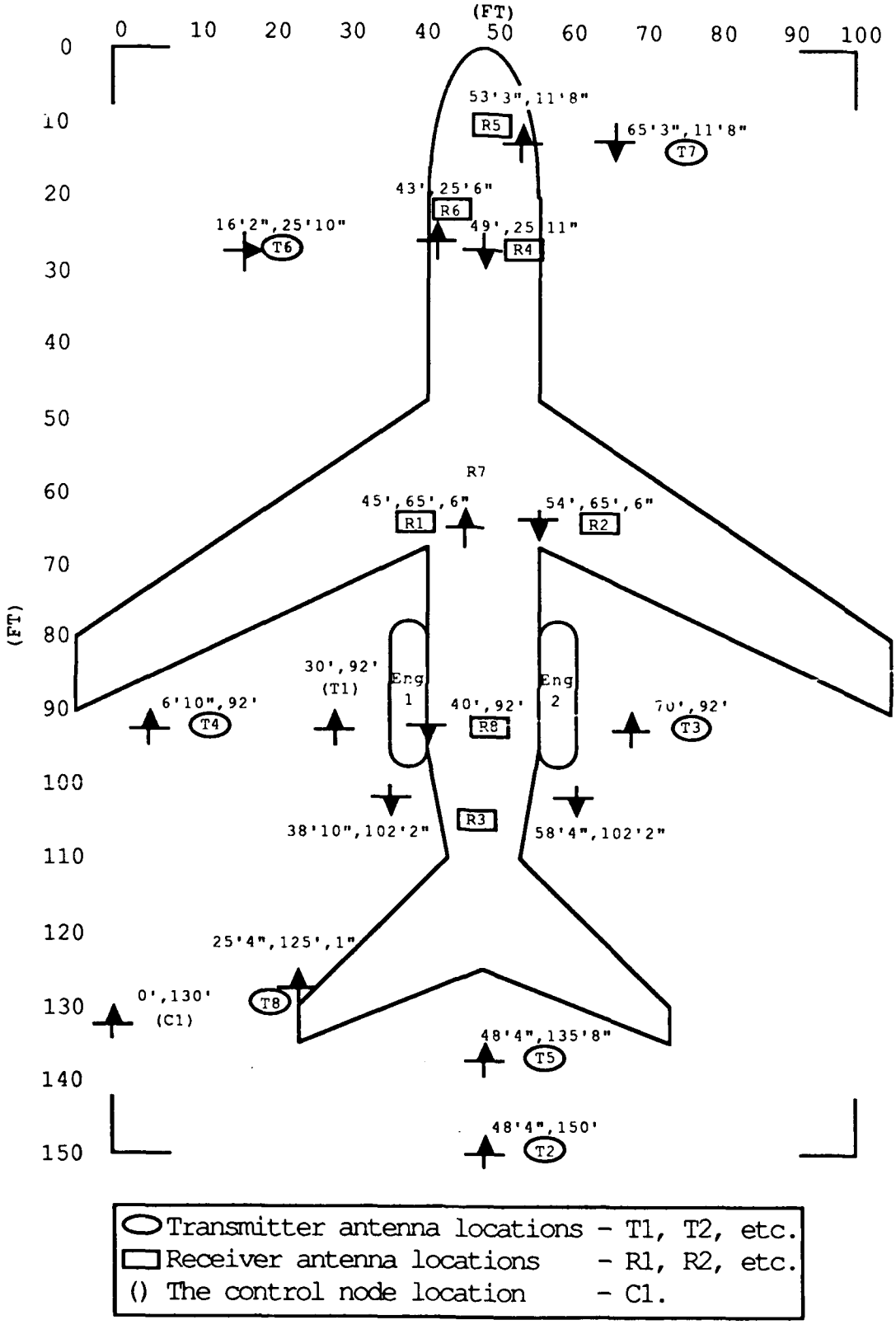

Figure 6.1.1. Measurement Locations in Graphical Form.

6.1.1 Description of Typical Field Test Data Set

The data set was obtained in the following steps.

1. Transmit antennas were located ten meters from the aircraft (for example in position T1 behind the left wing of the aircraft (see figure 6.1.1).

2. The receive antennas appropriate for each frequency range were placed in the cockpit in position R6.

3. The power was gradually raised for each frequency band until the maximum received field strength measured on the spectrum analyzer approached 1 volt/meter (so as not to exceed the limits set by the FAA). The receive antennas were rotated and moved to obtain some relative indication of maximum field strength. This maximum was found to be pointed at the transmit antennas and near the center of the aircraft.

4. A set of data was taken and recorded.

5. A calibration measurement was taken at the same power levels as the data set in step 4. This was done by placing the set of transmit antennas and the set of receive antennas opposite each other at a distance of ten meters. This calibration measurement was performed on a cement pad away from all buildings and encumbrances. This provided a reference field strength taking into account the path-loss due to the separation of the antennas.

6. In some cases, data were taken with the receive antennas positioned one at a time just outside of the aircraft, with the transmit location at the same point as when the receive antennas were on the inside of the aircraft as in step 4 above. This field strength measurement would include perturbations of the signal due to reflections from the aircraft. These reflections were somewhat changing and not the most meaningful data, but were taken for completeness.

7. The recorded data sets, taken outside and inside, were measured in dBM and subtracted to give the path-loss data. No antenna factors were required to be used because the receive and transmit antennas were identical.

8. The path-loss was then plotted by the computer providing a separate data plot for each band of frequencies.

6.2 CONDUCT OF FIELD TEST

The data acquisition system was designed, assembled from off the shelf equipment, and programmed. The equipment was shipped to the test site and the measurements were made. The test matrix and the data acquisition system are described in the following Sections. Photographs of the test equipment, various views of the aircraft, and photographs of some of the aircraft critical components are shown in appendix C as photographs 1 through 32. Brief descriptions of these photographs are contained in appendix C.

6.2.1 Test Matrix Summary

The test matrix is composed of a set of frequency bands which are lettered A-S and are the columns of the test matrix. The locations and descriptions of each test are the lines of the test matrix and are numbered 1-152. The test matrix is too large to print in matrix form on a reasonable size paper so it is written with the frequency bands as one list and the measurement locations as a second list. An original matrix which was very inclusive was prepared and is given in appendix A. This matrix was reduced to the critical measurements that were necessary without being excessively redundant and which could be accomplished in the ten days of testing allotted. The reduced matrix is presented in tables 6.2.1 and 6.2.2. An explanation of the vertical and horizontal columnar numbering system is given in appendix A.

Table 6.2.1
Reduced Test Matrix Horizontal (Column) Dimension

Frequency Band	Frequency Range	Antenna Description	Antenna Number
-	1 - 35 MHz	HF Monopole	1
A	1 - 35 MHz	HF Loop	2
B	20 - 300 MHz	Biconical	3
C	200 - 600 MHz	Log Periodic No. 1	4
D	600 MHz - 1.0 GHz	Log Periodic No. 1	4
E	1 - 1.5 GHz	Log Periodic No. 2	5
G	1.5 - 2.0 GHz	Log Periodic No. 2	5
H	2.0 - 2.5 GHz	Log Periodic No. 2	5

6.2.2 Description of the Data Acquisition System (DAS)

The DAS system is shown in figure 6.2.1 and is composed of six subsystems.

6.2.2.1 Computer Controller and Data Storage Unit

The computer controller (shown in figure 6.2.1 as node 1 and in photograph 3 in appendix C) furnishes the signals to the IEEE-488 interface controllers which will start, synchronize, and stop the RF transmitters, spectrum analyzer, and network analyzer. The computer controller also captured all the data digitally and stored the data on floppy discs.

6.2.2.2 RF Transmitters and Antennas

The RF transmitters and antennas subsystem (shown in figure 6.2.1 as nodes 2 and 3, and in more detail in figure 6.2.2, and in photographs 4 and 5 in appendix C) are composed of two signal generators and six separate power amplifiers each for a specific frequency range. The signal generators are swept through their specific frequency range sequentially, thereby covering the entire

Table 6.2.2
Reduced Test Matrix Vertical (line) Dimension

TEST NO.	CTRL NODE	TRANSMIT NODE	TRANS. ANTENNA					REC. ANT. NODE	SPECTRUM ANALYZER		NETWORK ANALYZER
			1	2	3	4	5		VOLTAGE PROBE	CURRENT PROBE	
1	1	1	1A	1A	1	1	1	1			
2									APU STOP SW		
8											APU STOP SW
10											APU START SW2
11											APU FIRE SW
12											APU SQUIB
13									SQUAT SW1		
15											SQUAT SW1
16											SQUAT SW2
17									HEAT SENSOR1		
20											HEAT SENSOR1
21											HEAT SENSOR2
22									APU FUEL SHUTOFF VALVE		
23											APU FUEL SHUTOFF VALVE
24									NO.1 FUEL SHUTOFF VALVE		
25									NO.2 FUEL SHUTOFF VALVE		
27											NO.1 FUEL SHUTOFF VALVE

Table 6.2.2
Reduced Test Matrix Vertical (line) Dimension (continued)

TEST NO.	CTRL NODE	TRANSMIT NODE	TRANS. ANTENNA 1	2	3	4	5	REC. ANT. NODE	SPECTRUM ANALYZER VOLTAGE PROBE	CURRENT PROBE	NETWORK ANALYZER
92	2	8	8	8	8	8	8	8			
93									ENG EXC BX IN		
									DC BUS		ENG IN
93A									ENG IGN BX IN		
									400 CYC. BUS		
94									ENG EXC BX OUT		ENG OUT
95									ENG HEAT SENS.		ENG HEAT SENS.
95A									ENG AIR VALVE		ENG AIR VALVE
125	2	7	7	7	7	7	7	5			
126									FIRE LIGHT		
127									PCD IND.		
128									FUEL IND.		
129									PNEUMATIC IND.		
130									TEMP IND.		
131									HYDRAULIC IND.		
132									400HZ ELEC.BUS		
133									DC ELEC. BUS		
134									OIL PRESS IND.		
135									VOLT METER		
136									CURRENT METER		
137									APU ON		
138									APU OFF		
139									APU FIRE SW		
140									SQ. SW		
141	ANT MID								HEAT SENSOR		
142	(125)	1		1	1	1	1	7			
143	(125)	1		1	1	1	1	5			
144	(138)			1	1	1	1	5	APU OFF		

Table 6.2.2
Reduced Test Matrix Vertical (line) Dimension (continued)

TEST NO.	CTRL NODE	TRANSMIT NODE	TRANS. ANTENNA					REC. ANT. NODE	SPECTRUM ANALYZER		NETWORK ANALYZER
			1	2	3	4	5		VOLTAGE PROBE	CURRENT PROBE	
145	(128)	1		1	1	1	1	5	FUEL IND.		
146	(126)	DROPPED									
147	(132)			1	1	1	1	5	400HZ ELECT. BUS		
149	(a,c,h)			1	1	1	1	8			
150	(a,c,h)			1	1	1	1	4			
151				1	1	1	1	7			
152	1	1		1	1	1	1	1			

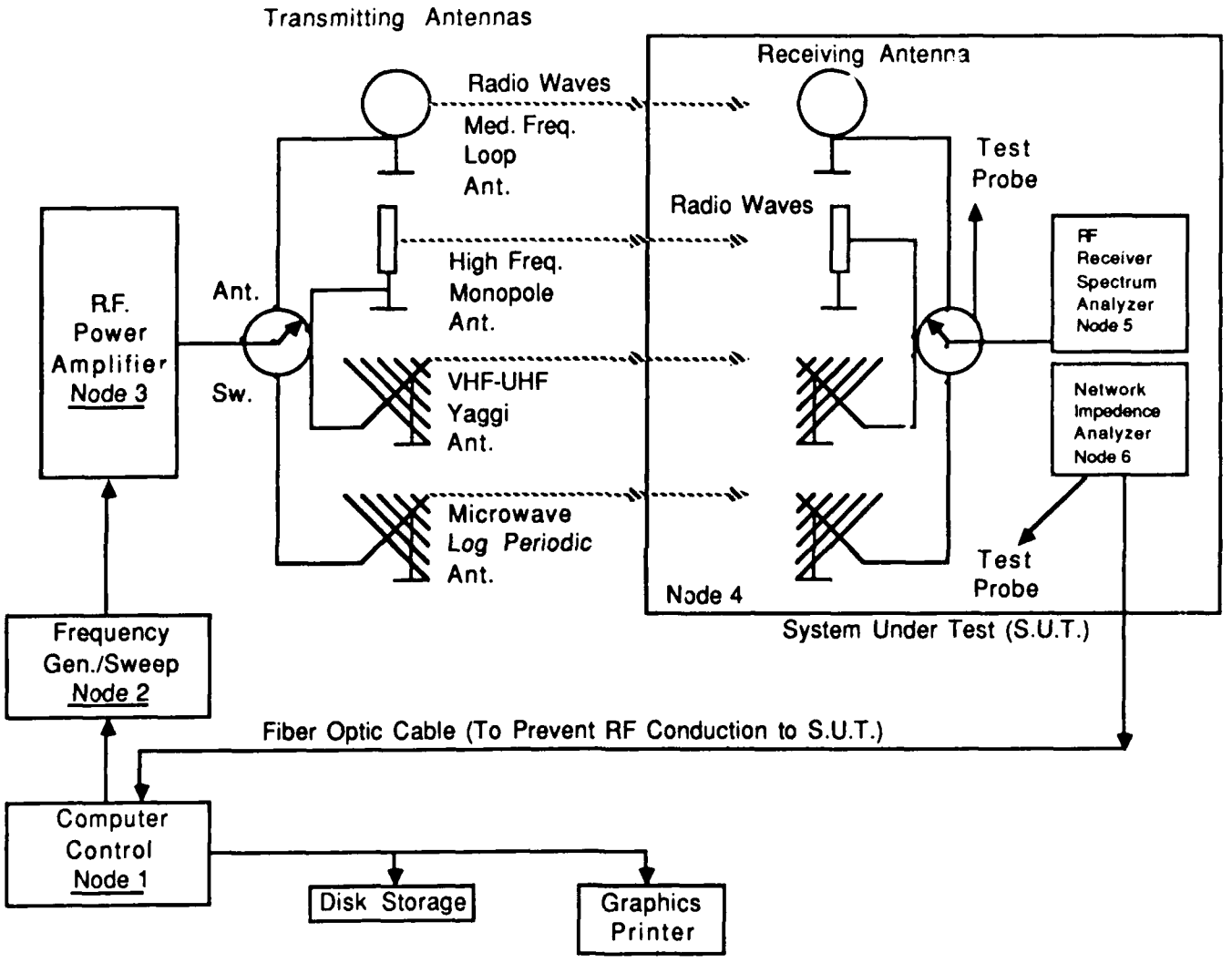

Figure 6.2.1 Field Test Data Acquisition System (DAS).

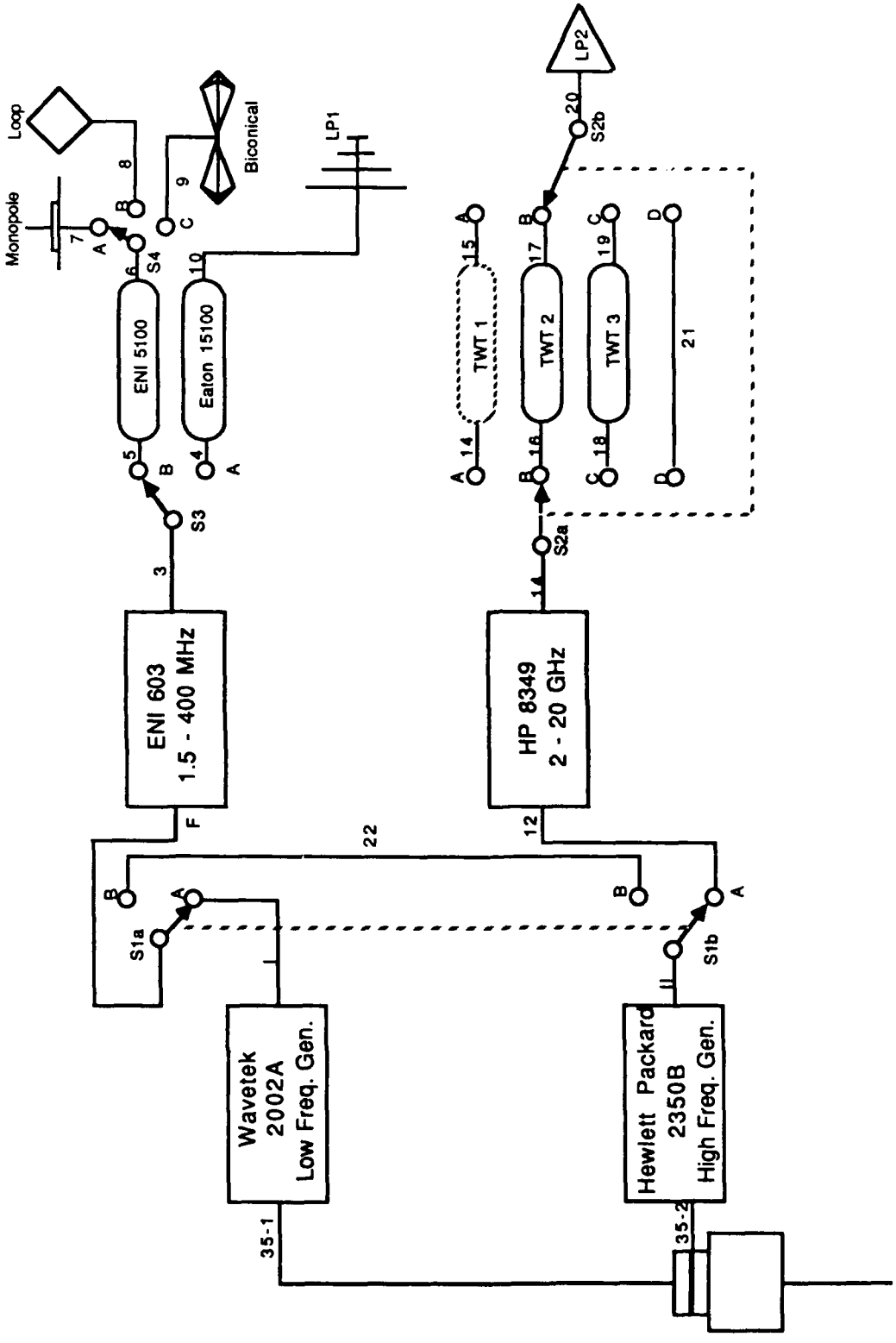

Figure 6.2.2 Field Test Transmit Node.

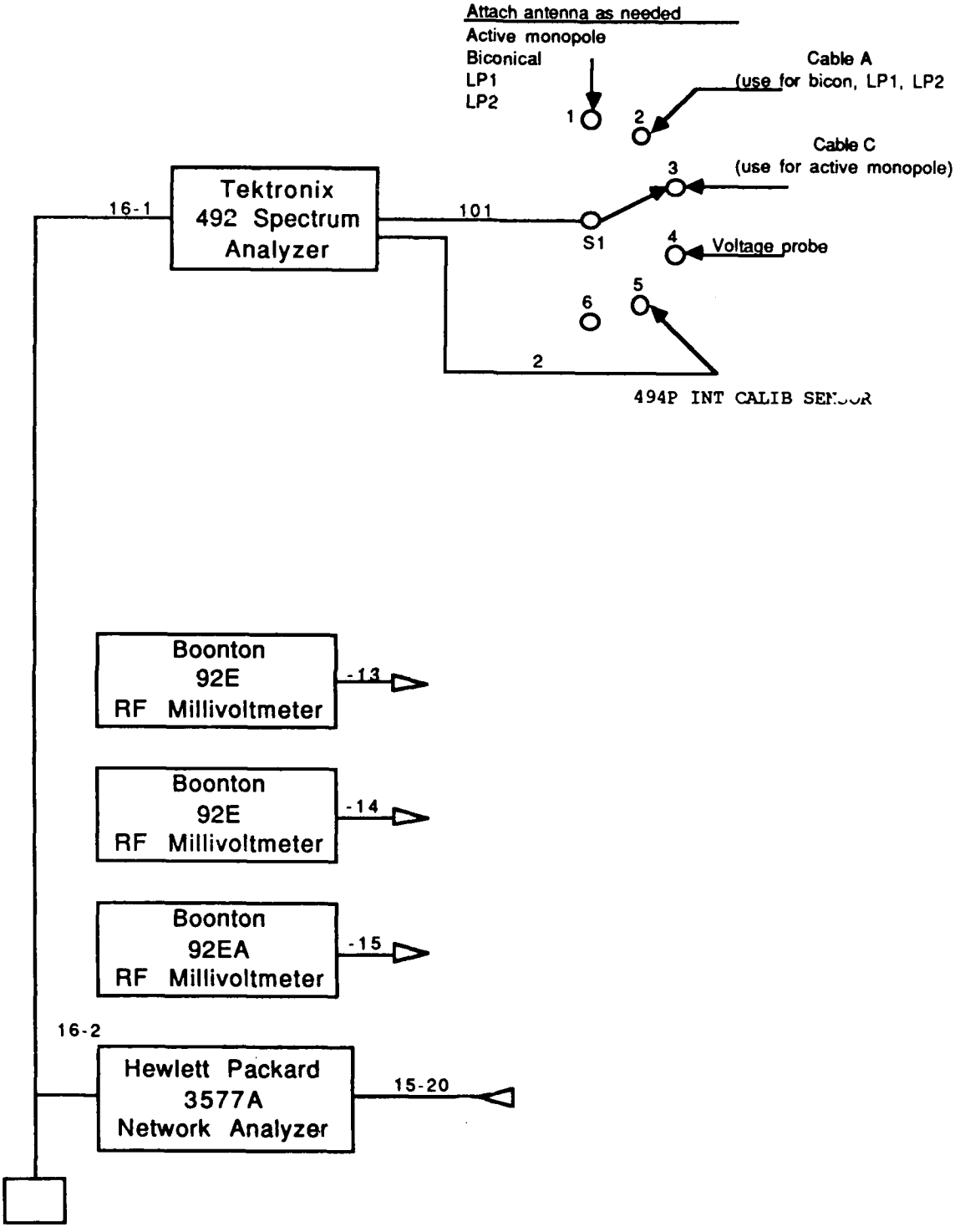

Figure 6.2.3 Field Test Receive Node

frequency spectrum required. As the power amplifiers are switched in and out by the computer controller (or by hand when prompted by the computer controller), their respective antennas are also switched.

6.2.2.3 Spectrum Analyzer

The spectrum analyzer is a self contained unit with RF receiver functions, computer controls, and data storage capabilities (shown in figure 6.2.1 as node 4 and in more detail in figure 6.2.3, and in photograph 6 in appendix C). The spectrum analyzer received the swept RF signal and digitized all data received both from the antennas and the direct line measurements. The data from the spectrum analyzer is transferred over an IEEE-488 bus via a fiber optic link to the computer controller for permanent storage.

6.2.2.4 Network Analyzer

The network analyzer (node 6 in figure 6.2.1, and in photograph 6 in appendix C) provides impedance information at selected test points for the frequencies being swept. This digital data is also transferred to the computer controller via an IEEE bus using a fiber optic link for permanent storage.

6.2.2.5 IEEE-488 Interface Controllers and Fiber Optic Interconnecting System

The IEEE-488 interface controllers allow the computer to control the signal generators, the spectrum analyzer, and the network analyzer. To insure that there are no RF signals taken inside the aircraft by the cables connecting the various instruments inside and outside the aircraft, fiber optic cables are used to penetrate the aircraft.

6.2.2.6 Software Control System

The software control system is, for the most part, written for the IBM AT to control and analyze data of the type gathered in this test program. All software programs are recorded and available for future uses.

6.2.3 Equipment and Software Used

A complete list of the equipment used in the receive, transmit, and control nodes and the software used to analyze the data is provided in appendix B.

7 RF ENERGY DATA ANALYSIS

The RF energy was measured and the data were used to calculate both the RF "path-losses" into the aircraft and the "transfer factor" relating to induced RF voltage onto aircraft wiring.

7.1 TRANSFER FACTOR AND PATH-LOSS THEORY AND MEASUREMENT

The data acquired from these tests are presented in the form of "path-loss" and "transfer factor" relationships. Path-loss is defined as the difference (attenuation), in dBM, between a reference measurement outside the aircraft and data measurements at certain locations inside the aircraft.

The transfer factor is a measure of induced RF energy on aircraft wiring related to RF field strength external to the aircraft. The transfer factor, as determined, was the actual induced RF energy measured on aircraft wiring related to measure RF field from a reference antenna external to the aircraft (see figure 7.1.1)

Path-loss and Transfer factor are tools which predict levels of RF within compartments and on wiring respectively when the aircraft is bathed in external RF fields of known strength.

7.1.1 Definition of the Path-Loss

The path-loss is measured in dB in order to cover the large dynamic range. The path-loss (P_L) is defined as:

$$P_L = P_t - P_r \qquad (1)$$

where,

P_r = power recorded by a 494P spectrum analyzer at free-air reference test point, in dBM and;

P_t = power recorded by a 494P spectrum analyzer inside an aircraft compartment.

The path-loss relationship is thus the difference of power (or field strength) external to the aircraft and the power received internal to the aircraft. The path-loss is then the attenuation, expressed in dB, of the external field.

7.1.2 Transfer Factor (TF) Derivation

A transfer factor (TF) of the same form as the antenna factor was derived to provide a relationship for interpretation of induced voltage on aircraft internal wiring as a function of external RF field (see appendix D for a detailed derivation of the individual elements of the transfer factor, TF). Figure 7.1.1 is a diagram of the test setup.

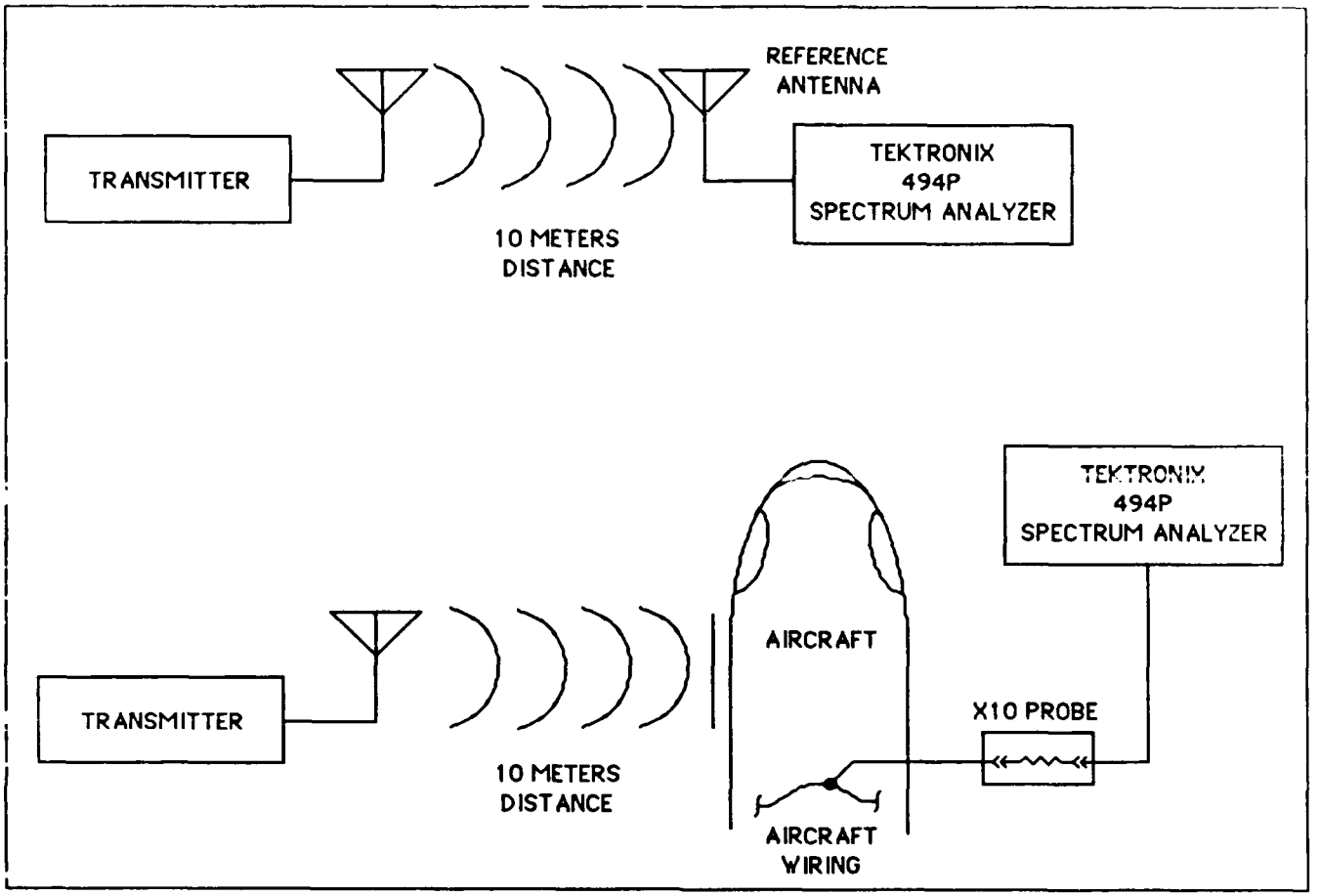

Figure 7.1.1 Test Setup - Measurement of Induced Voltage on Aircraft Internal Wiring

Assumptions inherent to the derivation are:

1. Field strength at the rcference receiving antenna equals field strength at aircraft surface;

2. Measurement inaccuracies, due to probe impedance, were not factored into the analysis.

From the antenna manufacturer data sheet (see appendix D), the equation for the antenna factor is:

$$dB\mu V + AF = dB\mu V/M \qquad (2)$$

where:

1. $dB\mu V$ is the voltage at the output of the reference receiving antenna, into a 50 ohm load, in dB referenced to 1.0 μV (V'_r in the following equation);

2. AF is the antenna factor in dB (see sample manufacturer's data sheet in appendix D);

3. dBμV/M is the field strength at the receiving antenna, in dB referenced to 1.0 μV/meter.

A similar relationship can be derived for externally induced voltage on internal aircraft wiring. The relationship is as follows:

$$dB\mu V_w + TF = dB\mu V/M \qquad (3)$$

where:

1. dBμVw is the voltage, induced on aircraft internal wiring, into a x10 probe (500 ohms), in dB referenced to 1.0 μV (V'_w in the following equation);

2. TF is the transfer factor, in dB;

3. dBμV/M is the field strength, in volts/meter, incident on the external surface of the aircraft, in dB referenced to 1.0 μV/M.

The field strength incident on the external surface of the aircraft is assumed to be equal to the field strength at the reference antenna. Therefore, equating the two expressions yields the transfer factor (TF):

$$dB\mu V_r + AF = dB\mu V_w + TF \qquad (4)$$

$$TF = dB\mu V_r - dB\mu V_w + AF \qquad (5)$$

Since a Tektronix 494P Spectrum Analyzer was used to measure the output of the reference antenna as well as the voltage induced on the internal aircraft wiring, the equation for the TF may be expressed as follows (when the units are converted to dBM):

$$TF = P'_r - P'_m + AF - 20 \qquad (6)$$

where:

1. TF is the transfer factor, in dB;

2. P'_r is the power reading, measured by the Tektronix 494P, in dB (referenced to 1 mw), at the terminals of the reference antenna (see figure 7.1.1 and D-1 respectively);

3. P'_m is the power reading, measured by the Tektronix 494P, in dB (referenced to 1 mw), connected through a x10 probe to internal wiring of the test aircraft (see figure 7.1.1 and D-1 respectively);

4. -20 is a conversion factor, in dB;

5. AF is the Antenna Factor, in dB, from the antenna manufacturer's AF versus Frequency chart (see appendix D).

7.2 TRANSFER FACTOR AND PATH-LOSS MEASUREMENT AND CALCULATION METHODOLOGY

Measurements were taken with the data acquisition system. The data was used to calculate the transfer factors and path-losses according to the theoretical equations just described. The measurement and calculational methods are described in the following sections.

7.2.1 Transfer Factor Measurement Methodology

7.2.1.1 Spectrum Analyzer Data

The measurement of the RF voltage (in dBM) on a test probe or on a receive antenna is collected and digitized by a spectrum analyzer. The computer control system collects, stores, and graphs this information as a function of frequency.

7.2.1.2 Network Analyzer Data

To avoid the necessity of measuring every point on a wire where the RF energy might cause some failure, the impedance of a wire was measured which provided the information necessary to describe the wire as a transmission line. Having the transmission line impedance vs. frequency for a wire, the voltage at one frequency at any point on a transmission line can be calculated knowing the voltage at the same frequency at any other point on the transmission line.

The impedance measurement as a function of frequency is obtained by using a network analyzer which is a self contained instrument which generates a small signal on a wire and calculates the resulting digital real and complex magnitudes of pulsed impedance vs. frequency over the frequency range of 1-200 MHz. Measurements of impedance above 200 MHz were deemed impractical in the test aircraft environment. The computer control system collects, stores, and graphs this information.

7.2.2 Transfer Factor and Path-Loss Calculation Methodology

The data from the spectrum analyzer was collected and recorded on floppy disk by the computer control mode. These data were plotted versus frequency and printed out. The plot frequency from 1 MHz to 2.5 GHz requires seven graphs.

7.3 DATA ANALYSIS

The data from the spectrum analyzer, network analyzer, and the calculated transfer factors and path-losses are analyzed as defined in the following sections.

7.3.1 Spectrum Analyzer Data

Figure 7.3.1 is a typical graph of spectrum analyzer data. The vertical axis is voltage measured on an antenna in dBM. The horizontal axis is frequency. This particular graph is a sweep of frequency from 20 MHz to 300 MHz using a biconical antenna. There are seven graphs for each frequency sweep of 1 MHz to 2,500 MHz. The date and time the data was recorded is shown also. Numerous graphs were made for various antenna locations and probes on wires taken at various locations (see tables 6.2.1 and 6.2.2). These raw data are not contained in this report but are archived for reference purposes in the SCIENTECH BOEING 727-100 RF TEST PROJECT files.

7.3.2 Network Analyzer Data

Figure 7.3.2 is a typical graph of network analyzer data and photograph 7 in appendix C shows a typical display. The vertical axis is divided into two parts. The lower half is the magnitude of the real part of the impedance on a wire measured in ohms. The upper half of the vertical scale is the magnitude of the imaginary part of impedance measured in ohms. The horizontal scale is frequency. This graph covers a sweep frequency of 0.1 to 50 MHz. It takes two graphs to cover from 0.1 to 200 MHz. All of these graphs are also archived for reference and are not contained in this report.

7.3.3 Transfer Factor and Path-Loss Data

The transfer factors and path-losses were calculated from the spectrum analyzer data according to the equations in Section 7.1.1 and are presented here in graphical form. There are two types of data: (1) antenna outside of the aircraft to antenna inside of the aircraft (path-loss), and (2) antenna outside of the aircraft to a probe on a wire in the aircraft (transfer factor). First the antenna path-losses and then the probe transfer factors will be presented.

7.3.3.1 Antenna Path-Loss Data

Figures 7.3.3 to 7.3.8 are antenna path-loss. The vertical scale is the transfer ratio in dB. The horizontal scale is frequency from 1 MHz to 2,500 MHz. Each figure is labeled according to the position of the antenna outside of the aircraft and the position of the antenna on the inside of the aircraft. The test number corresponding to the test matrix is shown in parenthesis after the title of each figure. The label in parenthesis next to the position description corresponds to the transmit and receive locations shown in figure 6.1.1.

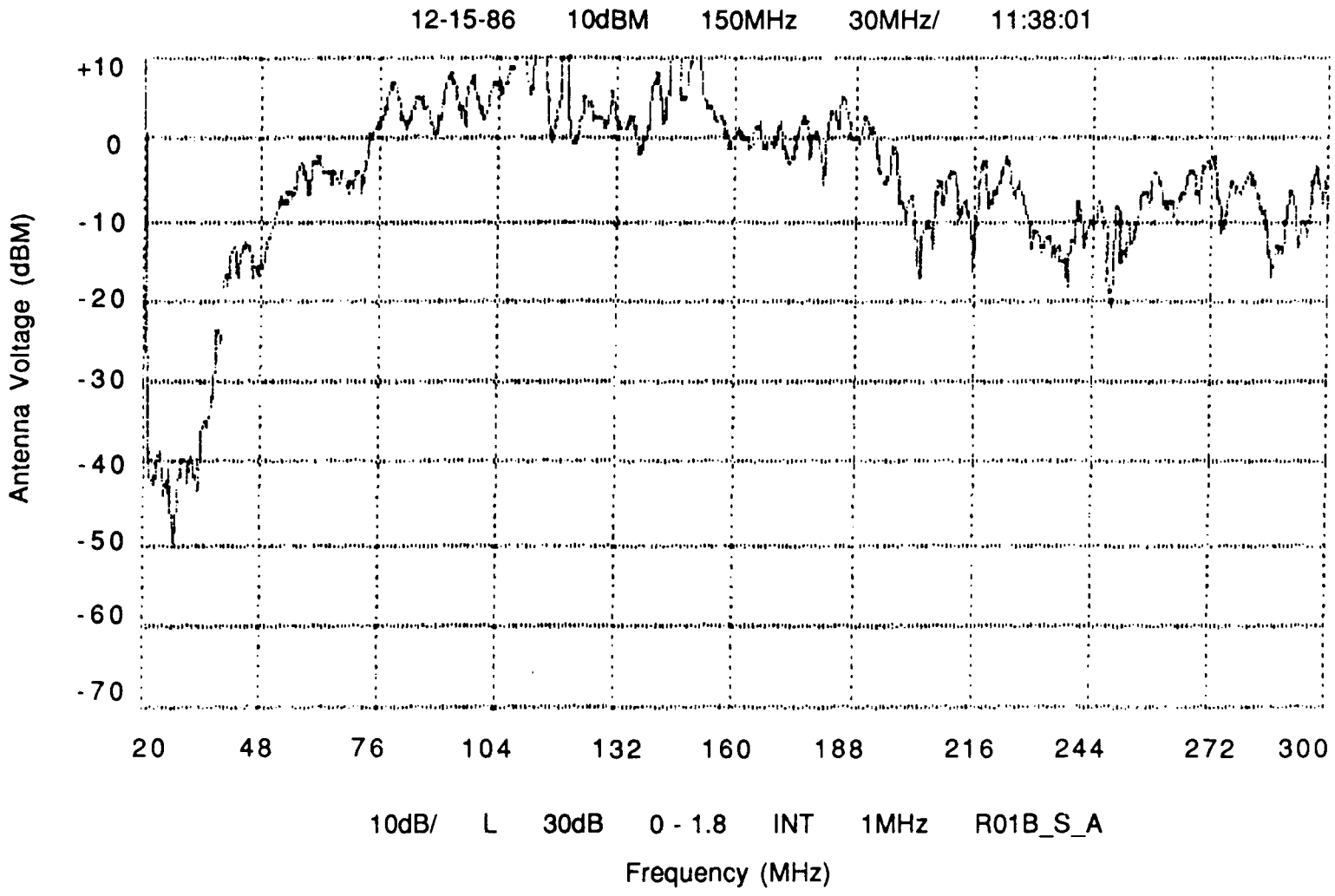

Figure 7.3.1 Typical Spectrum Analyzer Data (Test Sequence No.)

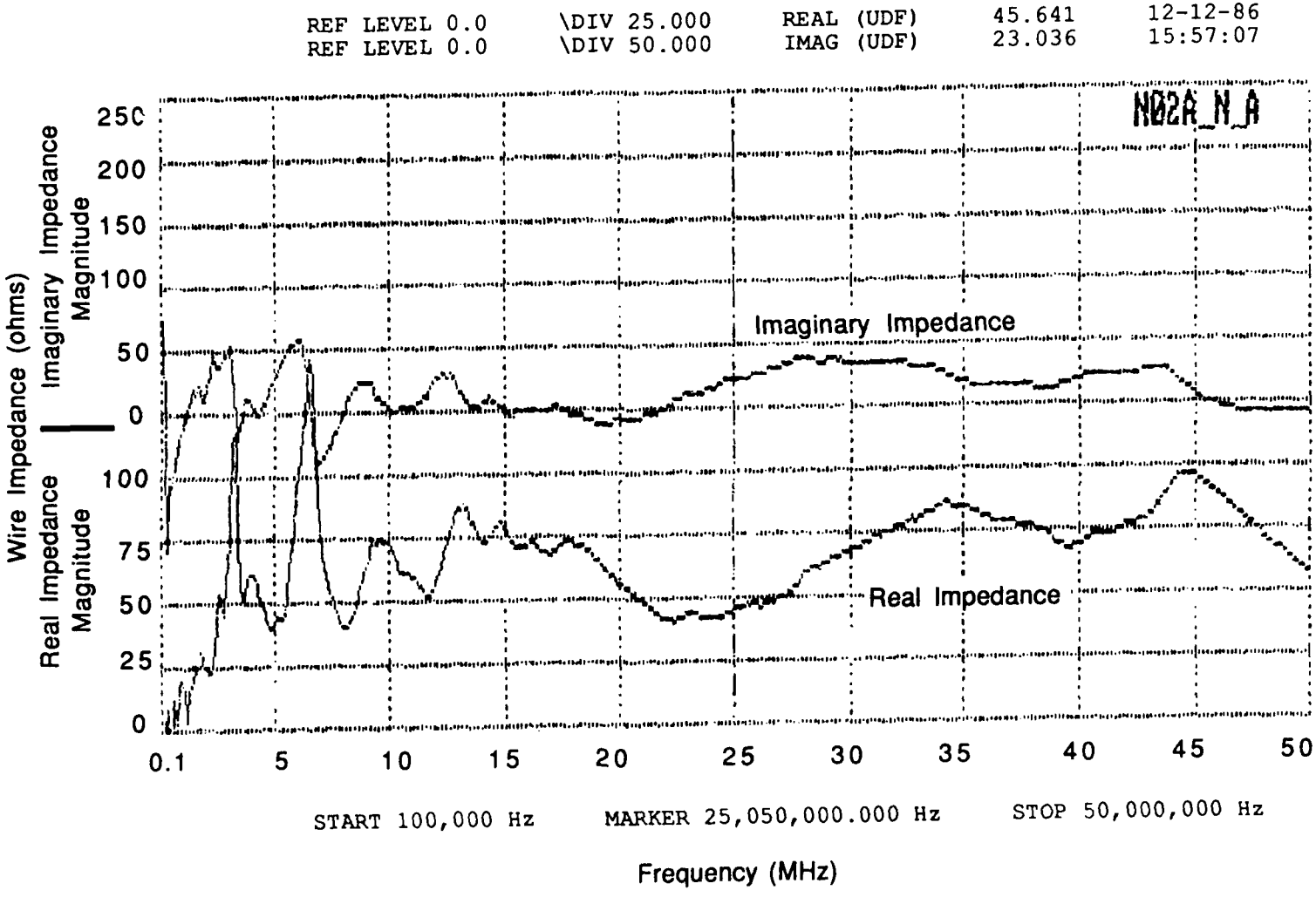

Figure 7.3.2 Typical Network Analyzer Data

The antenna path-losses show the decrease in signal levels due to going through the skin, windows, seams, etc. of the aircraft in decibels. In figure 7.3.3, the RF energy was transmitted directly at the right side of the cockpit at window height.

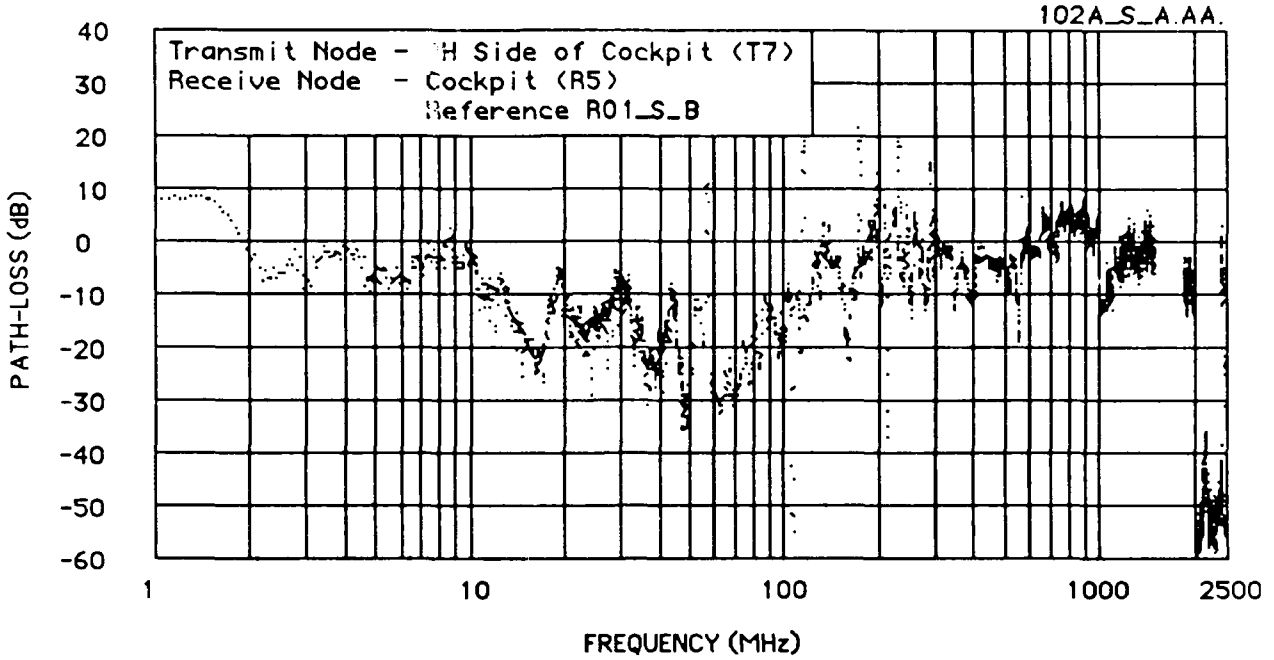

Figure 7.3.3 Antenna Path-Loss Function (Test 102A)

The signal levels were measured outside of the cockpit and compared to the signal levels inside of the cockpit. The figures have peaks and valleys which correspond to the frequencies where the aircraft dimensions resonate. The major resonant dimensions correspond to the length of the aircraft (approximately 5 MHz) and the cabin dimensions (approximately 35 MHz). Other peaks occur at dimensions of windows, seams, etc. In this figure, the average loss in the low frequency range (1 - 150 MHz) is about -12dB. The mid frequency range (150 - 1,000 MHz) averages about -5dB. The high frequency range (1,000 - 2,500 MHz) averages about -8dB.

Compare figure 7.3.3 to figure 7.3.4 where the transmitter is moved from outside of the cockpit to the left rear of the aircraft under the left engine. The major difference is in the high frequency range. When the transmitter was aiming in the windows of the cockpit the high frequency range came through the windows with an average loss of -8dB. When the transmitter was in the rear, the loss at the high frequency range was more like an average of -20dB. A loss of 20dB

means a loss of a factor of 100. This means that the signal level inside of the aircraft will be 100 times smaller than the signal outside of the aircraft.

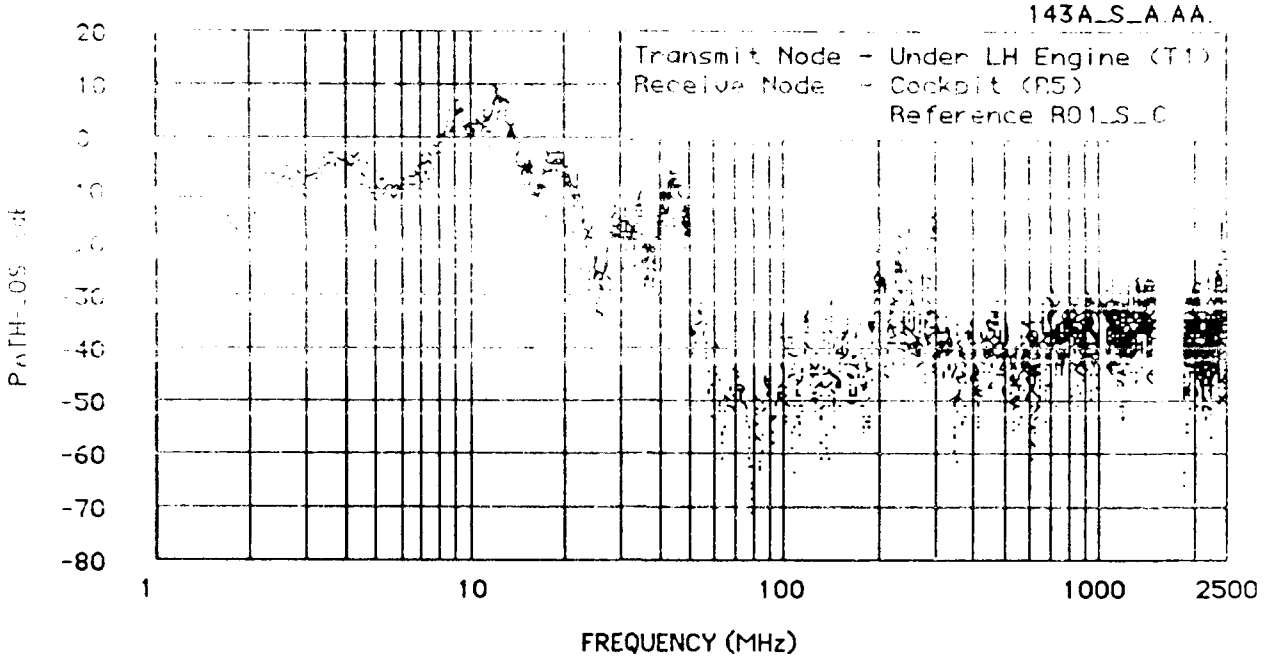

Figure 7.3.4 Antenna Path-Loss Function (Test 143A)

Figure 7.3.5 and figure 7.3.6 were taken for information of special interest to the FAA. The frequencies were swept over the low range and the high range. The mid range was not swept (represented by the straight line on the figures). Figure 7.3.5 was measured in the first class seating area with the outside transmitter in the rear. This shows that the frequencies critical to human passengers are so far below those in the cockpit area that passengers are well protected.

Figure 7.3.6 was taken in the equipment bay which is under the floor of the first class seating area. Most of the navigational equipment is installed in this equipment bay. The low frequencies are reduced in this protected area but the higher frequencies are about the same as the first class seating area.

Figure 7.3.7 and figure 7.3.8 are measured in the mid section of the aircraft with transmitter antennas in front of the cockpit and at the rear left side. The low range of frequencies hold at about -15dB. The mid frequency range varies from about -15dB in the front to -30dB in the rear. The high frequency range is about -25dB for both.

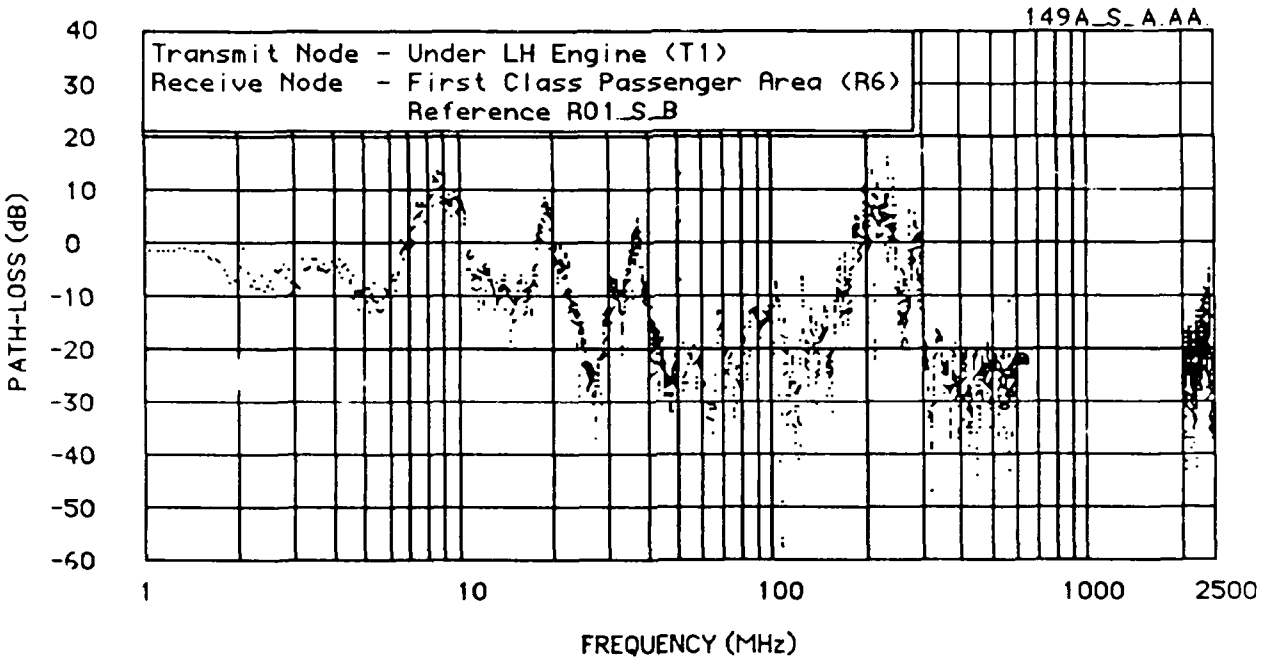

Figure 7.3.5 Antenna Path-Loss Function (Test 149A)

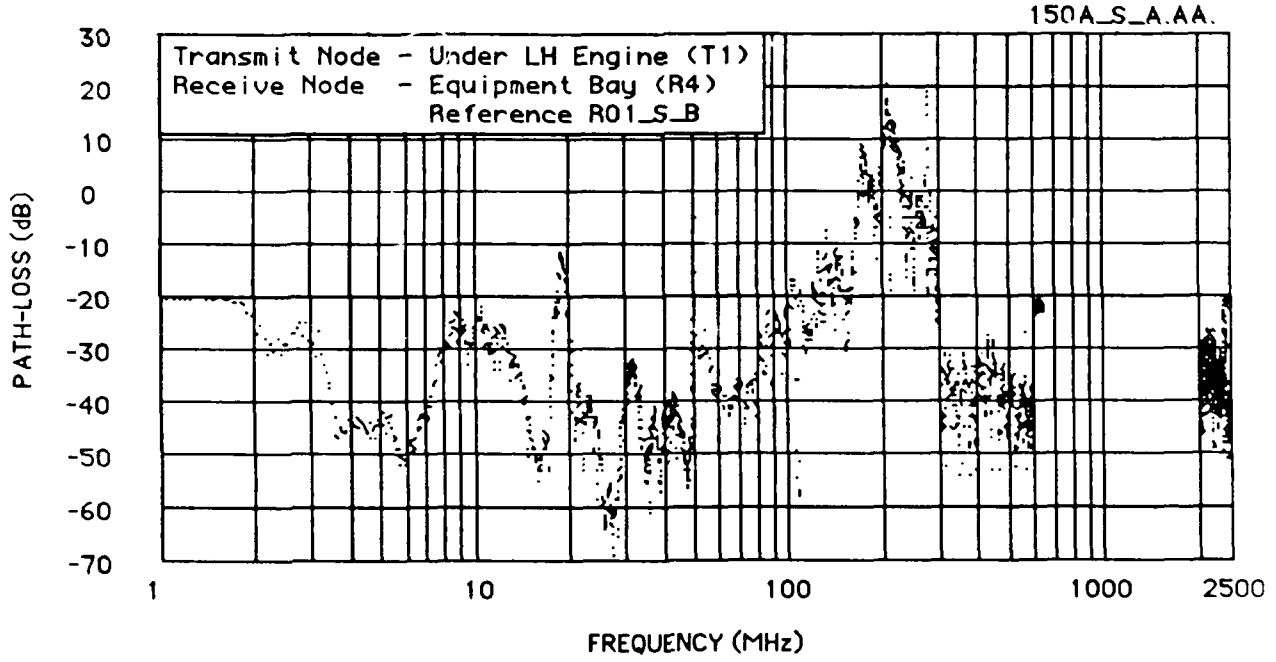

Figure 7.3.6 Antenna Path-Loss Function (Test 150A)

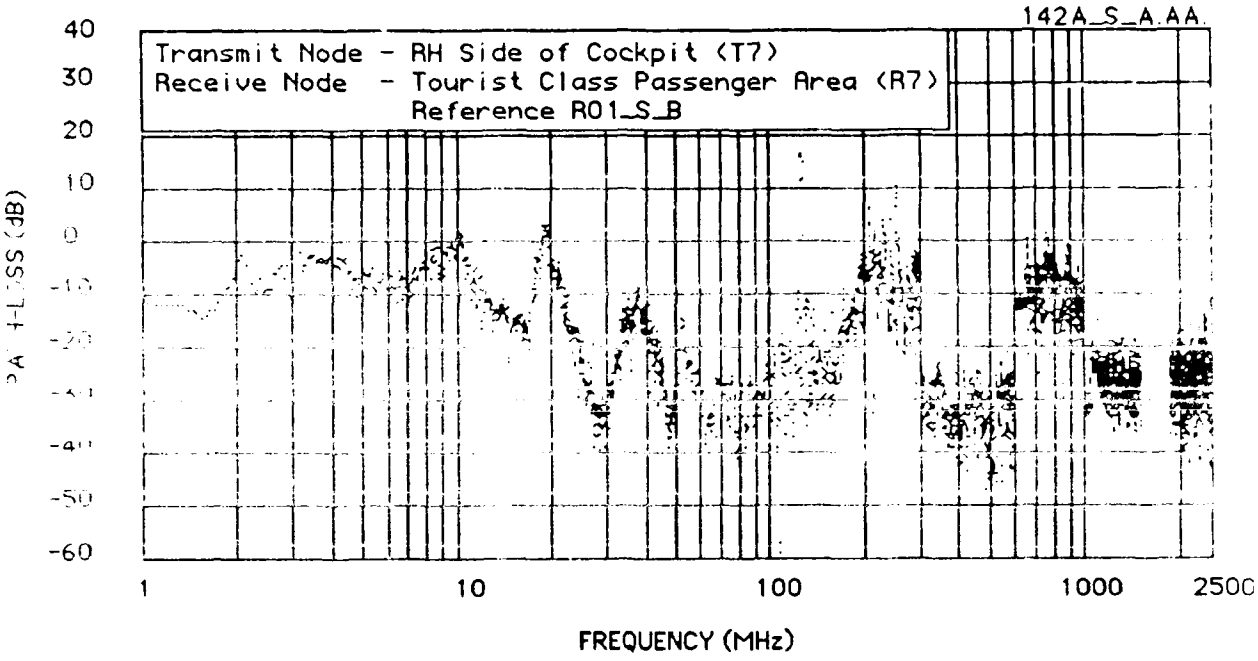

Figure 7.3.7 Antenna Path-Loss Function (Test 142A)

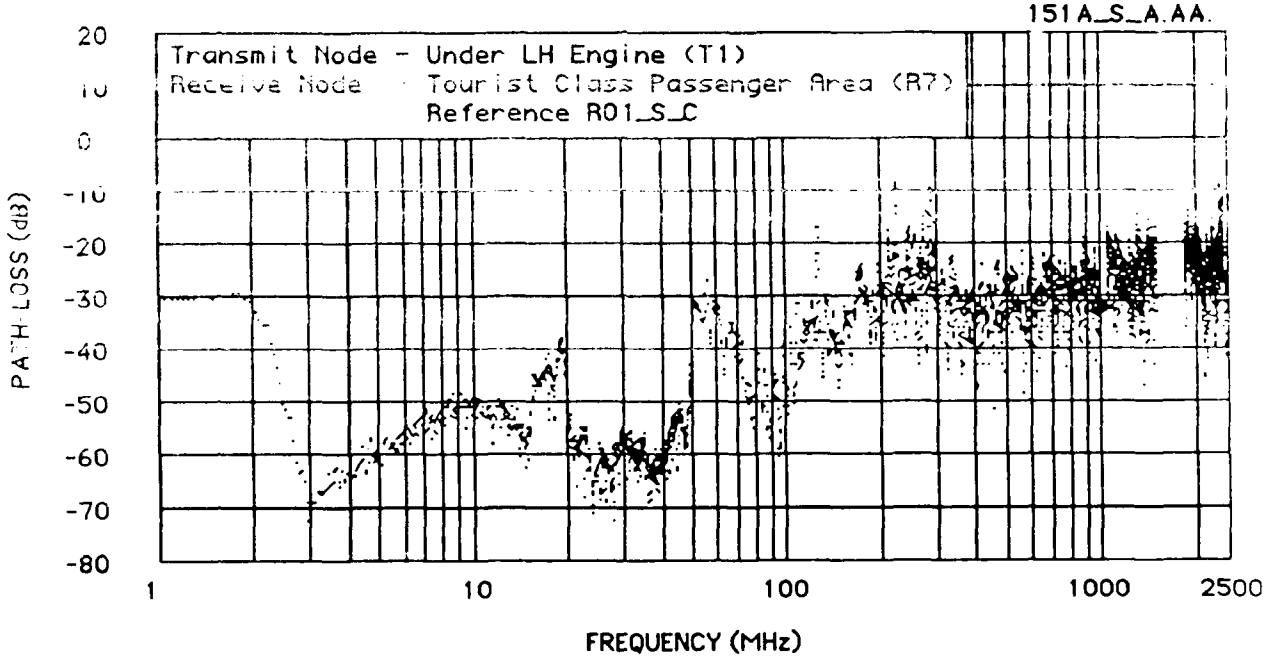

Figure 7.3.8 Antenna Path-Loss Function (Test 151A)

In summary, it appears from the antenna measurements that at a frequency of about 2 GHz, the average attenuation in the cabin areas where critical components could be damaged is about -25dB or a loss of about a factor of 300.

7.3.3.2 Probe Transfer Factor Data

Figures 7.3.9 to 7.3.19 are probe transfer factors. This transfer factor is a relationship of the power measured by a voltage probe and an impedance probe on a wire of the aircraft to the field strength (watts/meter^2) measured on an antenna outside of the aircraft (in decibels). The vertical axis is in dB and the horizontal axis is in frequency from 1 MHz to 2,500 MHz. The titles, antenna position and test number are shown in the same way as described for the antenna transfer factor figures.

Figures 7.3.9 and 7.3.10 are measured in the wheel well area. Figure 7.3.9 is measured with the probe on the APU off switch wire at pin I of the connections to the switch. Figure 7.3.10 is a verification that the signal in the probe picked up directly is not larger than the signal from the wire. Note: the straight line from 300 to 1,000 MHz and from 1,550 to 2,000 MHz means that no data was taken in this frequency range. This probe on/probe off test is repeated in various places in the aircraft and is denoted by the letter A after the test number for probe on and the letter B for the probe off.

The signal on the APU off switch wire, even though the wire location is outside of the aircraft, is many orders of magnitude lower than the signals on antennas inside of the aircraft.

Figures 7.3.11 through 7.3.13 are taken inside of the left engine cowling with the transmitter thirty feet to the left.

Figures 7.3.14 through 7.3.19 are taken on wires in the cockpit with the transmitter sometimes near the cockpit and sometimes under the left engine as indicated on the figures.

Almost all readings of RF energy picked up on the wiring are below -40dB at the low frequencies and below -60dB at the high frequencies.

These probe attenuation measurements indicate that the RF signal is attenuated nearly a million times and therefore it is not probable that damage will be caused by this mechanism except where antennas bring the RF energy directly into subsystems.

Because the probe transfer factors are so well attenuated, a detailed analysis of each figure will not be made. One exception to this is that on figure 7.3.12 there is a tremendous peak at 25 MHz on the wire that controls the opening and closing of the air valve for the engine. The engine cannot be started even with "shorepower" if this air valve is closed. This peak may be due to RF reflections

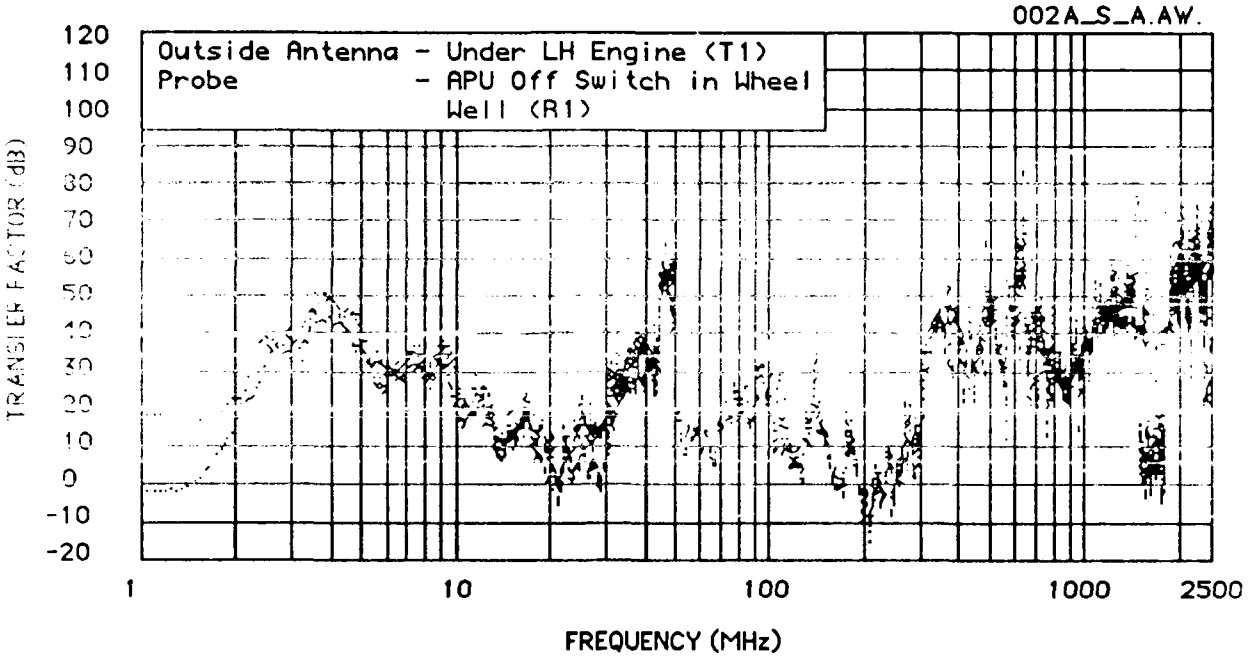

Figure 7.3.9 Probe Transfer Factor (Test 002A)

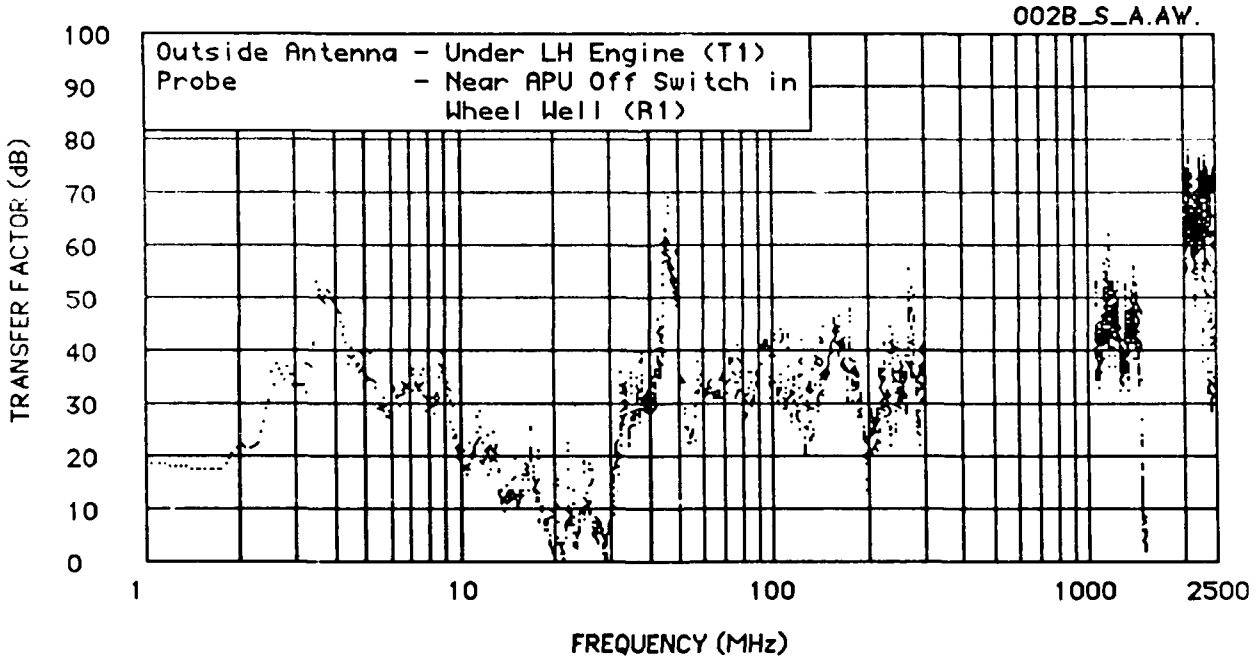

Figure 7.3.10 Probe Transfer Factor (Test 002B)

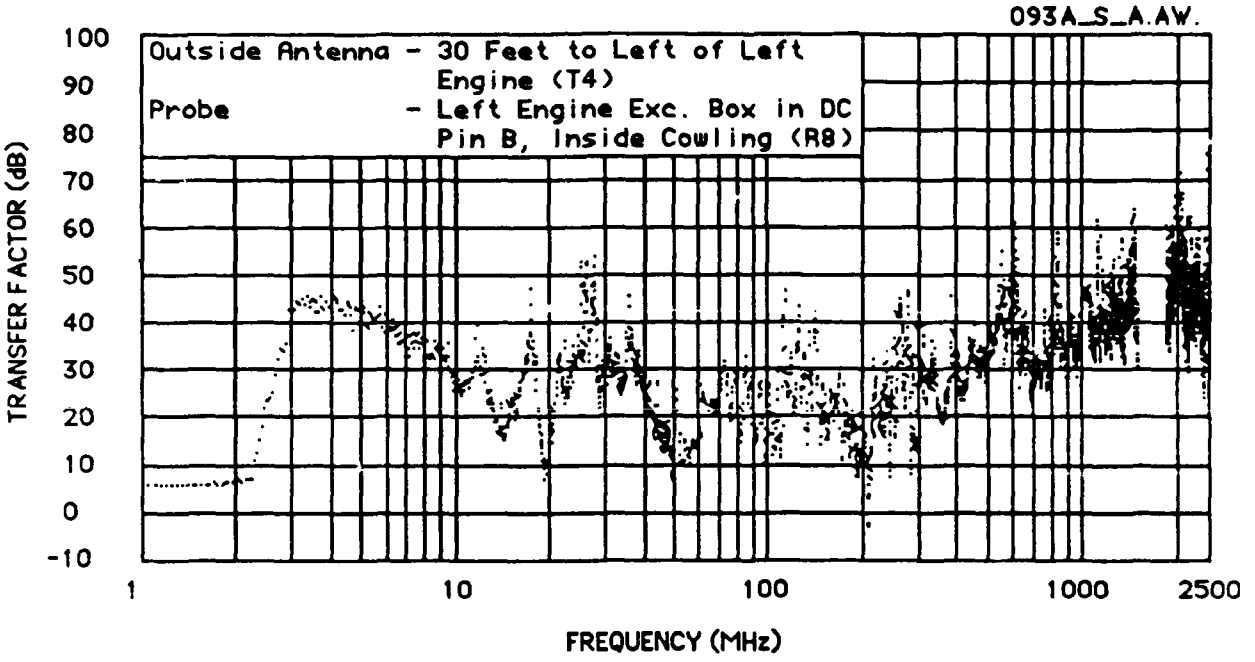

Figure 7.3.11 Probe Transfer Factor (Test 093A)

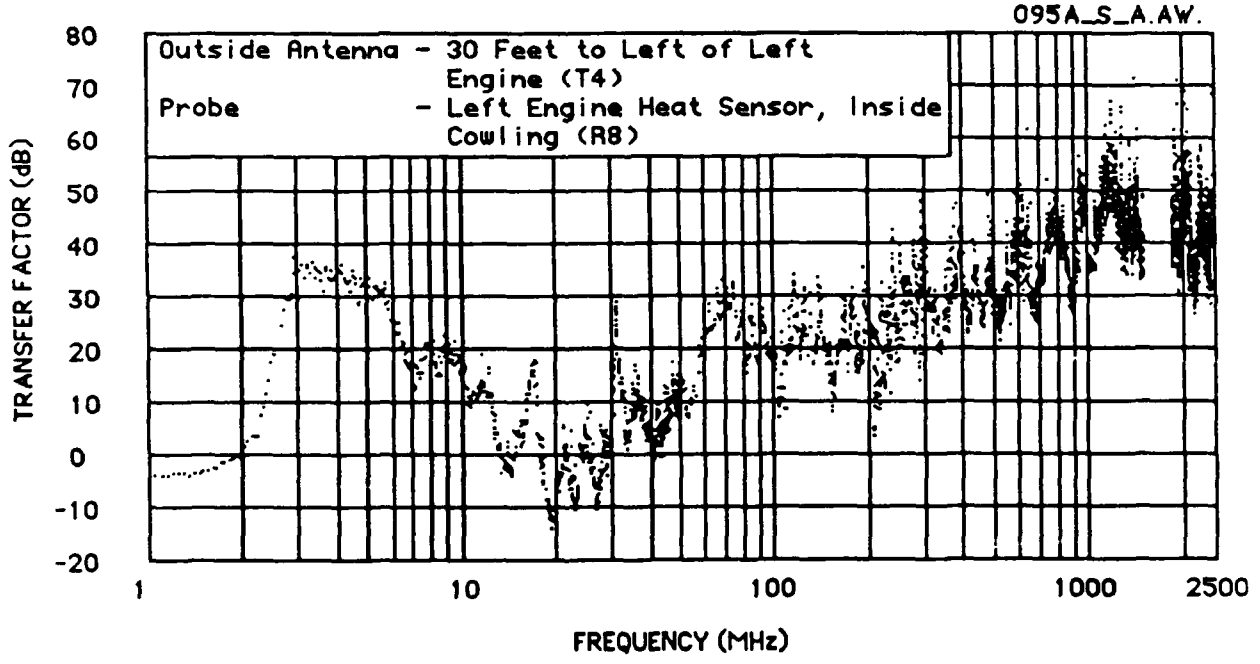

Figure 7.3.12 Probe Transfer Factor (Test 095A)

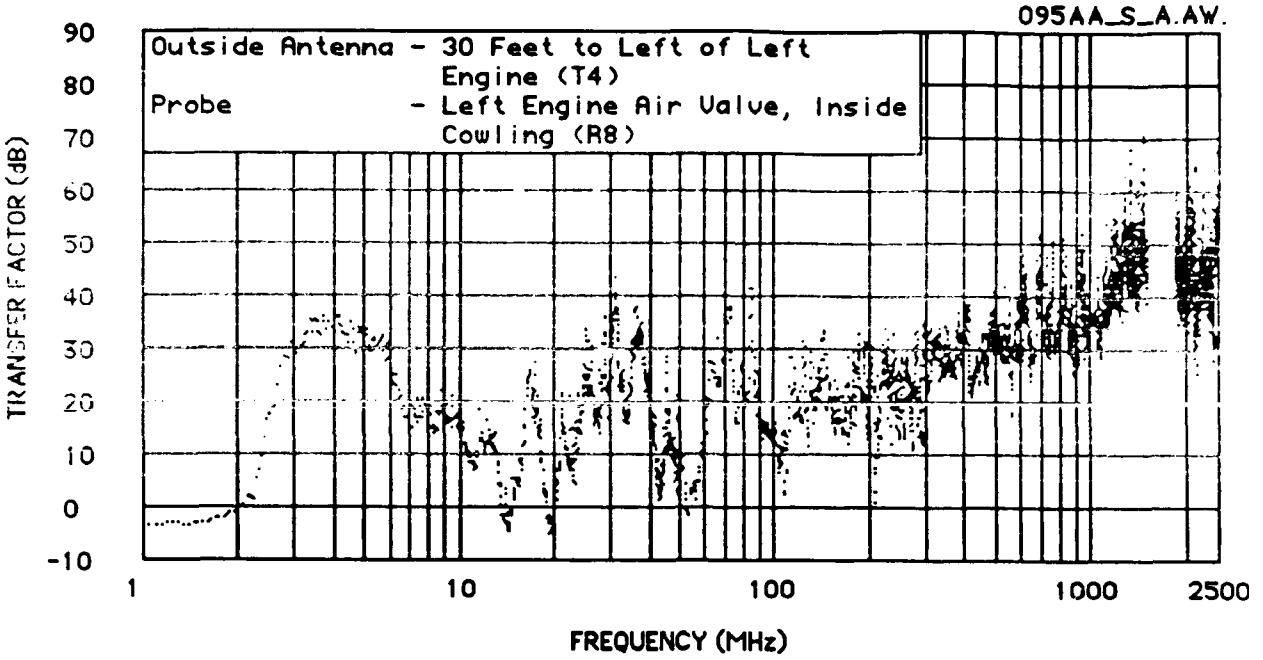

Figure 7.3.13 Probe Transfer Factor (Test 095AA)

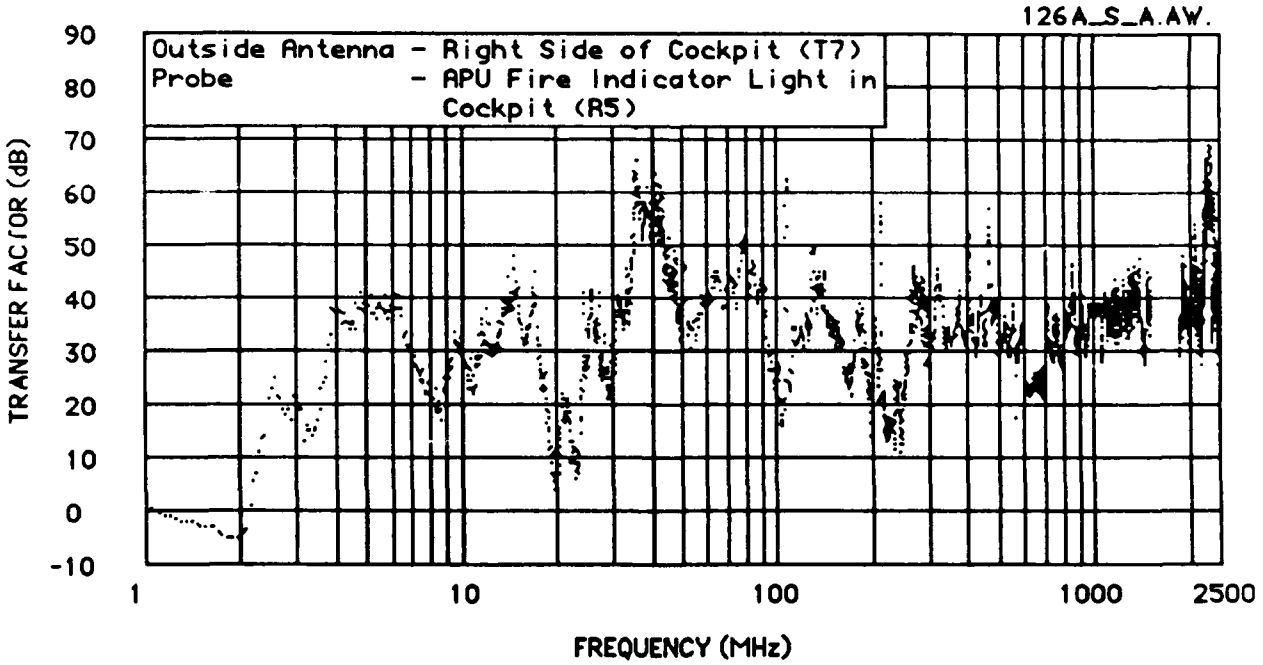

Figure 7.3.14 Probe Transfer Factor (Test 126A)

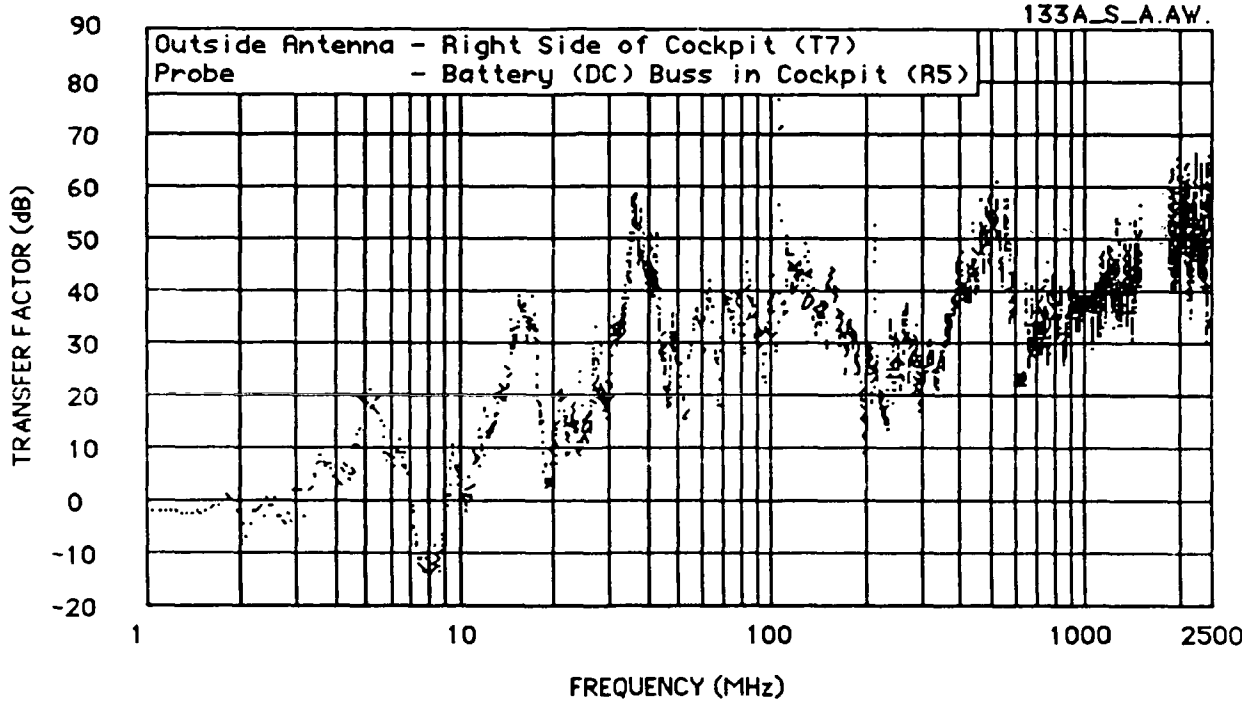

Figure 7.3.15 Probe Transfer Factor (Test 133A)

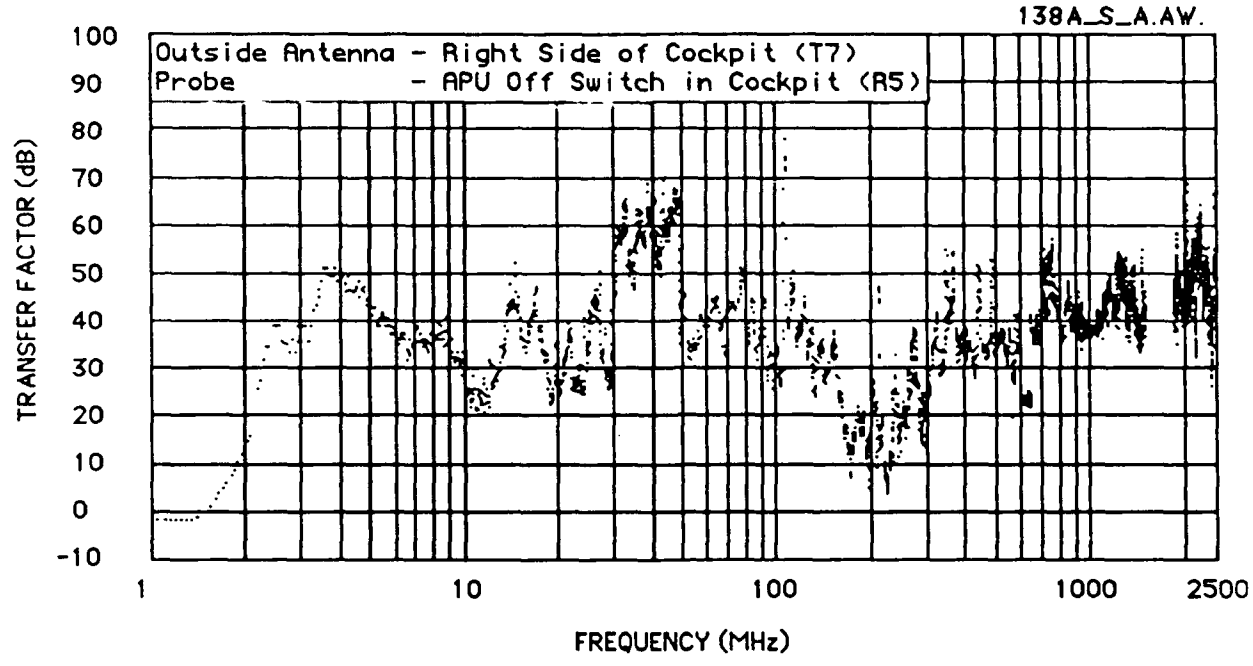

Figure 7.3.16 Probe Transfer Factor (Test 138A)

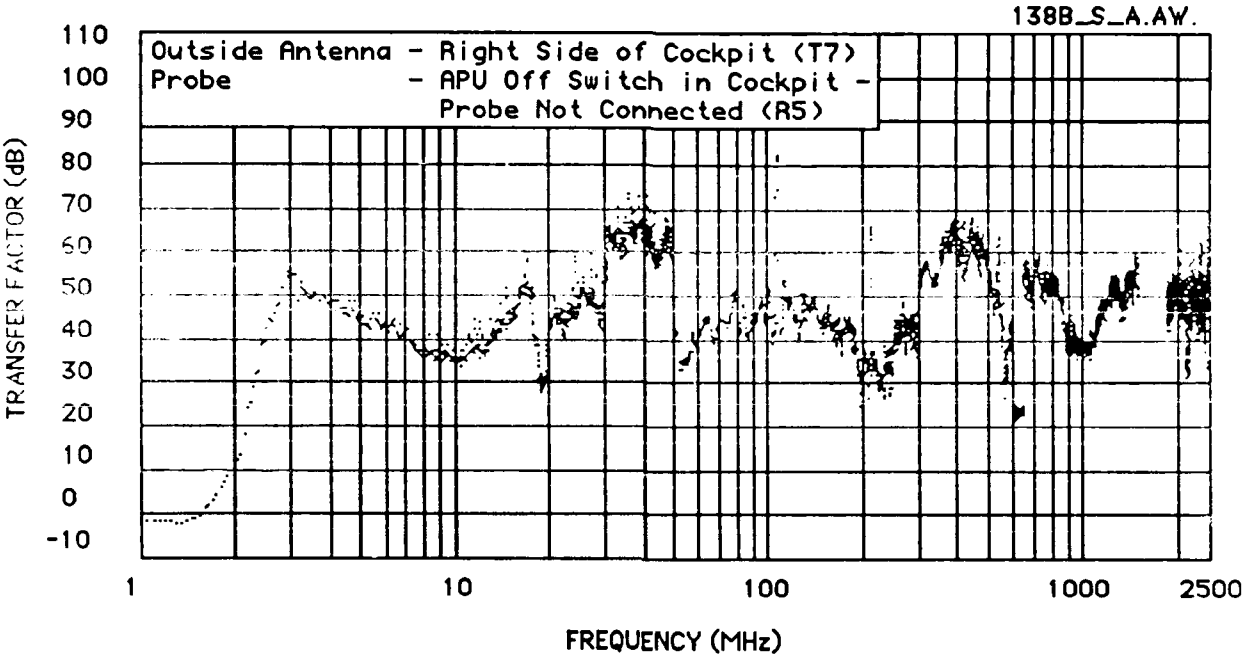

Figure 7.3.17 Probe Transfer Factor (Test 138B)

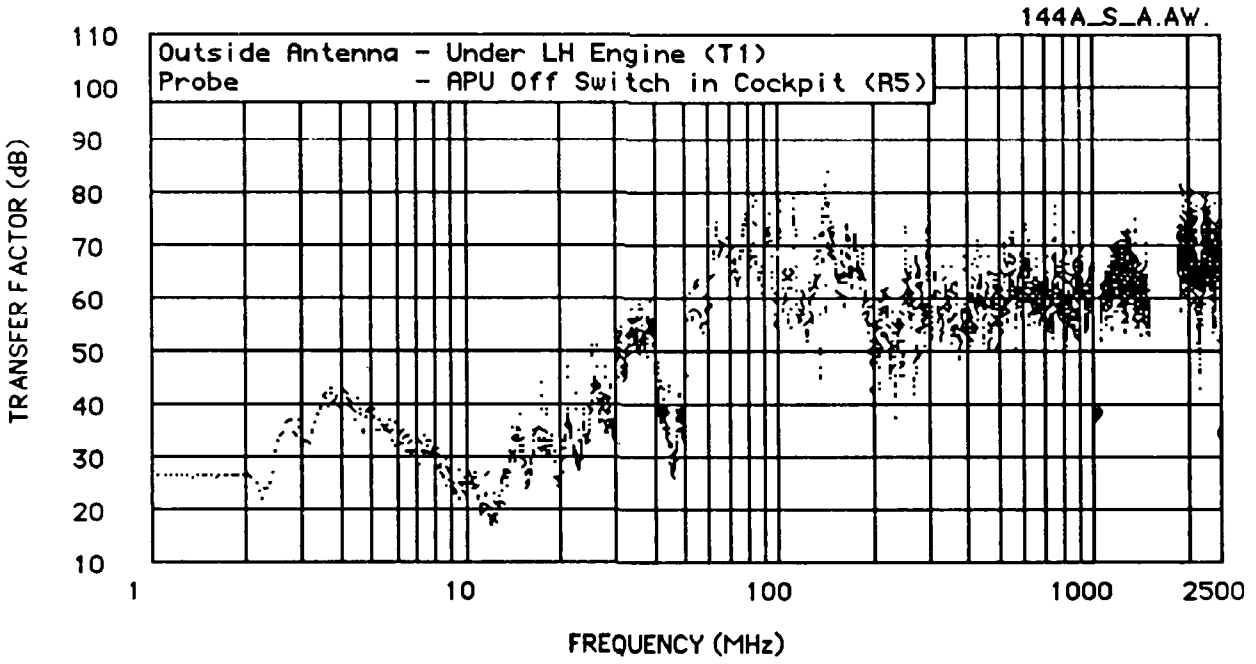

Figure 7.3.18 Probe Transfer Factor (Test 144A)

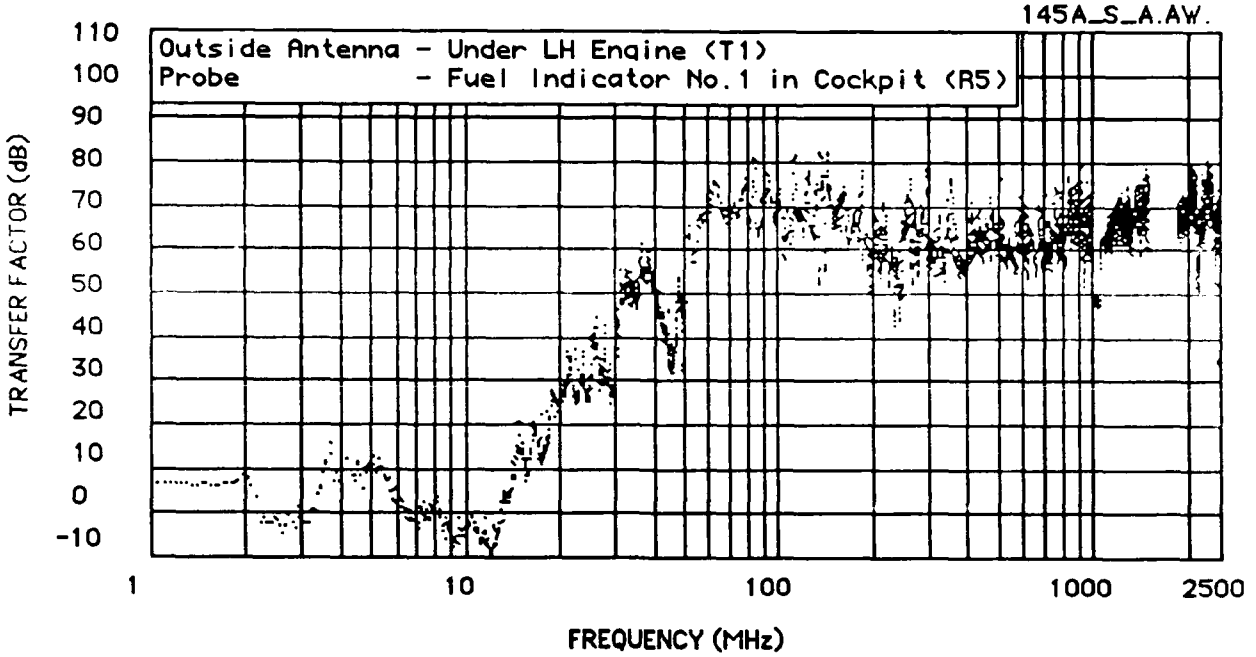

Figure 7.3.19 Probe Transfer Factor (Test 145A)

from the aircraft and the cowling of the engine. However, a probe off measurement was taken to determine what was really on the wire versus the probe pickup and the peak was 10 dB higher on the wire. Nevertheless, some caution on interpretation of this peak must remain until empirical tests can be made.

7.4 HEALTH HAZARDS

Comments on health hazards are discussed in the following sections.

7.4.1 Personnel Health Hazard

The 1982 American National Standards Institute (ANSI) standard for maximum public and occupational exposure to RF allows 0.4 watts per kilogram of body weight averaged over the entire body for 6 minutes. For average body size, the published limits of RF power versus frequency are:

Frequency	Maximum Exposure Power
1 MHz - 1 GHz	10 (Watts/meter squared)
1 GHz - 100 GHz	60 (Watts/meter squared)

In the frequency range near 2 GHz, 60 watts per meter squared is allowed for six minutes by the ANSI standards. The levels projected from this report may be above this level but not for the six minute maximum, since the aircraft would easily fly past the most intense RF fields in much less time than six minutes.

7.5 SUMMARY OF DATA ANALYSIS

The attenuation of external RF fields penetrating an airframe varies greatly. This data supports a conservative attenuation value of approximately -25dB (or a factor of 300). It should be noted that some locations show virtually no attenuation (wheel wells, cockpit, next to windows, etc...).

It is therefore possible to encounter external fields of sufficient intensity to induce potentially disruptive or even damaging voltages into the airplane electronics. This might take place at virtually any location on the aircraft.

8 SUMMARY

BOEING 727-100 RF TEST PROJECT was successfully completed. A brief reiteration of major results is given before the specific conclusions are discussed.

8.1 Literature Search

The project began with a literature search of material concerning such topics as EMI; RFI; EMC; affects of EMI on aircraft and aircraft components; and, aircraft systems critical to the safe operation of the aircraft. The results of the literature search are as follows:

1. Aircraft systems are susceptible to RFI. Older aircraft designs are susceptible to RFI but not to the same degree as newer aircraft designs. Aircraft designed in the 1980's are fly-by-wire designs containing microprocessor control systems without backup mechanical cables and pulleys and may be more susceptible to RFI than older designs.

2. The APU control circuits as well as wiring from systems affecting the airplane's air/ground sensing (i.e. squat switch), are visible in the main wheel well area when the wheels are lowered and are therefore more susceptible to RFI.

8.2 Aircraft Inspection

When the literature search was completed several different types of aircraft were inspected including C141, B-727-100, and B-737 with the help of the FAA. From these inspections it was determined that wiring external to the fuselage for systems such as the APU and air ground sensing were very similar and exposed in the wheel well area when the wheels are lowered.

8.3 Field Test

A commercial B-727-100 aircraft owned and operated by the FAA was tested at low levels of RF energy and it was determined that RF energy was attenuated by a factor of about three hundred (-25 dB) by the skin of the aircraft at low microwave frequencies.

8.4 Health Hazards

The American National Standards Institute (ANSI) has set a standard for human health hazard to RF energies. According to the latest ANSI standards, RF fields that would be encountered inside of the aircraft as it flies over intense RF fields at low microwave frequencies would not exceed the minimum health hazard levels for exposures of ten seconds or less.

9 CONCLUSIONS

Commercial aircraft such as a 727-100 are susceptible to RFI. The attenuation of RF fields from outside of the aircraft to the inside is about a factor of 300 (-25dB). This means that fields greater than one volt per meter are possible inside of the aircraft (one volt per meter is the tested "safe level" or "qualified" status of the instruments in a BOEING 727-100). Current generation aircraft are more susceptible to RFI than older designs of aircraft due to extensive use of sensitive electronic controls.

Because of the short times that people will be exposed to RF fields inside of the aircraft (as the aircraft flies over intense RF fields) the potential health hazard to personnel inside of the aircraft is very low.

The most significant technical aspect or finding of this effort is predicted induced voltage on internal wiring.

APPENDIX A
FULL TEST MATRIX

APPENDIX A
FULL TEST MATRIX

This appendix contains an explanation of the nomenclature used in the full test matrix originally designed for BOEING 727-100 RF TEST PROJECT. The full matrix is given in tables A.1 and A.2 because it is too large to fit on a single sheet of paper. The full matrix shows the maximum number of measurements which would have constituted a complete test. It was reduced at the time of the test to eliminate redundancy and to stay within the allotted test time. The reduced matrix is contained in the main body of the report as tables 6.2.1 and 6.2.2.

The test matrix is a two-dimensional matrix. The horizontal or column dimension contains the frequency bands through which the transmitter frequency is swept and the description of the type of antenna used for each frequency band, and is shown in table A.1. The frequency bands are lettered "A" through "S" with the addition of one band which is labeled "(-)". The type of antenna on both the receive and the transmit system has to be switched for each frequency band.

The vertical or line dimension represents a list of test points on the aircraft which are numbered 1 - 152 and are shown in table A.2. For each test number the location of the control node, the transmit node, the position of each of the five types of transmit antennas, and the receive node position (all five types of receive node antennas are located at the same position) are listed. It is further noted whether the test is an antenna test (also receive antenna node), a probe test on the spectrum analyzer (voltage or current probes), or a network analyzer impedance measurement (only one of the four types of measurements is listed for each test number).

There are three test equipment nodes as mentioned above. These nodes and a description of their positions are listed next. The position numbers are coordinated with the drawing shown in figure 6.1.1.

A. The three equipment carts called nodes are:
    1. Control Node
    2. Transmit Node
    3. Receive Node
B. The Control Node Location is:
    C1. Left side
C. The Transmit Locations are:
    T1. Under LH engine
    T2. 15 feet behind tail on LH side
    T3. Under RH wing
    T4. Left side facing engine No. 1
    T5. At tail
    T6. LH side near equipment bay
    T7. RH side of cockpit
    T8. Under left elevator

D. The Receiver Locations are:

R1. Under LH wing
R2. Under RH wing
R3. Tail stair case
R4. Equipment bay (antenna only)
R5. Cockpit
R6. First class passenger area
R7. Tourist class passenger area
R8. Engine No. 1

Table A.1
Full Test Matrix Horizontal (Column) Dimension

Frequency Band	Frequency Range	Antenna Description	Antenna Number
-	1 - 35 MHz	HF Monopole	1
A	1 - 35 MHz	HF Loop	2
B	20 - 300 MHz	Biconical	3
C	200 - 600 MHz	Log Periodic No. 1	4
D	600 MHz - 1.0 GHz	Log Periodic No. 1	4
E	1 - 1.5 GHz	Log Periodic No. 2	5
F	1.2 - 1.8 GHz	Log Periodic No. 2	5
G	1.5 - 2.0 GHz	Log Periodic No. 2	5
H	2.0 - 2.5 GHz	Log Periodic No. 2	5
I	2.5 - 3.0 GHz	Log Periodic No. 2	5
J	3.0 - 3.5 GHz	Log Periodic No. 2	5
K	3.5 - 4.0 GHz	Log Periodic No. 2	5
L	4.0 - 4.5 GHz	Log Periodic No. 2	5
M	4.5 - 5.0 GHz	Log Periodic No. 2	5
N	5.0 - 5.5 GHz	Log Periodic No. 2	5
O	5.5 - 6.0 GHz	Log Periodic No. 2	5
P	6.0 - 6.5 GHz	Log Periodic No. 2	5
Q	6.5 - 7.0 GHz	Log Periodic No. 2	5
R	7.0 - 7.5 GHz	Log Periodic No. 2	5
S	7.5 - 8.0 GHz	Log Periodic No. 2	5

Table A.2
Full Test Matrix Vertical (line) Dimension

TEST NO.	CTRL NODE	TRANSMIT NODE	TRANS. ANTENNA 1	2	3	4	5	REC. ANT. NODE	SPECTRUM ANALYZER VOLTAGE PROBE	CURRENT PROBE	NETWORK ANALYZER
1	1	1	1A	1A	1	1	1	1			
2									APU STOP SW		
3									APU START SW1		
4									APU START SW2		
5									APU FIRE SW		
6									APU SQUIB		
7										STOP SW	
8											APU STOP SW
9											APU START SW1
10											APU START SW2
11											APU FIRE SW
12											APU SQUIB
13									SQUAT SW1		
14									SQUAT SW2		
15											SQUAT SW1
16											SQUAT SW2
17									HEAT SENSOR1		
18									HEAT SENSOR2		
19										HEAT SENSOR1	
20											HEAT SENSOR1
21											HEAT SENSOR2
22									APU FUEL SHUTOFF VALVE		
23											APU FUEL SHUTOFF VALVE
24									NO.1 FUEL SHUTOFF VALVE		
25	1	1	1A	1A	1	1	1	1	NO.2 FUEL SHUTOFF VALVE		

Table A.2
Full Test Matrix Vertical (line) Dimension (continued)

TEST NO.	CTRL NODE	TRANSMIT NODE	TRANS. ANTENNA					REC. ANT. NODE	SPECTRUM ANALYZER		NETWORK ANALYZER
			1	2	3	4	5		VOLTAGE PROBE	CURRENT PROBE	
26	1	1	1A	1A	1	1	1	1	NO.3 FUEL SHUTOFF VALVE		
27											NO.1 FUEL SHUTOFF VALVE
28											NO.2 FUEL SHUTOFF VALVE
29											NO.3 FUEL SHUTOFF VALVE
30									APU 110% OVER-SPEED SOLENOID		
31									APU OIL PRESS. SENSOR		
32											APU 110% OVERSPEED SOLENOID
33											APU OIL PRESSURE SENSOR
34									MISC.1		
35									MISC.2		
36									MISC.3		
37									MISC.4		
38									MISC.5		
39											MISC.1
40											MISC.2
41											MISC.3
42											MISC.4
43	1	1	1A	1A	1	1	1	1			MISC.5

Table A.2
Full Test Matrix Vertical (line) Dimension (continued)

TEST NO.	CTRL NODE	TRANSMIT NODE	TRANS. ANTENNA					REC. ANT. NODE	SPECTRUM ANALYZER		NETWORK ANALYZER
			1	2	3	4	5		VOLTAGE PROBE	CURRENT PROBE	
44	1	2	2	2	2	2	2	1			
45									APU STOP SW		
46									APU START SW1		
47									APU START SW2		
48									APU FIRE SW		
49									APU SQUIB		
50										APU STOP SW	
51											APU STOP SW
52											APU START SW1
53											APU START SW2
54											APU FIRE SW
55											APU SQUIB
56									SQUAT SW1		
57									SQUAT SW2		
58											SQUAT SW1
59											SQUAT SW2
60									HEAT SENSOR1		
61									HEAT SENSOR2		
62										HEAT SENSOR1	
63											HEAT SENSOR1
64											HEAT SENSOR2
65									APU FUEL SHUTOFF VALVE		
66											APU FUEL SHUTOFF VALVE
67									NO.1 FUEL SHUTOFF VALVE		
68	1	2	2	2	2	2	2	1	NO.2 FUEL SHUTOFF VALVE		

Table A.2
Full Test Matrix Vertical (line) Dimension (continued)

TEST NO.	CTRL NODE	TRANSMIT NODE	TRANS. ANTENNA					REC. ANT. NODE	SPECTRUM ANALYZER		NETWORK ANALYZER
			1	2	3	4	5		VOLTAGE PROBE	CURRENT PROBE	
69	1	2	2	2	2	2	2	1	NO.3 FUEL SHUTOFF VALVE		
70											NO.1 FUEL SHUTOFF VALVE
71											NO.2 FUEL SHUTOFF VALVE
72											NO.3 FUEL SHUTOFF VALVE
73									APU 110% OVER-SPEED SOLENOID		
74									APU OIL PRESS. SENSOR		
75											APU 110% OVERSPEED SOLENOID
76											APU OIL PRESSURE SENSOR
77									MISC.1		
78									MISC.2		
79									MISC.3		
80									MISC.4		
81									MISC.5		
82											MISC.1
83											MISC.2
84											MISC.3
85											MISC.4
86											MISC.5

Table A.2
Full Test Matrix Vertical (line) Dimension (continued)

TEST NO.	CTRL NODE	TRANSMIT NODE	TRANS. ANTENNA 1	2	3	4	5	REC. ANT. NODE	SPECTRUM ANALYZER VOLTAGE PROBE	CURRENT PROBE	NETWORK ANALYZER
87	1	3	3	3	3	3	3	2			
88									EXHAUST DOOR		
89									STACK DISCONN.		
90											EXHAUST DOOR
91											STACK DISCONN.
92	2	6	6	6	6	6	6	6			
93									ENG EXC BX IN DC BUS		
93A									ENG EXC BX IN 400HZ BUS		
94									ENG EXC BX OUT		
95									ENG HEAT SENS.		
95A									AIR VALVE		
95AA									AIR VALVE WITH PROBE DISCONN.		
96	1	4	4	4	4	4	4	3			
97									SQUIB		
98											SQUIB
99	1	5	5	5	5	5	5	3			
100									SQUIB		
101											SQUIB
102	1	6	6	6	6	6	6	4			
103									APU ON		
104									APU OFF		
105									APU FIRE		
106									SQ. SW		
107	1	6	6	6	6	6	6	4	HEAT SENSOR		

Table A.2
Full Test Matrix Vertical (line) Dimension (continued)

TEST NO.	CTRL NODE	TRANSMIT NODE	TRANS. ANTENNA 1	2	3	4	5	REC. ANT. NODE	SPECTRUM ANALYZER VOLTAGE PROBE	CURRENT PROBE	NETWORK ANALYZER
108	1	6	6	6	6	6	6	5			
109									FIRE LIGHT		
110									PCD IND.		
111									FUEL IND.		
112									PNEUMAT. IND.		
113									TEMP. IND.		
114									HYDRAUL. IND.		
115									400HZ ELEC.BUS		
116									DC ELEC. BUS		
117									OIL PRESS IND.		
118									VOLT METER		
119									CURRENT METER		
120									APU ON		
121									APU OFF		
122									APU FIRE SW		
123									SQ. SW.		
124	1	6	6	6	6	6	6	5	HEAT SENSOR		
125	2	7	7	7	7	7	7	5			
126									FIRE LIGHT		
127									PCD IND.		
128									FUEL IND.		
129									PNEUMAT. IND.		
130									TEMP. IND.		
131									HYDRAUL. IND.		
132									400HZ ELEC.BUS		
133									DC ELEC. BUS		
134									OIL PRESS IND.		
135									VOLT METER		
136	2	7	7	7	7	7	7	5	CURRENT METER		

Table A.2
Full Test Matrix Vertical (line) Dimension (continued)

TEST NO.	CTRL NODE	TRANSMIT NODE	TRANS. ANTENNA 1	2	3	4	5	REC. ANT. NODE	SPECTRUM ANALYZER VOLTAGE PROBE	CURRENT PROBE	NETWORK ANALYZER
137	7	7	7	7	7	7	7	5	APU ON		
138									APU OFF		
139									APU FIRE SW		
140									SQ. SW.		
141	ANT MID								HEAT SENSOR		
142	(125)	1		1	1	1	1	7			
143	(125)	1		1	1	1	1	5			
144	(138)			1	1	1	1	5	APU OFF		
145	(128)			1	1	1	1	5	FUEL IND.		
146	(126)	DROPPED									
147	(132)			1	1	1	1	5	400HZ ELEC.BUS		
149	(a,c,h)			1	1	1	1	8			
150	(a,c,h)			1	1	1	1	4			
151				1	1	1	1	7			
152	1	1		1	1	1	1	1			

APPENDIX B
EQUIPMENT LIST AND SOFTWARE

APPENDIX B
EQUIPMENT LIST AND SOFTWARE

Equipment Description	Manufacturer	Model No.
1.Rx Node		
Spectrum Analyzer	Tektronix	494P
Coax Switch - 6p	Dow-Key	780602
IEEE-488 buss. conv.	IOtech	Extender 488
Buss - Fiber Optic	BB	FO-232
HF-MW Voltage Probe	Tektronix	P-6056-9, 6057-9
HF-MW Current Probe w/adapter	CT	1-08, 1-09,
HF-VHF Clamp C. Probe	BCP	511
Active Antenna	SAS	200/550
HF-VHF Antenna	SAS	200/542
UHF Antenna	SAS	200/530
UHF Antenna	SAS	200/510
Microwave Antenna	SAS	200/511
Fiber Optic Cable 1	***	***
HF-VHF Network An/S	HP	3577A
2. Tx Node		
HF Signal Generator	WaveTek	2002
Microwave Sig Gen	HP	8350
Microwave RF Plug-in	HP	83595
HF-UHF PreAmp	ENI	603L
HF Power Amp	ENI	5100LA
UHF Power Amp	Ailtech	15100B
Microwave PreAmp	HP	8349A
Microwave TWT PA	Hughes	8020H01
Microwave TWT PA	Hughes	8020H02
RF MilliVoltmeter	Boonton	92A w/Loads
Coax Switch - 6p	Dow-Key	780602
Coax Switch - 6p	Dow-Key	116-220202
Coax Switch - 2p	Dow-Key	780702
HF Loop Antenna	Locally Fabricated	
Equipment Description	Manufacturer	Model No.
2. Tx Node (continued)		
HF Vertical Antenna	Locally Fabricated	
HF-VHF Antenna	SAS	200/541
UHF Antenna	SAS	200/512
Microwave Antenna 1	SAS	200/511
DC Supply	AE	95-513

3. Control Node

Computer Controller	iBM	PC-AT
Printer	Okidata	MicroLine 294
IEEE-488 conv.-3	IOtech	Extender 488
Buss - Fiber Optic 2	BB	FO-232
Expansion Hardware	IOTECH	Pers 488

SOFTWARE

1. Control Node Software
   Menu System
   Custom Test Software
   Fastback
   Quick Basic 3.0

2. Software used to Analyze Data
   Plot program written for the project is archived in the SCIENTECH project file.

APPENDIX C
PHOTOGRAPHS

PHOTOGRAPHS

NUMBER	DESCRIPTION
1	Honolulu FAA staff.
2	FAA 727 - N77.
3	Computer control node display of DAS selection menu.
4	Transmit Node Frequency Generators.
5	Transmit Node cart (right), Receive Node carts (left).
6	Receive Node equipment, Network Analyzer (left), Spectrum Analyzer (right).
7	Typical Network Analyzer Display.
8	Transmit Node with antennas below engine number 1 (location T1).
9	Transmit Node at location T1.
10	Receive Node under left wing near wheel well (location R1).
11	Receive dipole antenna near left wheel showing open equipment bay (location R1).
12	Transmit antennas at right side of cockpit (location T7).
13	View from cockpit of transmit antennas positioned at right side of cockpit (location T7).
14	Engine number 1.
15	Air start valve on engine number 1 (Test 95A).
16	Ceiling of wheel well with viewport and wheel well heat-sensing wire.
17	Wheel well heat sensor, Test 20.
18	Wheel well heat sensor, Test 20.
19	APU fire switch in wheel well, Test 5.
20	APU off switch with probe on, Test 2.
21	APU off switch with antenna, Test 1.
22	Right side of wheel well near APU exhaust door switch.
23	APU exhaust door switch under right wing.
24	View of pilot's instruments showing red-colored engine fire switches at top of photo.

PHOTOGRAPHS (continued)

NUMBER	DESCRIPTION
25	View showing panel to engine fire switches removed for access to wiring.
26	Engine fire switch wiring in cockpit.
27	View of flight engineer's instrument panel.
28	Connector for fuel indicator on flight engineer's panel.
29	Probe measurement of fuel indicator at flight engineer's panel.
30	Circuit breaker panel in rear of cockpit with one tray open.
31	APU stop switch in cockpit.
32	DC electrical buss in cockpit .

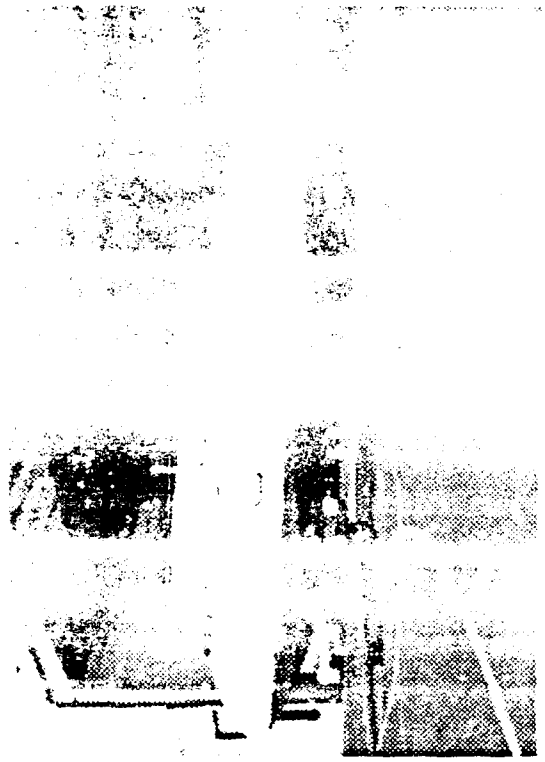

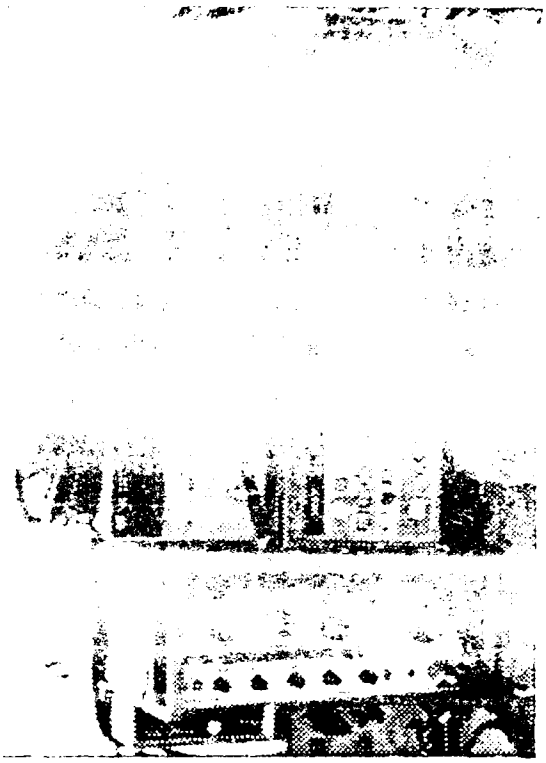

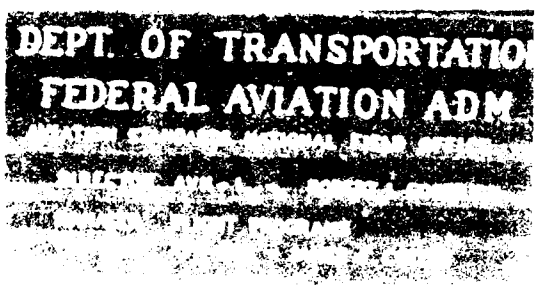
DEPT. OF TRANSPORTATIO
FEDERAL AVIATION ADM.

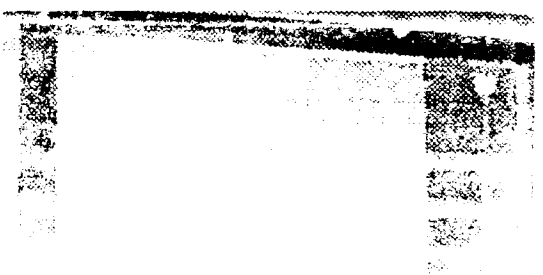

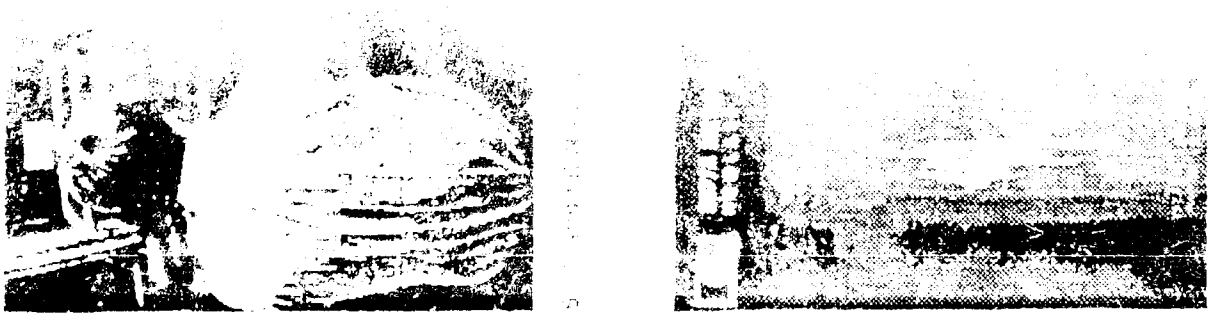

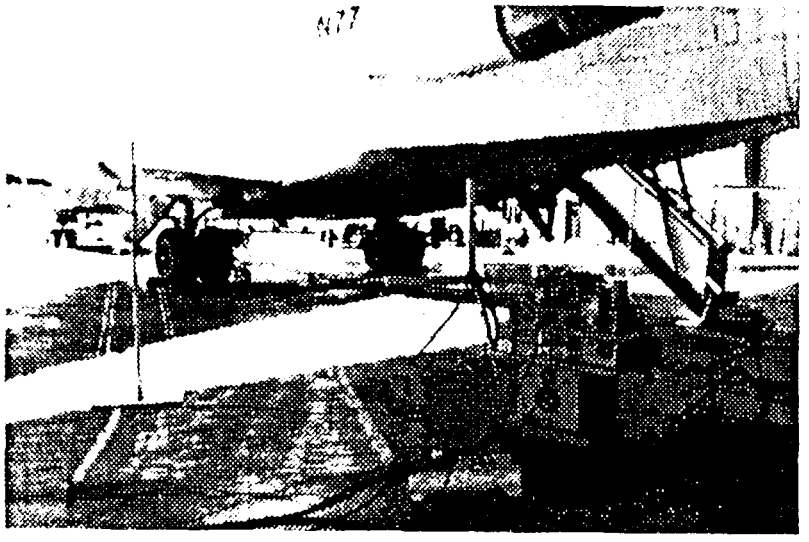

9 Transmit Node at location T1.

1 Rece under wheel well (location

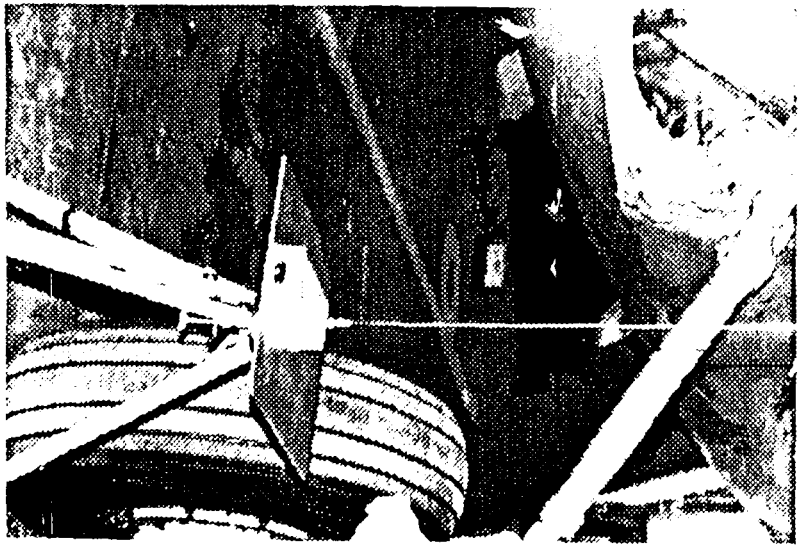

11. Receive dipole antenna near left wheel showing open equipment bay (location R1).

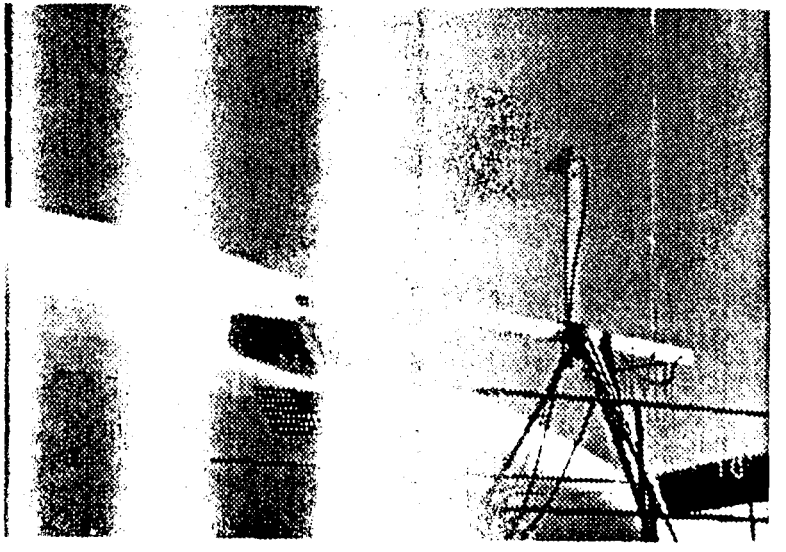

Fra mas bolt (location T7)

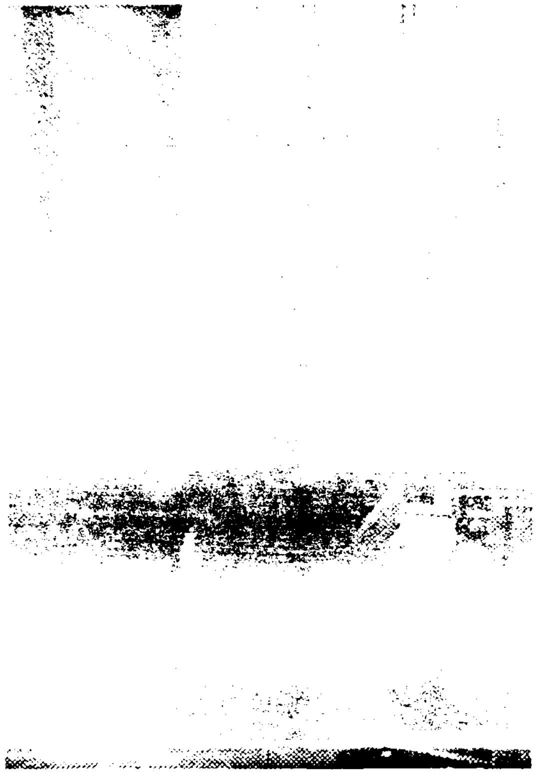

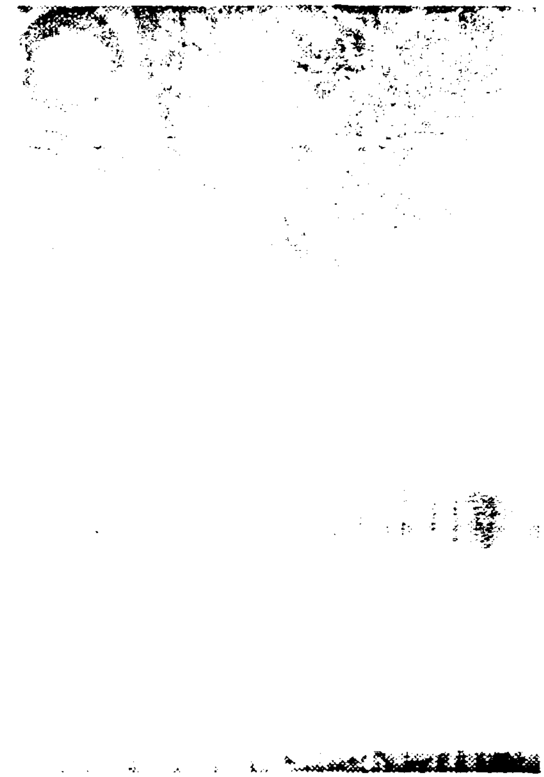

side of

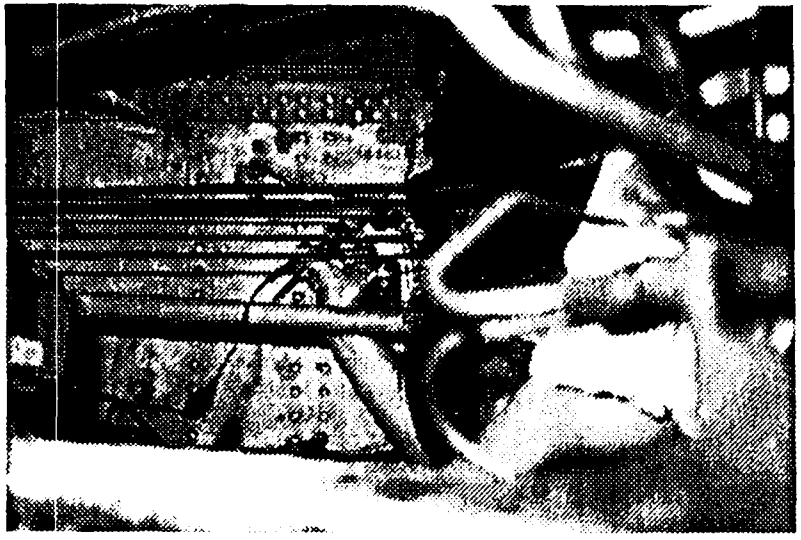

17. Wheel well heat sensor, Test 20

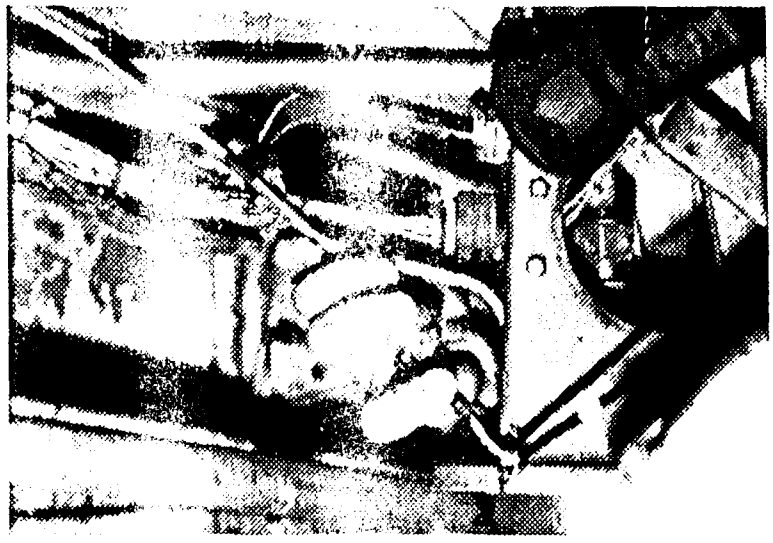

18. Wheel well heat sensor, Test 20

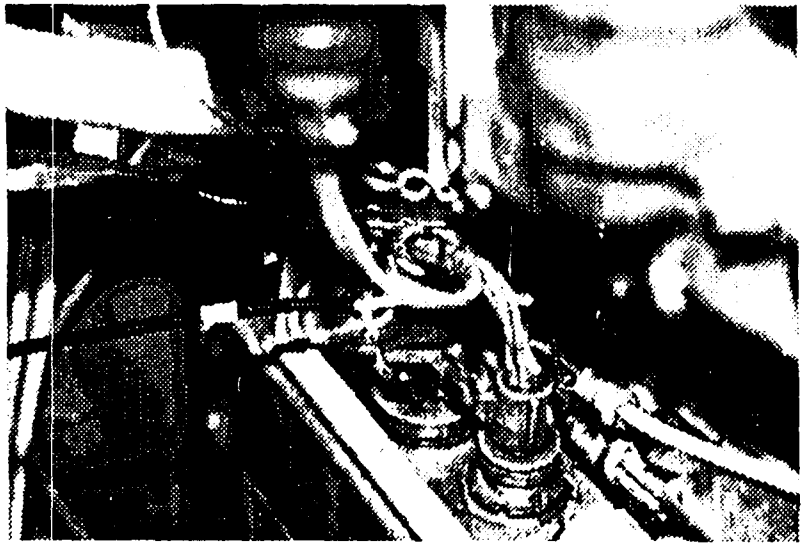

19. APU fire switch in wheel well, Test 5.

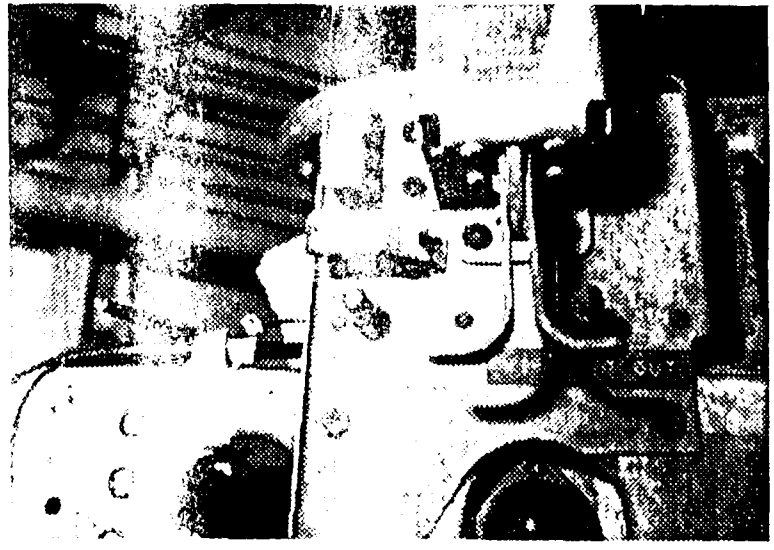

20. APU fire switch with protection, Test 2.

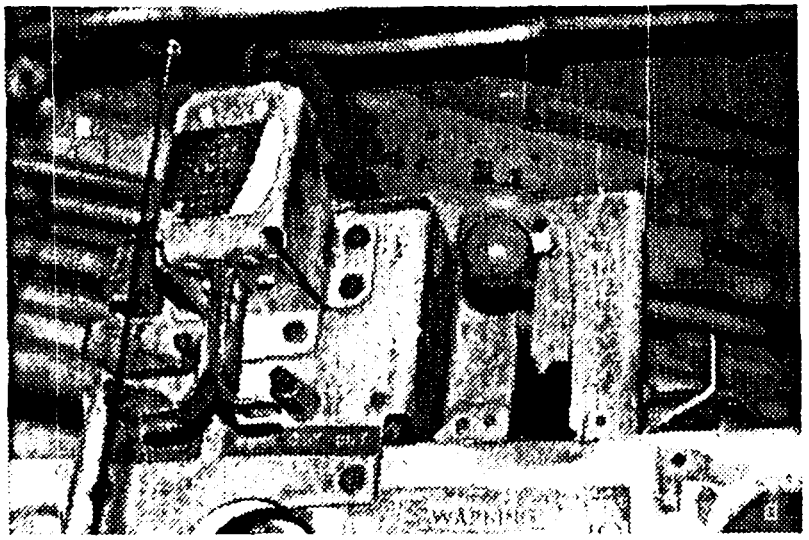

21. APU off switch with antenna, Test 1.

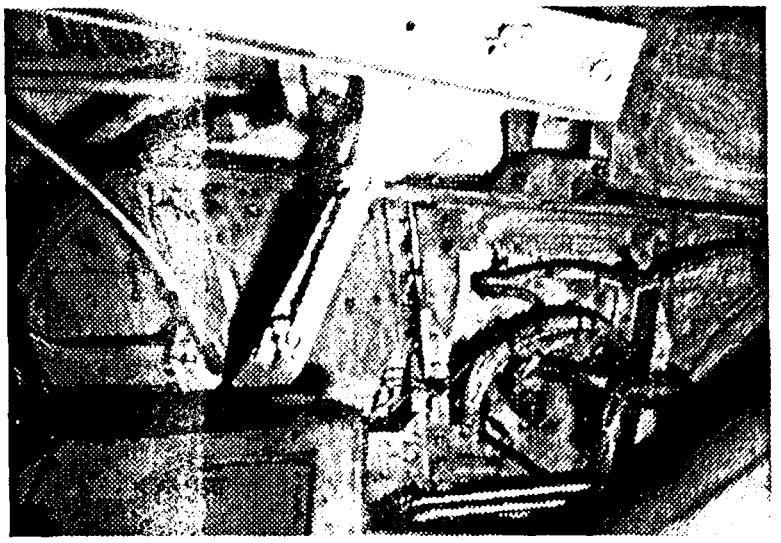

22. Right side of wheel well near APU exhaust door switch.

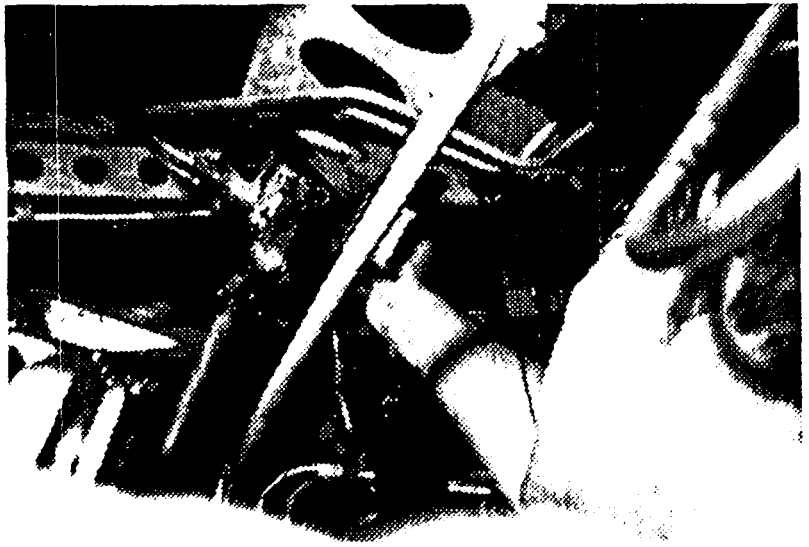

23. APU exhaust door switch under right wing.

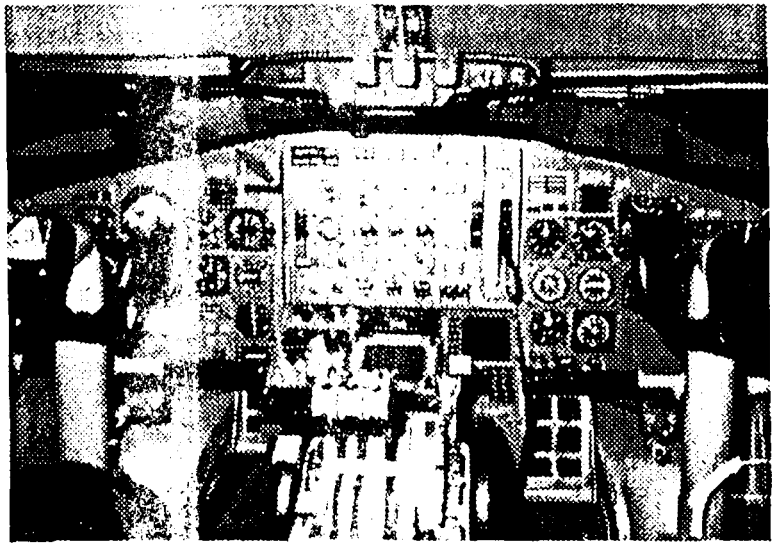

24. View of pilot's instrument panel, showing red-colored engine fire switches at top of photo.

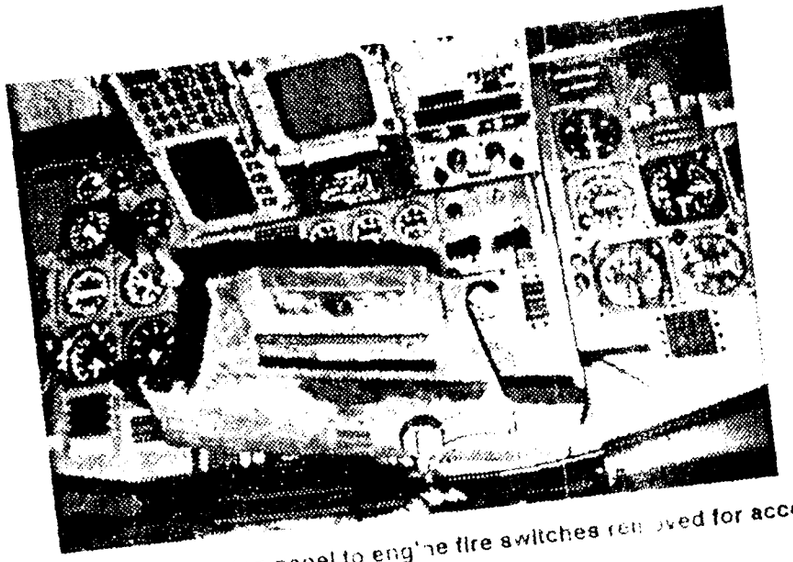

25. View showing panel to engine fire switches removed for access to wiring.

26. Engine [illegible] switch [illegible].

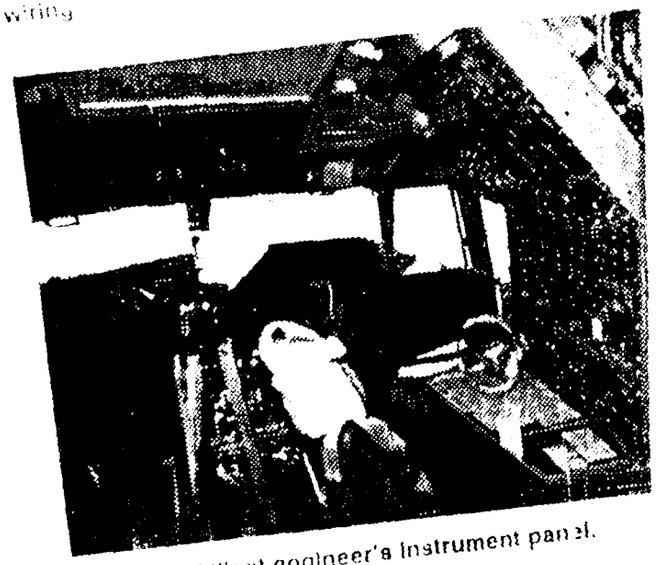

27. View of flight engineer's instrument panel.

[illegible] engineer's panel.

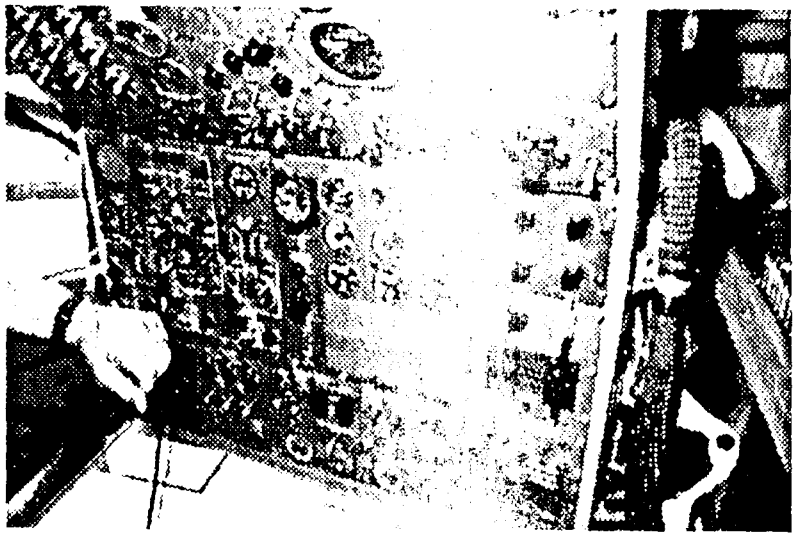

29. Probe measurement of f[illegible]ght engineer's panele

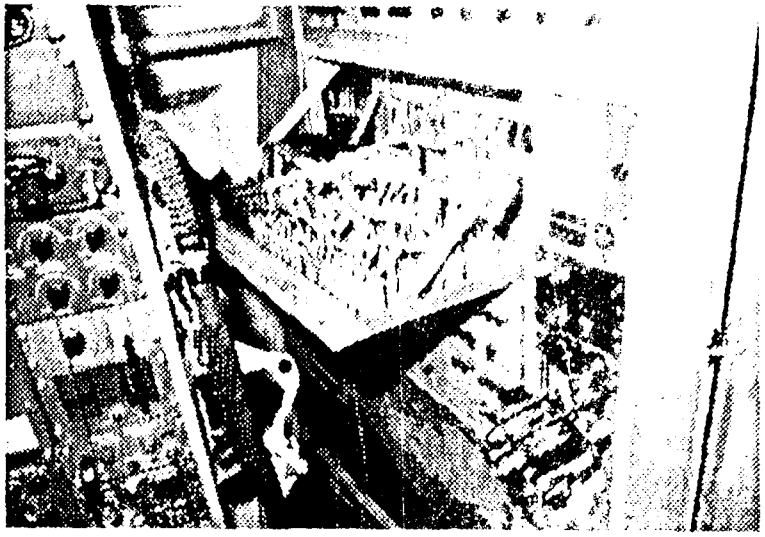

30. Circuit breaker panel in [illegible] tray open.

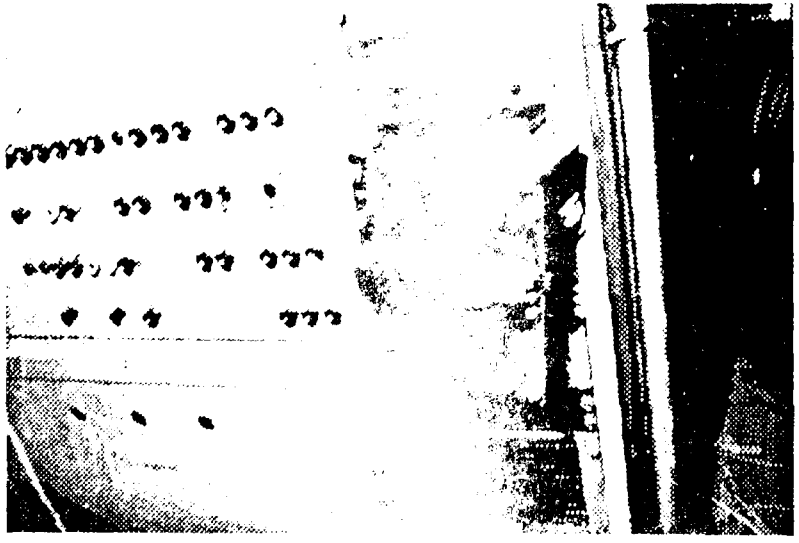

31. APU stop switch in co[illegible]

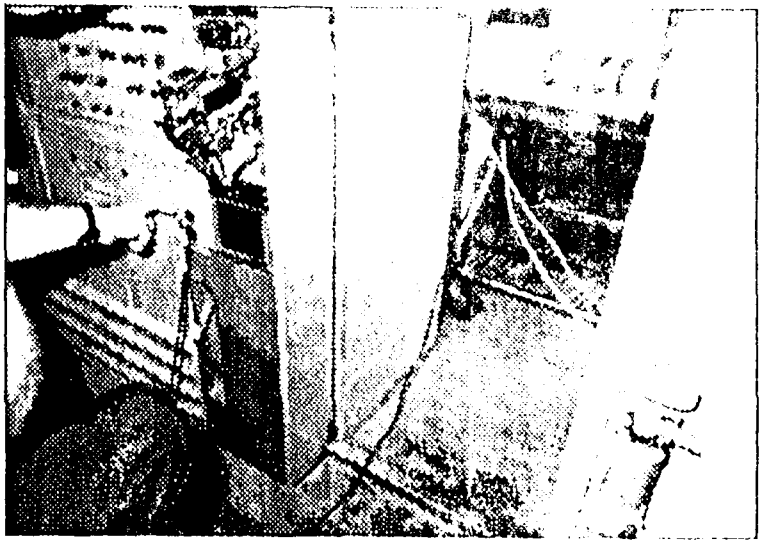

32. DC electrical bus in cockpit.

APPENDIX D
DETAILED DERIVATION OF TRANSFER FACTOR (TF)

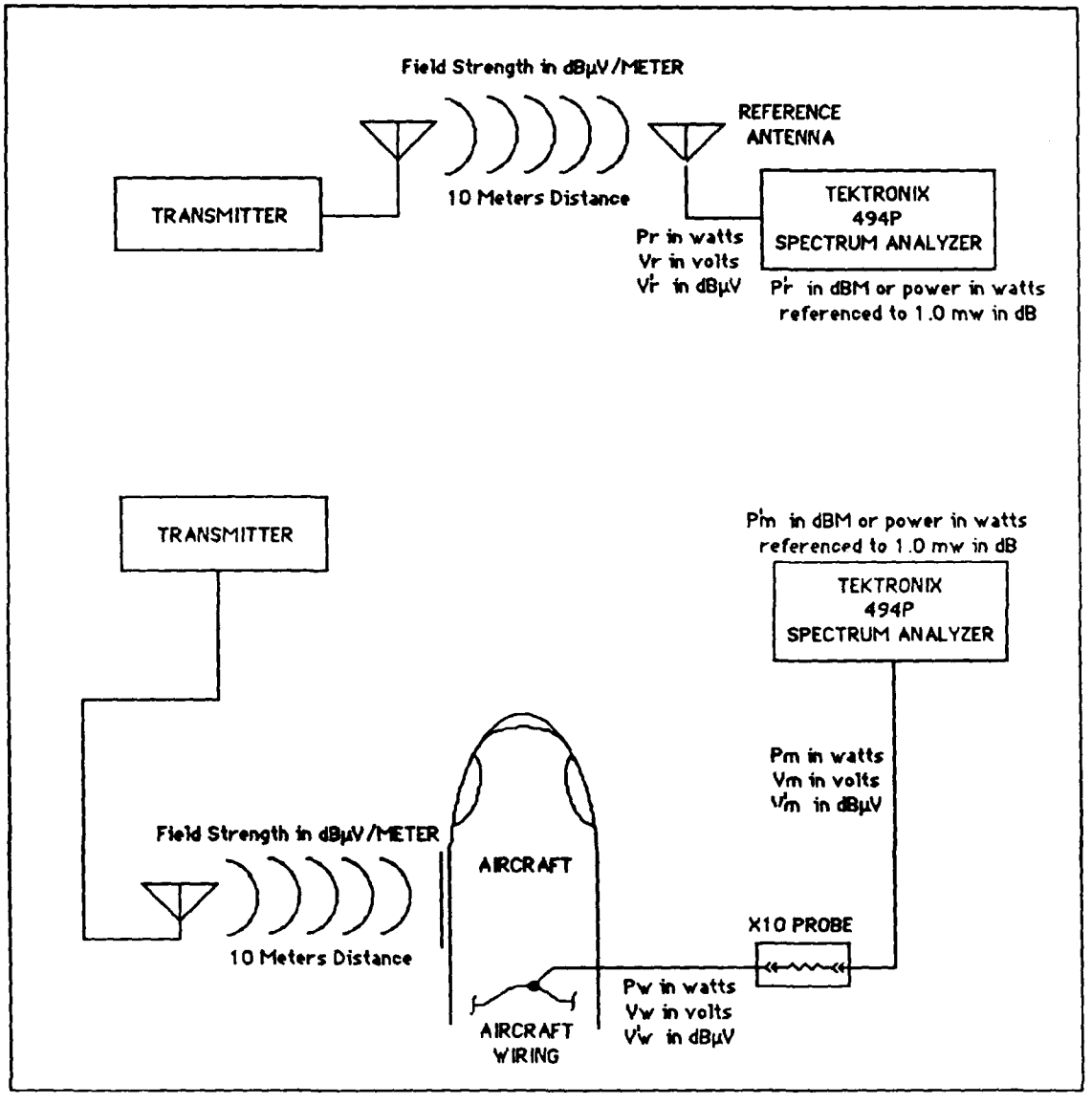

Figure D-1 Detailed Test Setup - Measurement of Induced Voltage on Aircraft Internal Wiring

The two basic equations:

$$dB\mu V_r + AF = dB\mu V/M \qquad (D\text{-}1)$$

$$dB\mu V_w + TF = dB\mu V/M \qquad (D\text{-}2)$$

where:

1. $dB\mu V_r$ is the voltage, at the output of the reference receiving antenna, into a 50 ohm load (Tektronix 494P), in dB referenced to 1.0 μV;

2. AF is the antenna factor in dB (see sample manufacturers data sheet);

3. dBμV/M is the field strength in volts/meter at the receiving antenna, in dB referenced to 1.0 μV;

4. $dB\mu V_w$ is the voltage, induced on aircraft internal wiring, into or measured by a x10 probe (500 ohms), in dB referenced to 1.0 μV;

5. TF is the transfer factor, in dB;

6. dBμV/M is the field strength, in volts/meter, adjacent to the external surface of the aircraft and at the receiving reference antenna, in dB referenced to 1.0 μV.

These two basic equations may be equated since the reference antenna and the external surface of the aircraft are illuminated by equivalent electromagnetic fields:

$$dB\mu V_r + AF = dB\mu V_w + TF \qquad \text{(D-3)}$$

Next, the unknowns, dBμVr and dBμVw, are solved in terms of measured power, in dBM, on the Tektronix 494P screen. For the reference antenna (see figure D-1):

1. Power at the input to the 494P is:

$$P_r = \frac{V_r^2}{50\Omega} \text{ ; Watts} \qquad \text{(D-4)}$$

2. Power as measured on the Tektronix 494P is:

$$P_r' = 10\,\text{Log}_{10}\left(\frac{P_r}{1\text{ mw}}\right) \qquad \text{(D-5)}$$

$$P_r' = 10\,\text{Log}_{10}\left(\frac{V_r^2/50\Omega}{10^{-3}}\right) \qquad \text{(D-6)}$$

Next, solve for Vr' (dBμV):

$$\frac{P_r'}{10} = \text{Log}_{10}\left(\frac{V_r^2}{.05}\right) \qquad \text{(D-7)}$$

$$\left[\frac{P_r'}{10}\right]\text{Log}_{10}[10] = \text{Log}_{10}\left(\frac{V_r^2}{.05}\right) \qquad \text{(D-8)}$$

$$\text{Log}_{10}\left[10^{\frac{P_r'}{10}}\right] = \text{Log}_{10}\left(\frac{V_r^2}{.05}\right) \qquad \text{(D-9)}$$

$$V_r^2 = 0.05\left(10^{\frac{P_r'}{10}}\right) \quad \text{(D-10)}$$

$$V_r^2 = \left(10^{\frac{P_r'}{10}}\right)10^{-1.3} \quad \text{(D-11)}$$

$$V_r^2 = \left(10^{\frac{P_r' - 13}{10}}\right) \quad \text{(D-12)}$$

$$V_r = \left(10^{\frac{P_r' - 13}{20}}\right) \quad \text{(D-13)}$$

Converting V_r to dBμV (V'_r):

$$V_r' = 20\,\text{Log}_{10}\left(\frac{10^{\frac{P_r - 13}{20}}}{10^{-6}}\right) \quad \text{(D-14)}$$

$$V_r' = 20\,\text{Log}_{10}\left(10^{\frac{P_r' + 107}{20}}\right) \quad \text{(D-15)}$$

$$V_r' = \text{Log}_{10}\left(10^{P_r' + 107}\right) \quad \text{(D-16)}$$

$$V_r' = \left(P_r' + 107\right)(\text{dB}\mu\text{V})_r \quad \text{(D-17)}$$

Solving for V_w:

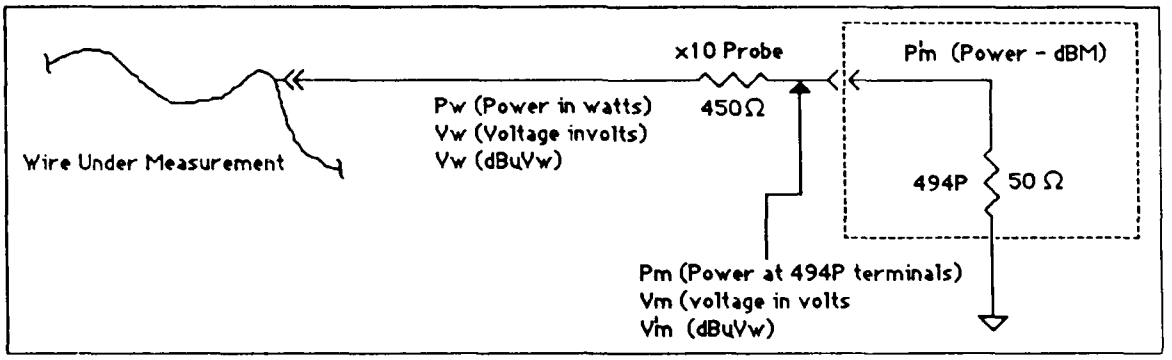

$$V_m = 10^{\frac{P_m' - 13}{20}} \quad \text{(D-18)}$$

$$V_w = 10\,V_m \quad \text{(D-19)}$$

$$\therefore \quad V_w = 10^{\frac{P_m' + 7}{20}} \quad \text{(D-20)}$$

Converting V_w to $dB\mu V_w$ (V'_w):

$$V'_w = 20 \text{ Log}_{10}\left(\frac{10^{\frac{P_m + 7}{20}}}{10^{-6}}\right) \quad \text{(D-21)}$$

$$V'_w = 20 \text{ Log}_{10}\left(10^{\frac{P_m + 127}{20}}\right) \quad \text{(D-22)}$$

$$V'_w = (P'_m + 127)\ (dB\mu V)_w \quad \text{(D-23)}$$

From the initial equations:

$$TF = dB\mu V_r + AF - dB\mu V_w \quad \text{(D-24)}$$

$$TF = V'_r + AF - V'_w \quad \text{(D-25)}$$

$$TF = P'_r + 107 + AF - (P'_m + 127) \quad \text{(D-26)}$$

$$TF = P'_r - P'_m + AF - 20 \quad \text{(D-27)}$$

Figure D-2 shows a typical manufacturer antenna factor chart.

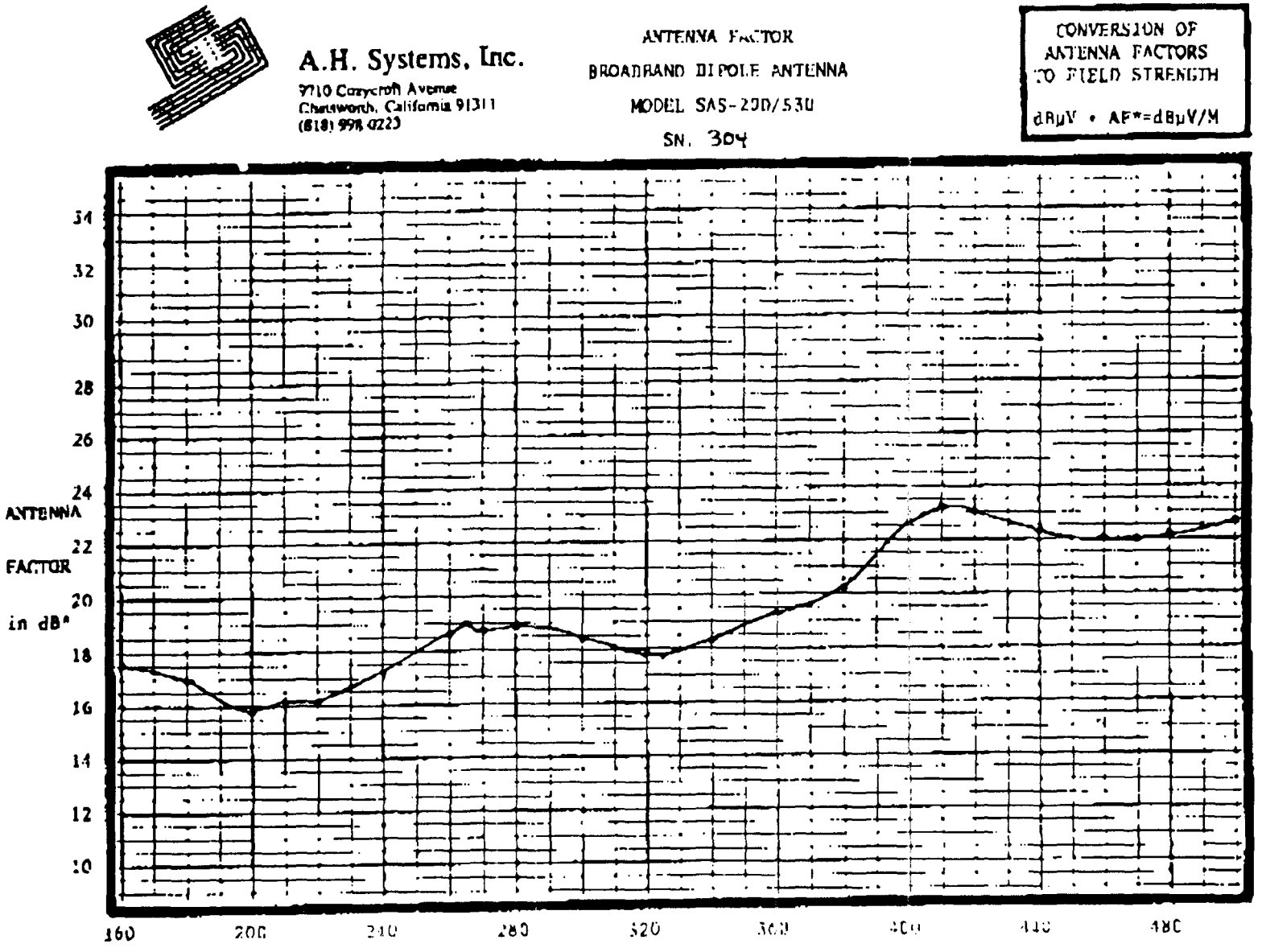

Figure D-2 Typical Antenna Factor Chart

APPENDIX E
TEST DATA

Air-To-Wire Data Reduction

The derivation of the air-to-wire transfer factor, X_{tf}, was addressed in the main body of the report (see Section 7). In brief, it was demonstrated that the transfer factor could be expressed as:

$$X_{tf}(dB) = \text{Reference data(dB)} - \text{Probe data(dB)} + \text{Antenna Factor(dB)} + \text{Constant} - 10^{*}\,\text{Log}\left[\frac{450 + \text{Imped}}{500 + \text{Imped}}\right]$$

For practical applications, the last two terms of the correlation may be replaced with a constant value of -20:

$$X_{tf}(dB) = \text{Reference data(dB)} - \text{Probe data(dB)} + \text{Antenna Factor(dB)} - 20$$

The probe and reference data were gathered with a programmable Tektronix 494P Spectrum Analyzer. The evaluation of the transfer factor for any given test configuration requires not only probe and reference data, but the incorporation of antenna factors and the impedance of the wire under investigation (as-well-as a constant, -13). Figure E-1 illustrates the implementation of the various data required to calculate X_{tf}. Figure E-2 shows the frequency dependance of the antenna factors over the entire frequency spectrum employed in the field tests.

Table E-1 lists the associated data files for each air-to-wire test. The probe and reference data for a given test each consist of two data files per frequency band (*.WAV, and .*.WBV). The *.WAV files contain the raw probe and reference data gathered with the Tektronix 494P Spectrum Analyzer. Before the data were used in the calculation of X_{tf}, it was necessary to convert the data to engineering units, and frequency stamp each data item, using the test parameter information contained in the *.WBV files.

The network analyzer data are contained in three files for each test (*.WAV, *,WDV, *.WBV). The *.WAV and *.WDV files contain the frequency dependent real and imaginary impedances of the test wire. The *.WAV and *.WDV files were used in conjunction with the test parameter information contained in the *.WBV file to determine the total impedance of the wire (wire impedance is required for evaluating the transfer factor) and to frequency stamp each data item. Figures E-4 through E-23 present the complete set of available air-to-wire data.

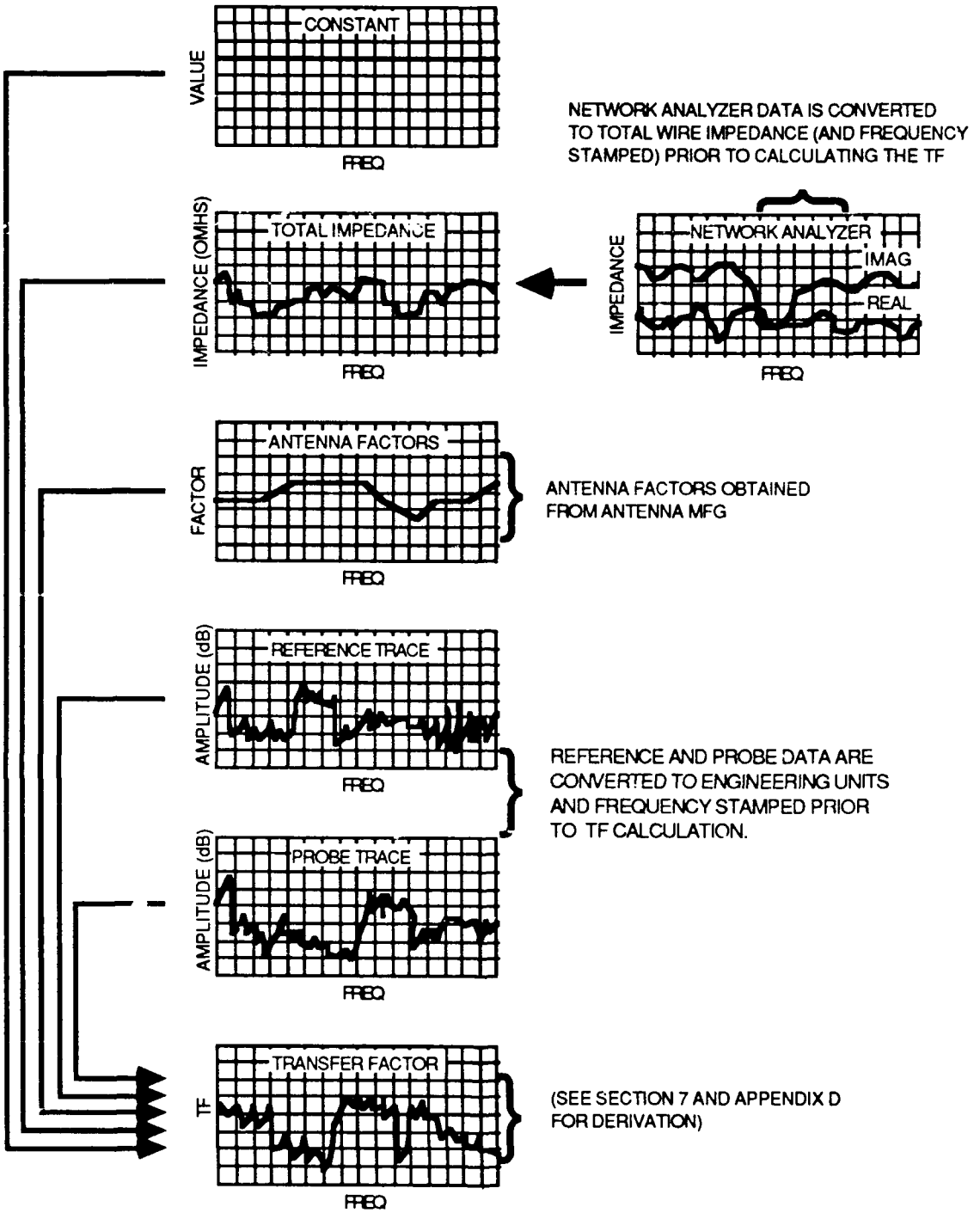

Figure E-1 Air - to - Wire Transfer Factor Calculation Sequence

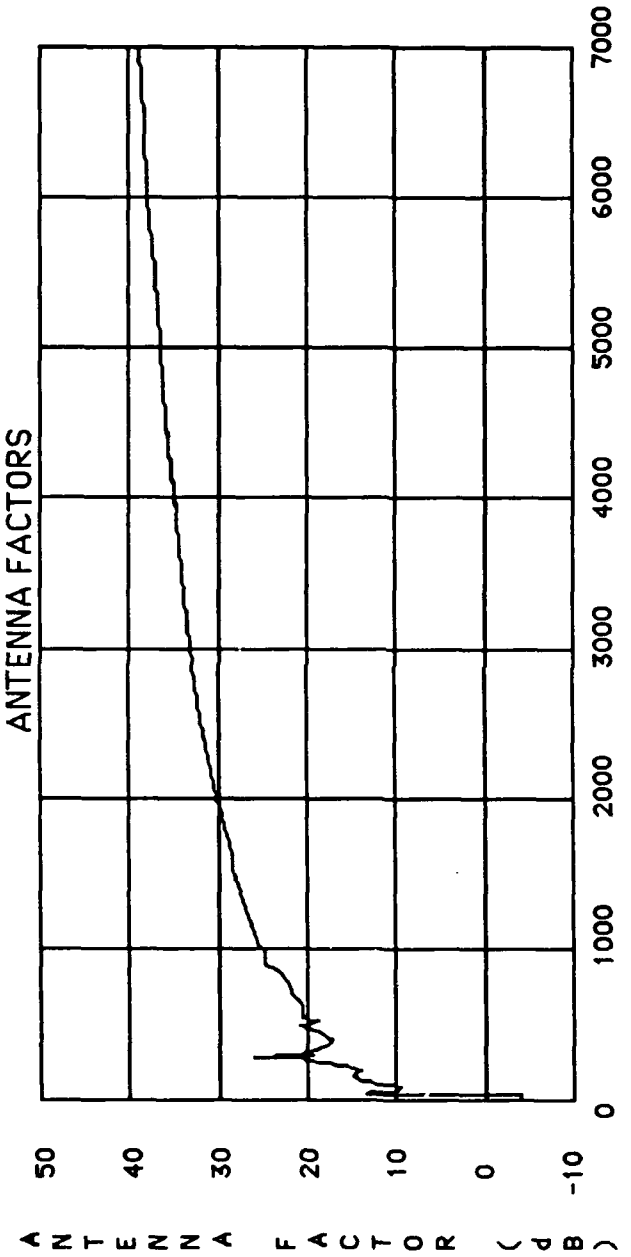

Figure E-2 Antenna Factors vs. Frequency

Table E-1
AIR-TO-WIRE DATA FILES

PROBE DATA FILE	REFERENCE DATA FILE	NETWORK ANALYZER DATA FILE	BAND ID*	PROBE LOCATION	TRANS. LOCATION
002_S_A.WAV/WBV	R01_S_A	N02B_N_A.WAV/WDV	-,A,B,C,D E,F,G,H I,J,K,L M,N,O	APU STOP SW BACK OF SW NC=2 WIRE #5457 CONN #5515 (R1)	T1
002B_S_A.WAV/WBV	R01_S_A	N/A	-,B,E,H,O	SAME AS ABOVE WITH PROBE OFF (R1)	T1
013_S_A.WAV/WBV	R01_S_A	N03B_N_F.WAV/WDV	A,B,C,D E,G,H,P	SQUAT SWITCH IN WHEEL WELL D262/B (R1)	T1
017_S_A.WAV/WBV	R01_S_A	N03B_N_H.WAV/WDV	A,B	LEFT ENGINE HEAT SENSOR #1 (R1)	T1
022_S_A.WAV/WBV	R01_S_A	N03B_N_I.WAV/WDV	A,B,C,D E,G,H,P	APU FUEL SHUT-OFF VALVE (R1)	T1
024A_S_A.WAV/WBV	R01_S_A	N03B_N_J.WAV/WDV	A,B,C,D E,G,H,P	APU FUEL SHUT-OFF VALVE (R1)	T1
093_S_A.WAV/WBV	R01_S_C	N04B_N_A.WAV/WDV	A,B,C,D E,G,H,P	ENG. EXC. BOX IN D.C. PIN B (R8)	T4

Table E-1 (continued)
AIR-TO-WIRE DATA FILES

PROBE DATA FILE	REFERENCE DATA FILE	NETWORK ANALYZER DATA FILE	BAND ID*	PROBE LOCATION	TRANS. LOCATION
093A_S_A.WAV/WBV	R01_S_C	N04B_N_B.WAV/WDV	A,B,C,D E,G,H,P	ENG. EXC. BOX IN 400Hz PIN C (R8)	T4
094_S_A.WAV/WBV	R01_S_C	N04B_N_D.WAV/WDV	A,B,C,D E,G,H,P	ENG. EXC. BOX OUT (R8)	T4
095_S_A.WAV/WBV	R01_S_C	N04B_N_C.WAV/WDV	A,B,C,D E,G,H,P	ENGINE HEAT SENSOR, PIN A (R8)	T4
095A_S_A.WAV/WBV	R01_S_C	N04B_N_E.WAV/WDV	A,B,C,D E,G,H,P	ENGINE AIR VALVE (R8)	T4
126_S_A.WAV/WBV	R01_S_B	N02B_N_E.WAV/WDV	A,B,C,D E,G,H,P	COCKPIT FIRE LIGHT (R5)	T7
128_S_A.WAV/WBV	R01_S_B	N02B_N_C.WAV/WDV	A,B,C,D E,G,H,P	COCKPIT FUEL IND. (R5)	T7
132_S_A.WAV/WBV	R01_S_B	N02B_N_D.WAV/WDV	A,B,C,D E,G,H,P	400Hz BUS (R5)	T7
133_S_A.WAV/WBV	R01_S_B	N02B_N_E.WAV/WDV	A,B,C,D E,G,H,P	D.C. BUS (R5)	T7

Table E-1 (continued)
AIR-TO-WIRE DATA FILES

PROBE DATA FILE	REFERENCE DATA FILE	NETWORK ANALYZER DATA FILE	BAND ID*	PROBE LOCATION	TRANS LOCATION
138_S_A.WAV/WBV	R01_S_B	N02B_N_A.WAV/WDV	A,B,C,D E,G,H,P	APU OFF SWITCH (R5)	T7
138B_S_A.WAV/WBV	R01_S_B	N/A	A,B,C,D E,G,H,P	SAME AS ABOVE PROBE OFF (R5)	T7
144_S_A.WAV/WBV	R01_S_C	N02B_N_A.WAV/WDV	A,B,C,D E,G,H,P	APU OFF SWITCH (R5)	T1
145_S_A.WAV/WBV	R01_S_C	N02B_N_C.WAV/WDV	A,B,C,D E,G,H,P	FUEL INDICATOR (R5)	T1
147_S_A.WAV/WBV	R01_S_C	N02B_N_D.WAV/WDV	A,B,C,D E,G,H,P	400Hz BUS (R5)	T1

Frequency Band	Frequency Range	Antenna Description	Antenna Number
-	1 - 35 MHz	HF Monopole	1
A	1 - 35 MHz	HF Loop	2
B	20 - 300 MHz	Biconical	3
C	200 - 600 MHz	Log Periodic No.1	4
D	600 - 1.0 GHz	Log Periodic No.1	4
E	1 - 1.5 GHz	Log Periodic No.2	5
F	1.2 - 1.8 GHz	Log Periodic No.2	5
G	1.5 - 2.0 GHz	Log Periodic No.2	5
H	2.0 - 2.5 GHz	Log Periodic No.2	5
I	2.5 - 3.0 GHz	Log Periodic No.2	5
J	3.0 - 3.5 GHz	Log Periodic No.2	5
K	3.5 - 4.0 GHz	Log Periodic No.2	5
L	4.0 - 4.5 GHz	Log Periodic No.2	5
M	4.5 - 5.0 GHz	Log Periodic No.2	5
N	5.0 - 5.5 GHz	Log Periodic No.2	5
O	5.5 - 6.0 GHz	Log Periodic No.2	5
P	6.0 - 6.5 GHz	Log Periodic No.2	5
Q	6.5 - 7.0 GHz	Log Periodic No.2	5
R	7.0 - 7.5 GHz	Log Periodic No.2	5
S	7.5 - 8.0 GHz	Log Periodic No.2	5

Air-To-Air Data Reduction

The air-to-air data are used to evaluate the path-losses associated with RF penetration of various aircraft components. By definition, the path-loss is calculated as:

Path-loss(dB) = Antenna data(dB) - Reference data(dB)

Table E-2 lists the associated data files for each air-to-air test. As with the air-to-wire data, the results of each air-to-air test (antenna data and reference data) are stored in two data files for each frequency band investigated, a *.WAV file for raw data and a *.WBV file which contains test parameter information. Figure E-3 portrays graphically the utilization of the antenna and reference data for calculating path-loss. Figures E-24 through E-32 represent the complete set of available air-to-air data

Copies of the air-to-wire and air to air data files are available on IBM (3.5" or 5.25") or Macintosh formatted diskettes upon written request to:

SCIENTECH, Inc.
Dept. 2003
P.O. Box 1406
Idaho Falls, ID 83403-1406

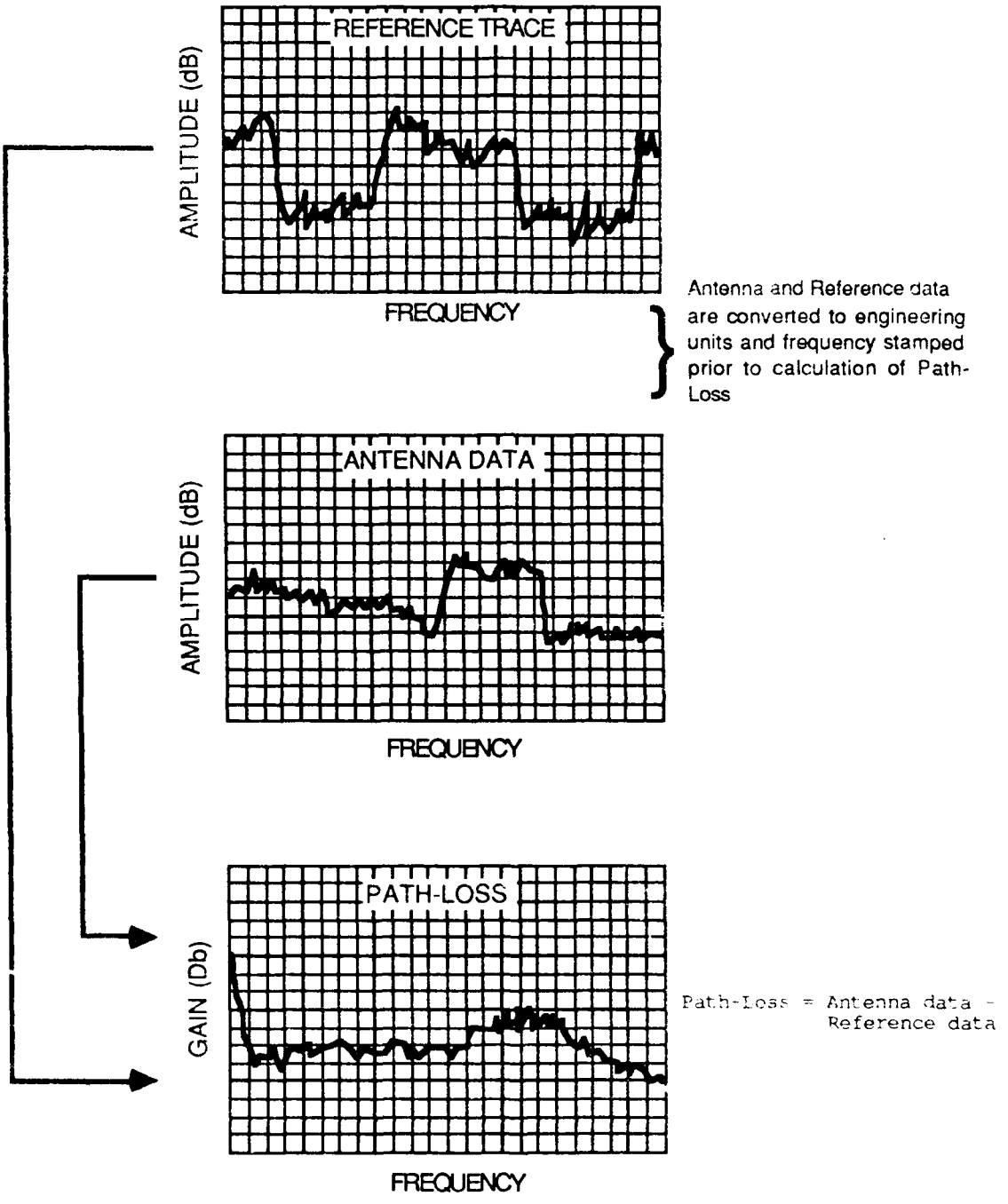

Figure E-3 Air - to - Air Path-Loss Calculation Sequence

Table E-2
AIR-TO-AIR DATA FILES

PROBE DATA FILE	REFERENCE DATA FILE	PROBE LOCATION	TRANS. LOCATION	BAND ID*
001_S_A.WAV/WBV	R01_S_A	UNDER LEFT WHEEL WELL (R1)	UNDER LEFT ENGINE (T1)	A,B,C,D E,F,G,H I,J,K,L M,N,O,P Q,R,S
092_S_A.WAV/WBV	R01_S_A	UNDER LEFT ENGINE (R8)	UNDER LEFT ELEVATOR FACING ENGINE (T8)	A,B,C,D E,G,H,P
102_S_A.WAV/WBV	R01_S_B	COCKPIT (R5)	RIGHT SIDE OF COCKPIT (T7)	A,B,C,D E,G,H
142_S_A.WAV/WBV	R01_S_B	TOURIST CLASS SEATING AREA (R7)	RIGHT SIDE OF COCKPIT (T7)	A,B,C,D E,G,H,P
143_S_A.WAV/WBV	R01_S_C	COCKPIT (R5)	UNDER LEFT ENGINE (T1)	A,B,C,D E,G,H,P
149_S_A.WAV/WBV	R01_S_B	FIRST CLASS SEATING AREA (R6)	UNDER LEFT ENGINE (T1)	A,B,C,H
150_S_A.WAV/WBV	R01_S_B	EQIPMENT BAY (R4)	UNDER LEFT ENGINE (T1)	A,B,C,H

Table E-2
AIR-TO-AIR DATA FILES (continued)

PROBE DATA FILE	REFERENCE DATA FILE	PROBE LOCATION	TRANS. LOCATION	BAND ID*
151_S_A.WAV/WBV	R01_S_C	TOURIST CLASS SEATING AREA (R7)	UNDER LEFT ENGINE (T1)	A,B,C,D E,G,H,P
152_S_A.WAV/WBV	R01_S_A	UNDER LEFT WHEEL WELL (R1)	UNDER LEFT ENGINE (T1)	A,B,C,D E,G,H,P

Frequency Band	Frequency Range	Antenna Description	Antenna Number
-	1 - 35 MHz	HF Monopole	1
A	1 - 35 MHz	HF Loop	2
B	20 - 300 MHz	Biconical	3
C	200 - 600 MHz	Log Periodic No.1	4
D	600 - 1.0 GHz	Log Periodic No.1	4
E	1 - 1.5 GHz	Log Periodic No.2	5
F	1.2 - 1.8 GHz	Log Periodic No.2	5
G	1.5 - 2.0 GHz	Log Periodic No.2	5
H	2.0 - 2.5 GHz	Log Periodic No.2	5
I	2.5 - 3.0 GHz	Log Periodic No.2	5
J	3.0 - 3.5 GHz	Log Periodic No.2	5
K	3.5 - 4.0 GHz	Log Periodic No.2	5
L	4.0 - 4.5 GHz	Log Periodic No.2	5
M	4.5 - 5.0 GHz	Log Periodic No.2	5
N	5.0 - 5.5 GHz	Log Periodic No.2	5
O	5.5 - 6.0 GHz	Log Periodic No.2	5
P	6.0 - 6.5 GHz	Log Periodic No.2	5
Q	6.5 - 7.0 GHz	Log Periodic No.2	5
R	7.0 - 7.5 GHz	Log Periodic No.2	5
S	7.5 - 8.0 GHz	Log Periodic No.2	5

AIR-TO-WIRE DATA

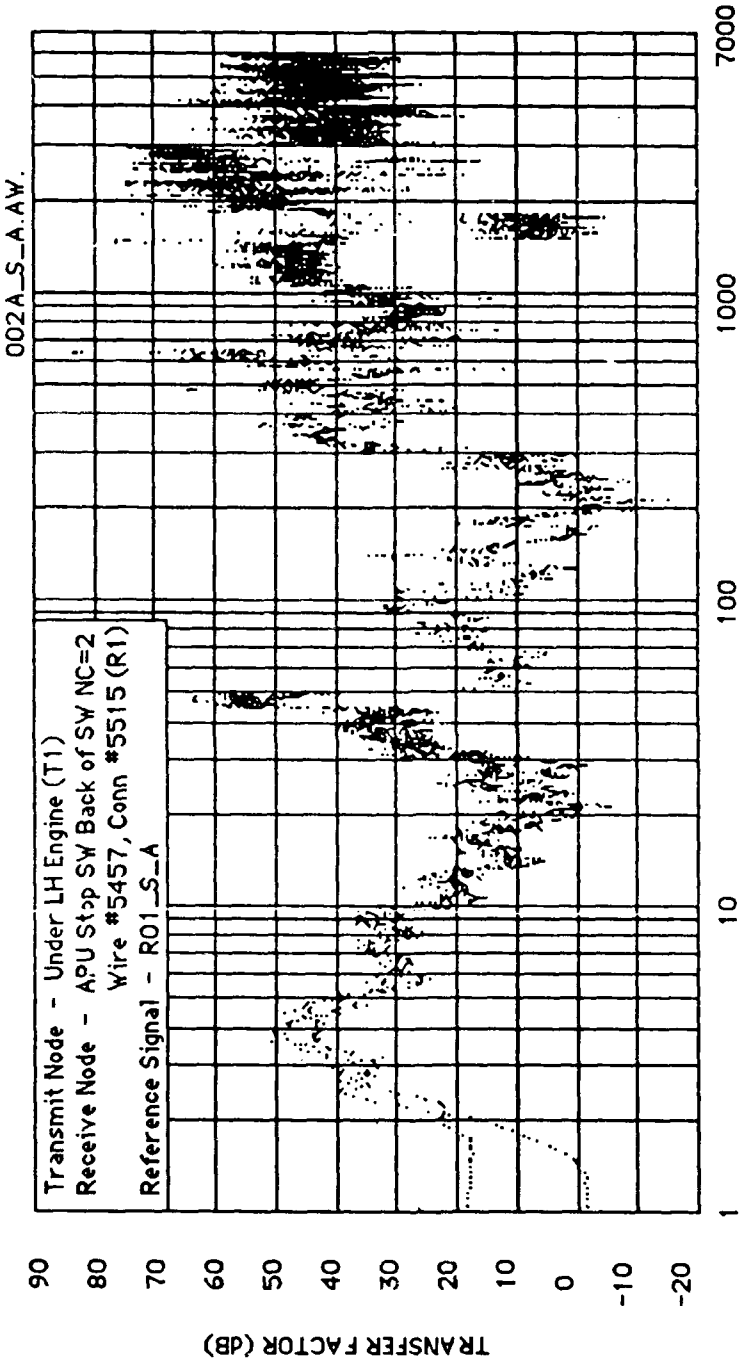

Figure E-4 Probe Transfer Factor (Test 002A)

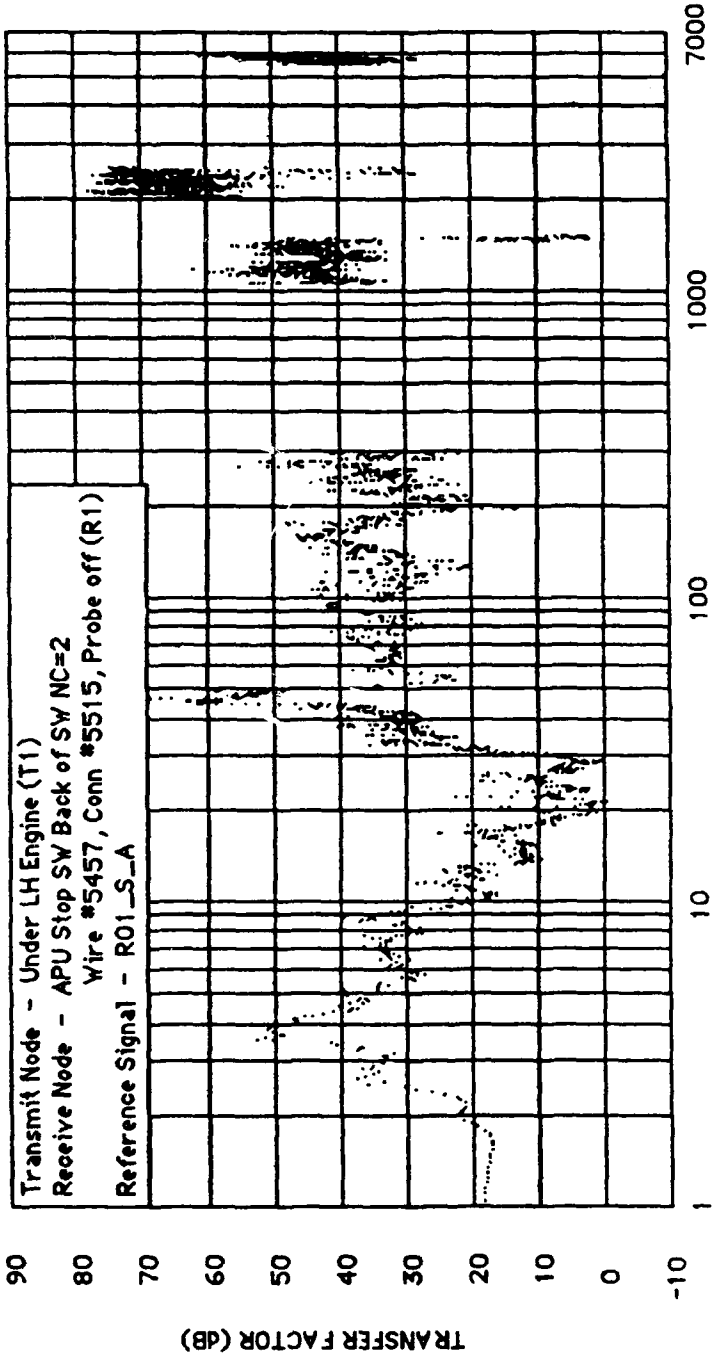

Figure E-5 Probe Transfer Factor (Test 002B)

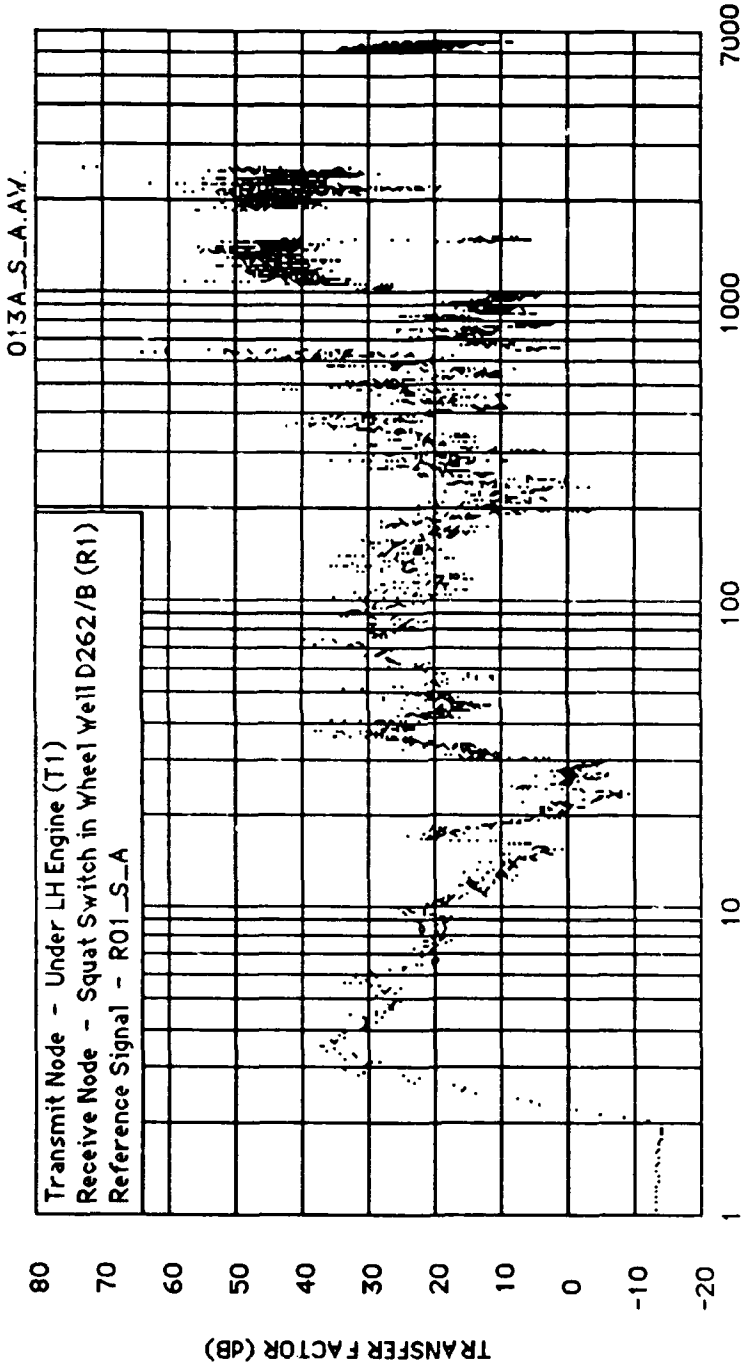

Figure E-6 Probe Transfer Factor (Test 013A)

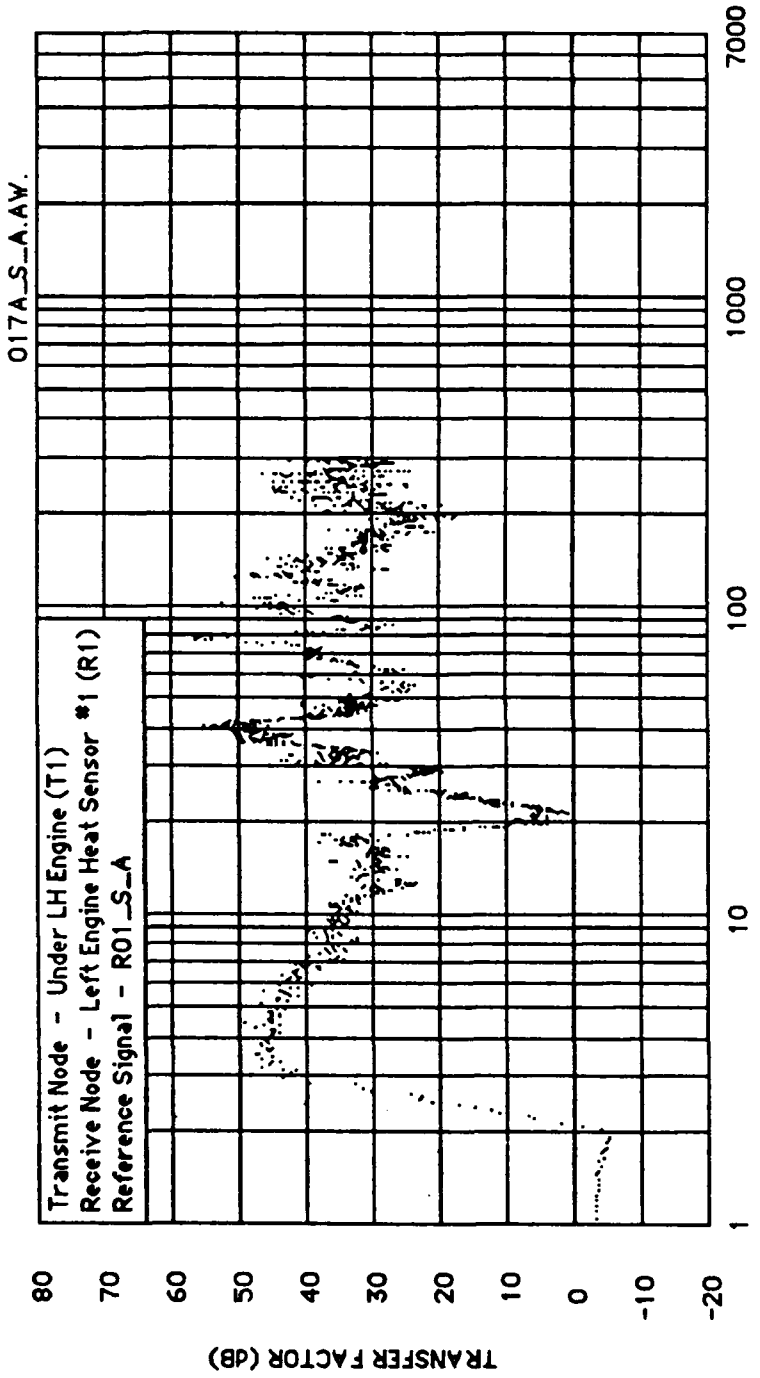

Figure E-7 Probe Transfer Factor (Test 017A)

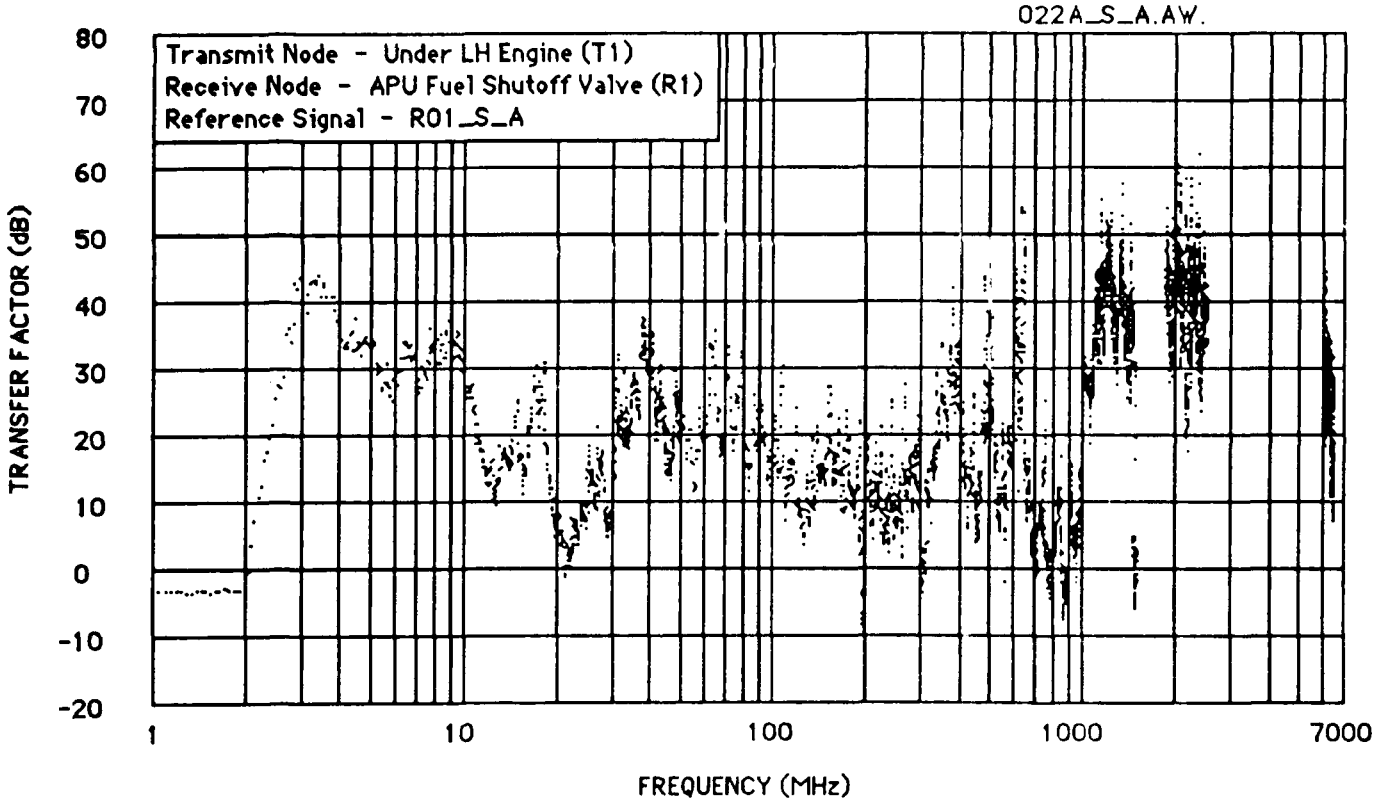

Figure E-8 Probe Transfer Factor (Test 022A)

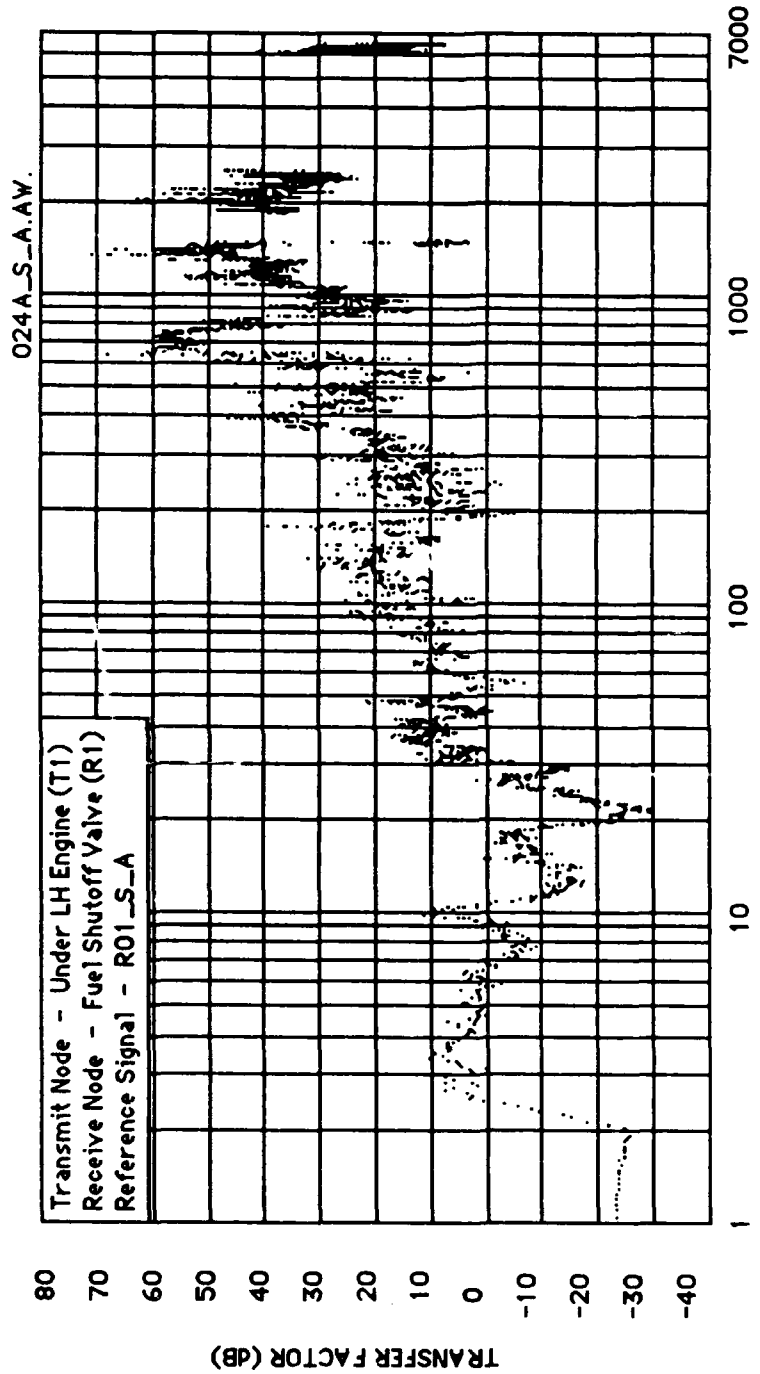

Figure E-9 Probe Transfer Factor (Test 024A)

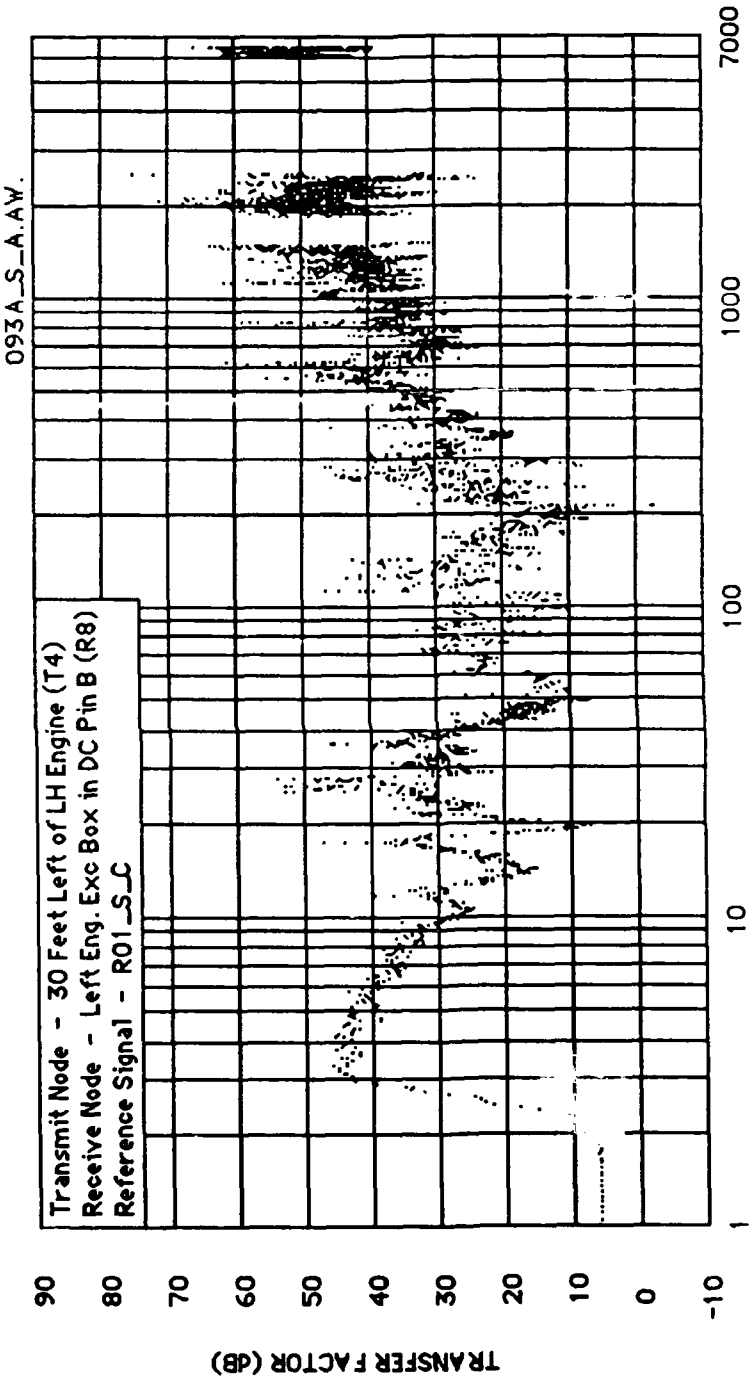

Figure E-10 Probe Transfer Factor (Test 093A)

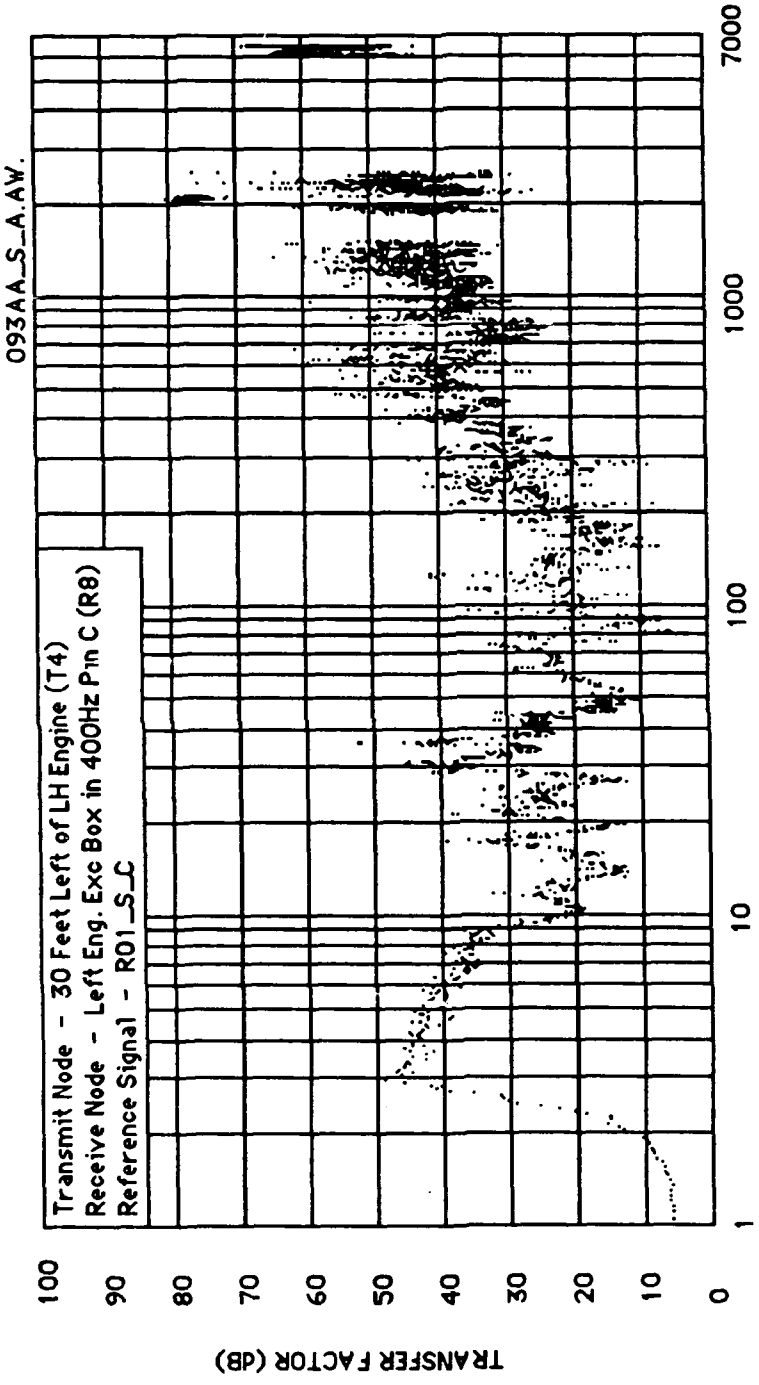

Figure E-11 Probe Transfer Factor (Test 093AA)

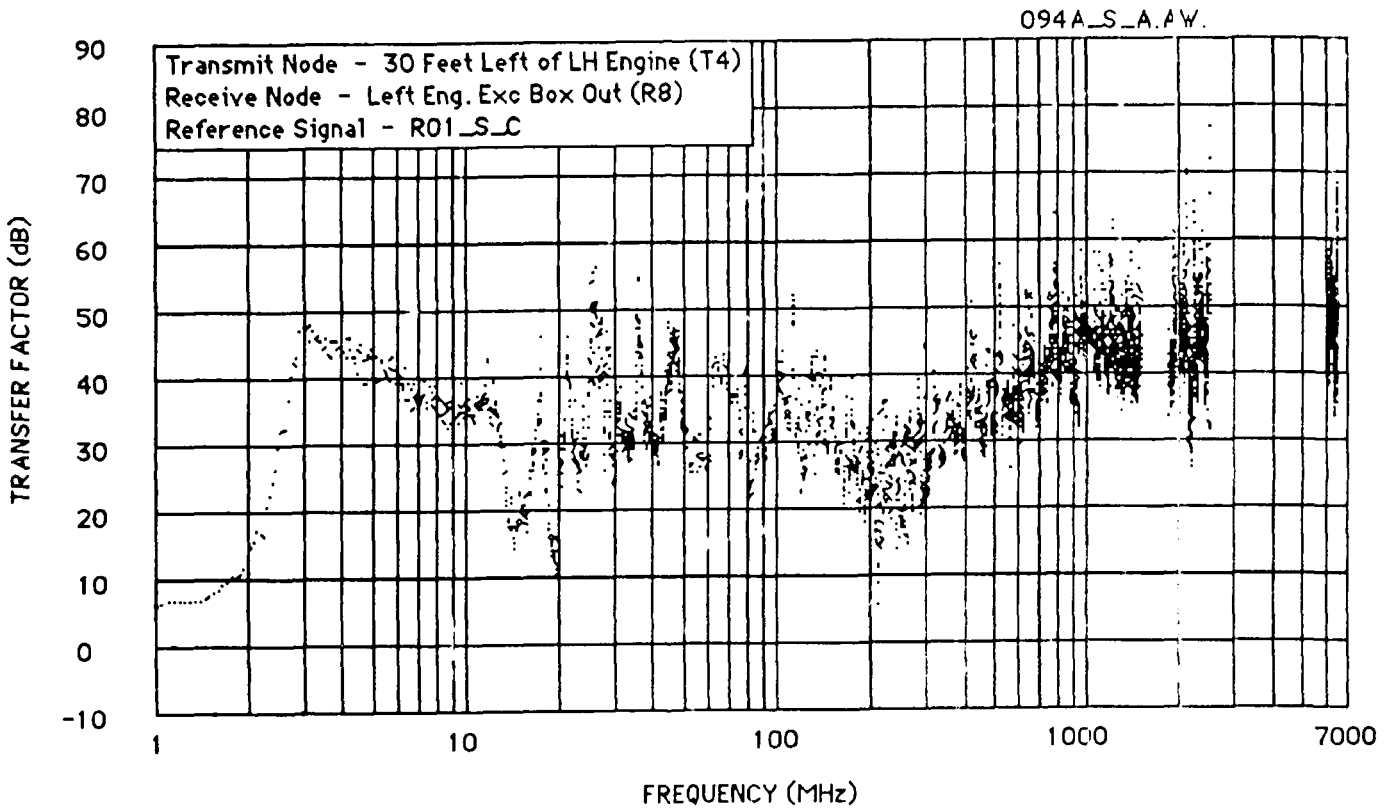

Figure E-12 Probe Transfer Factor (Test 094A)

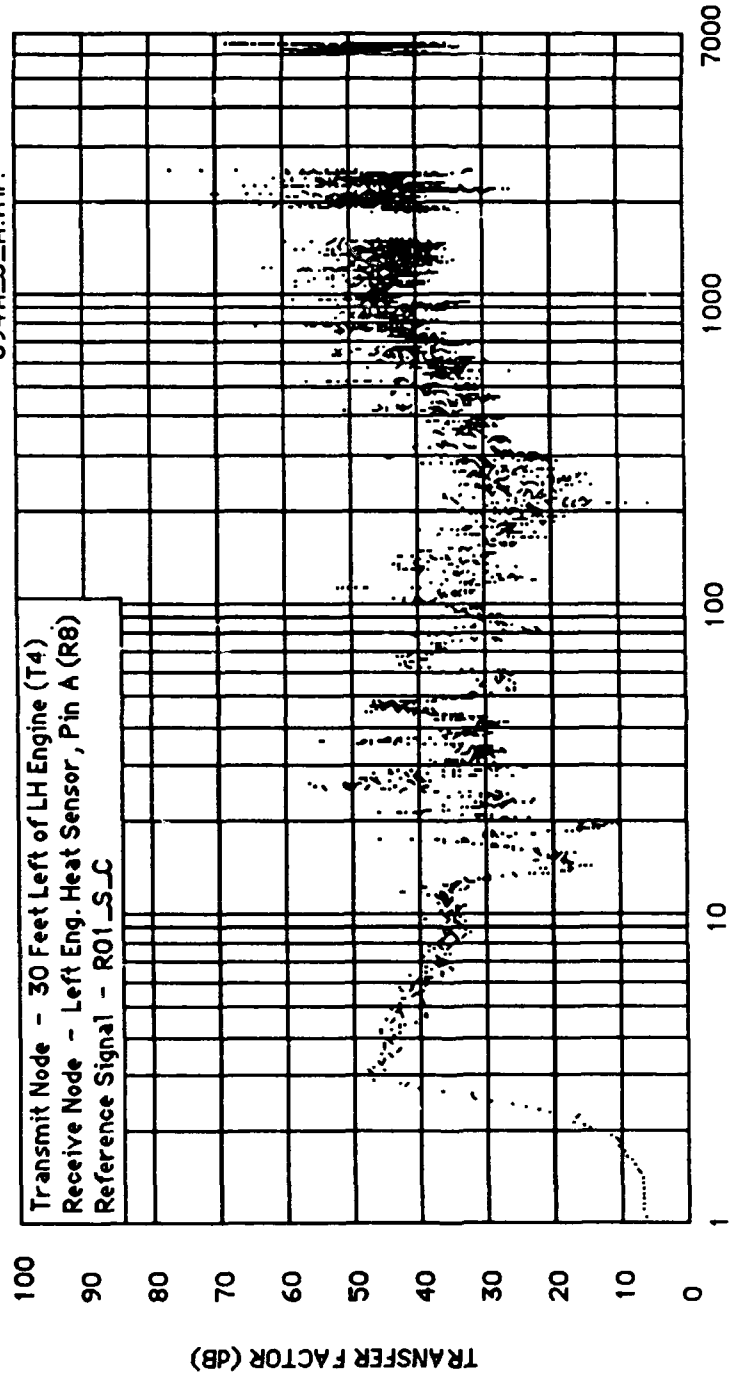

Figure E-13 Probe Transfer Factor (Test 095A)

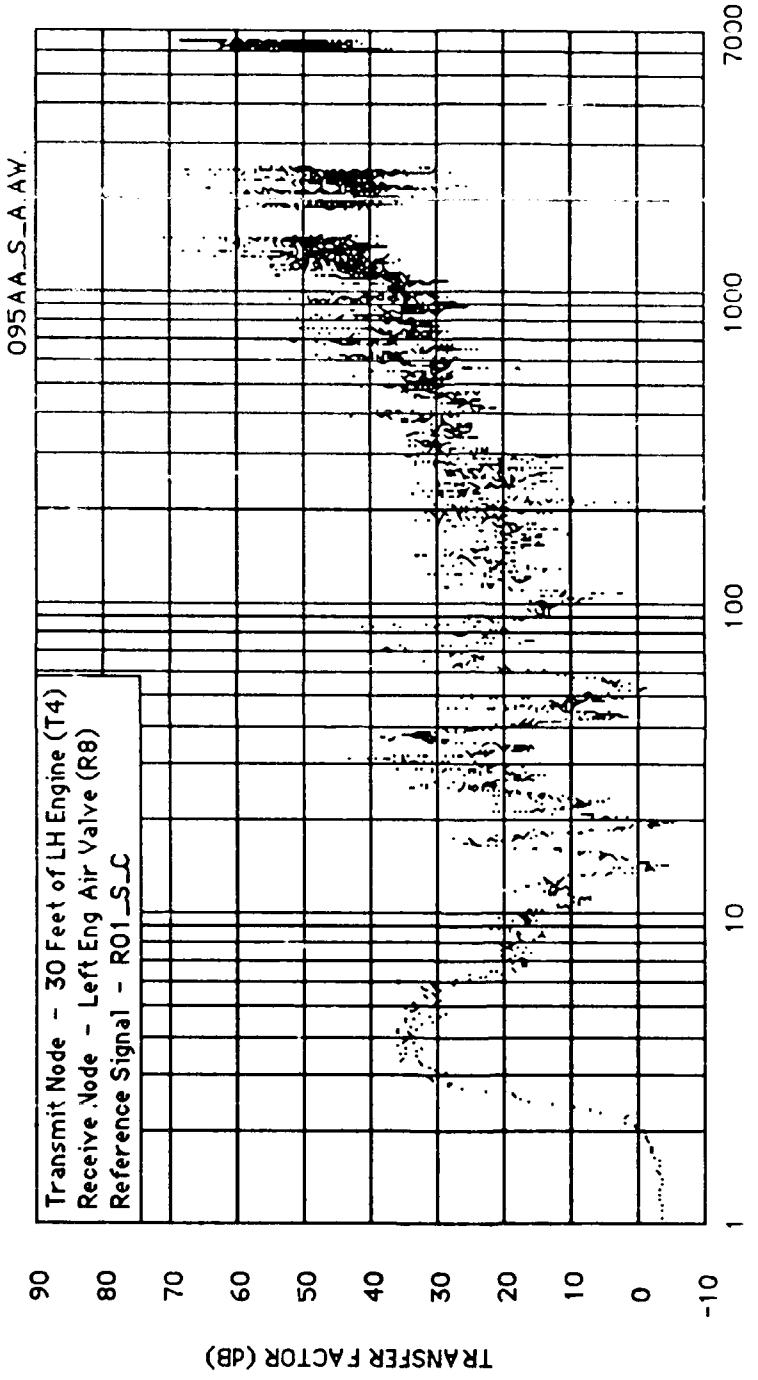

Figure E-14 Probe Transfer Factor (Test 095AA)

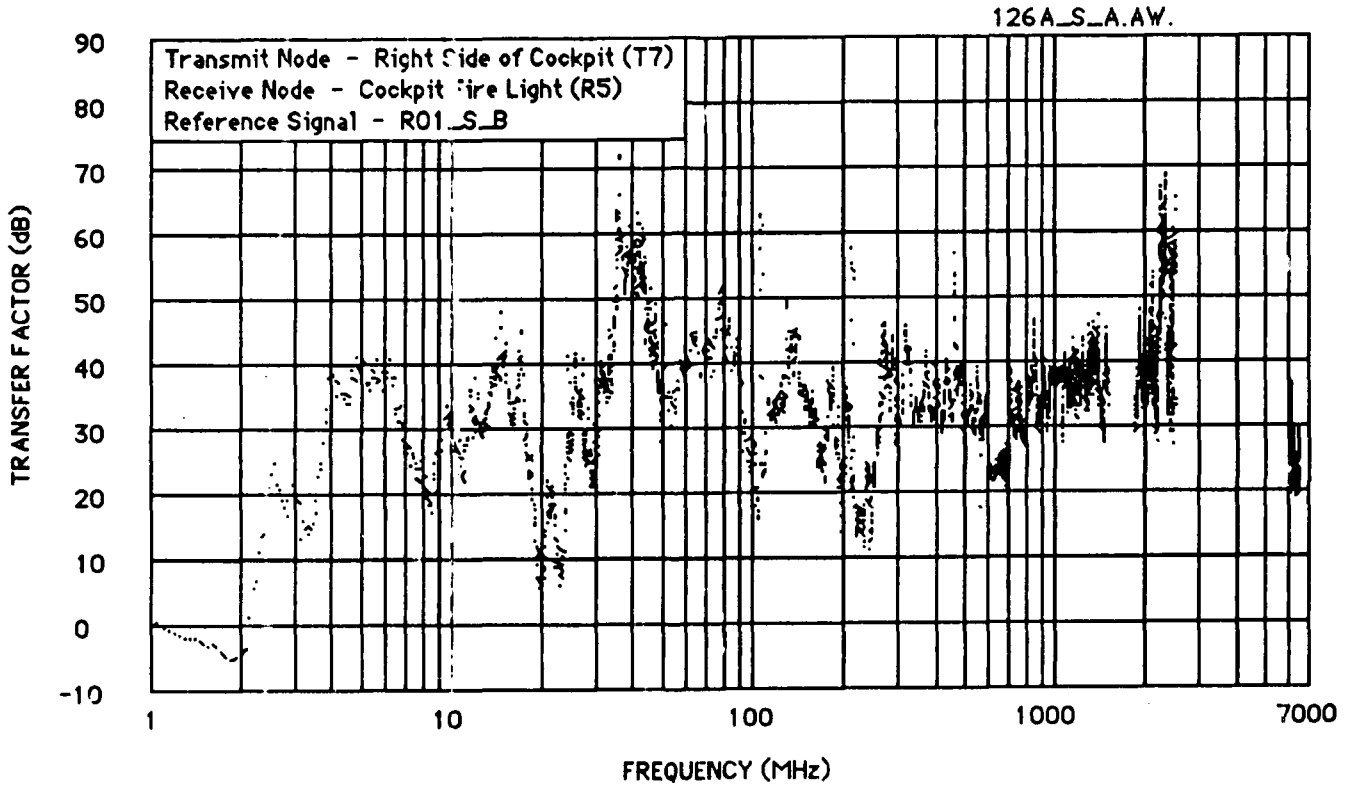

Figure E-15 Probe Transfer Factor (Test 126A)

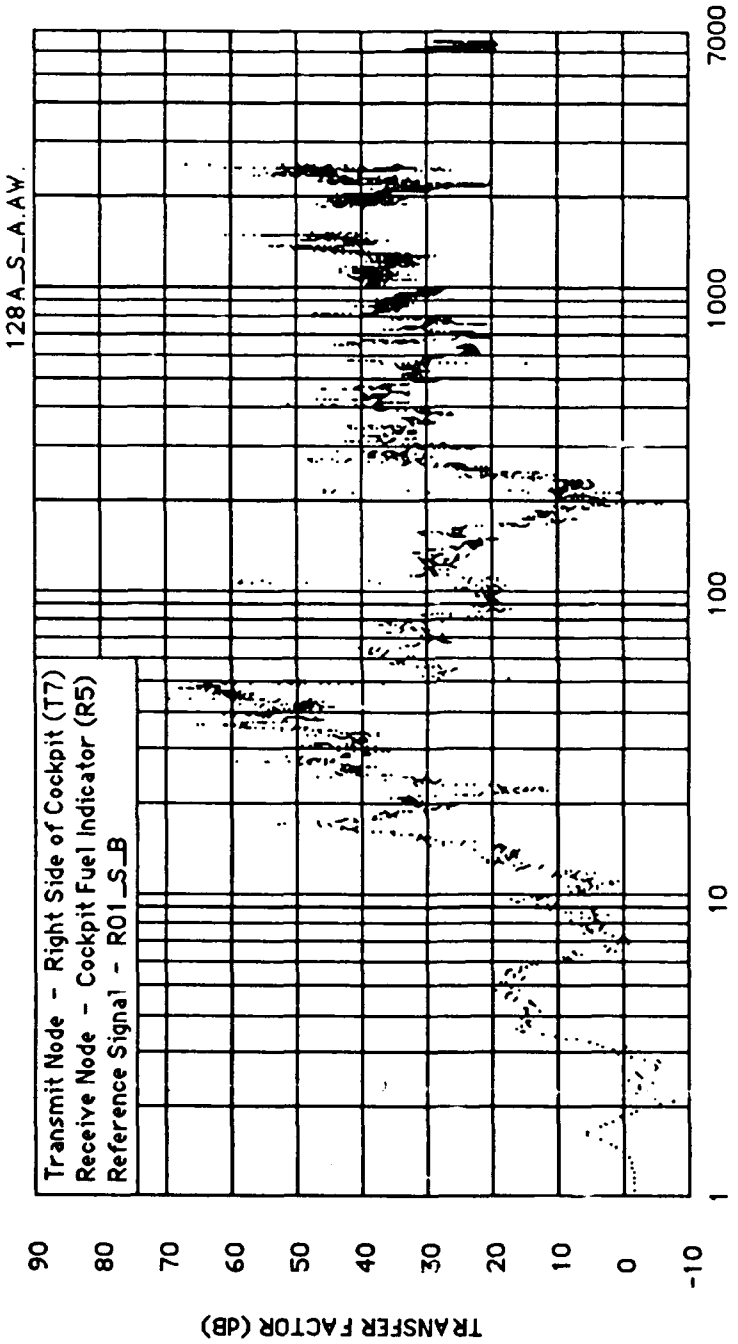

Figure E-16 Probe Transfer Factor (Test 128A)

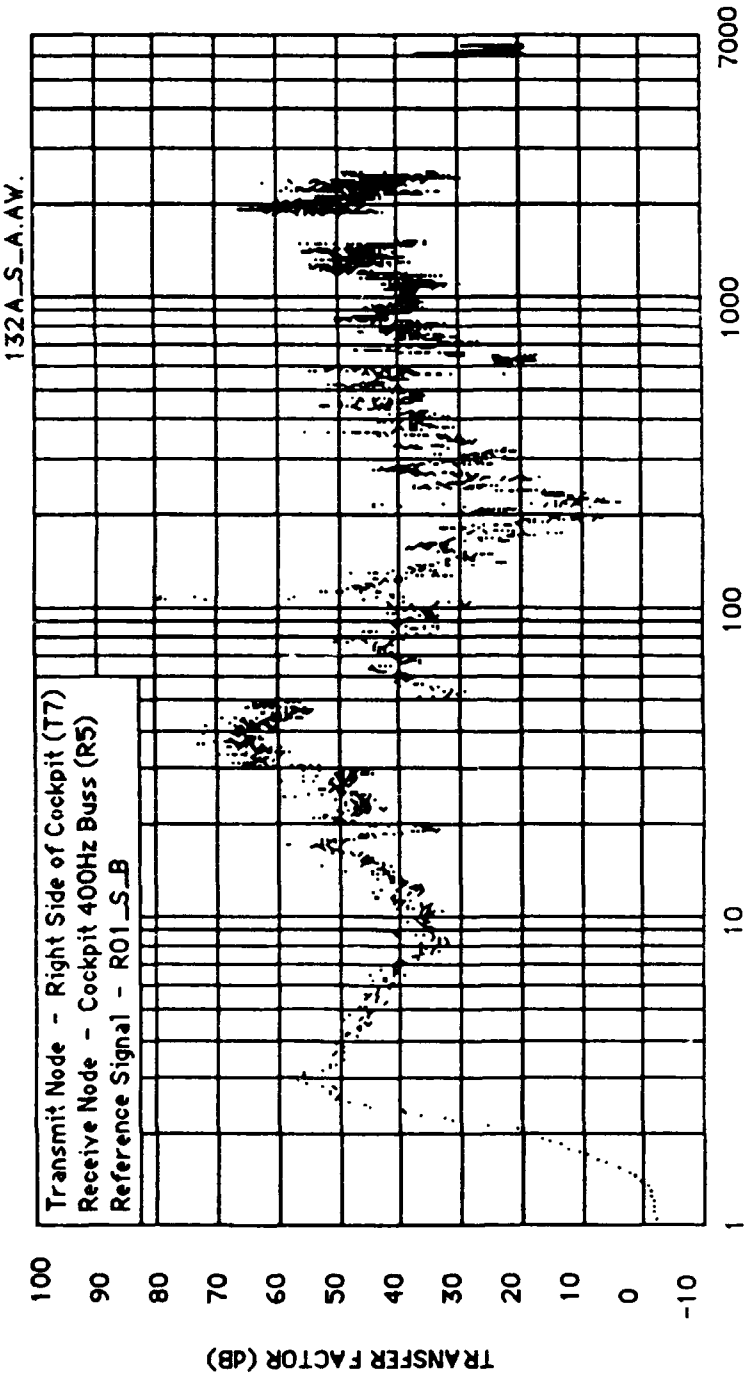

Figure E-17 Probe Transfer Factor (Test 132A)

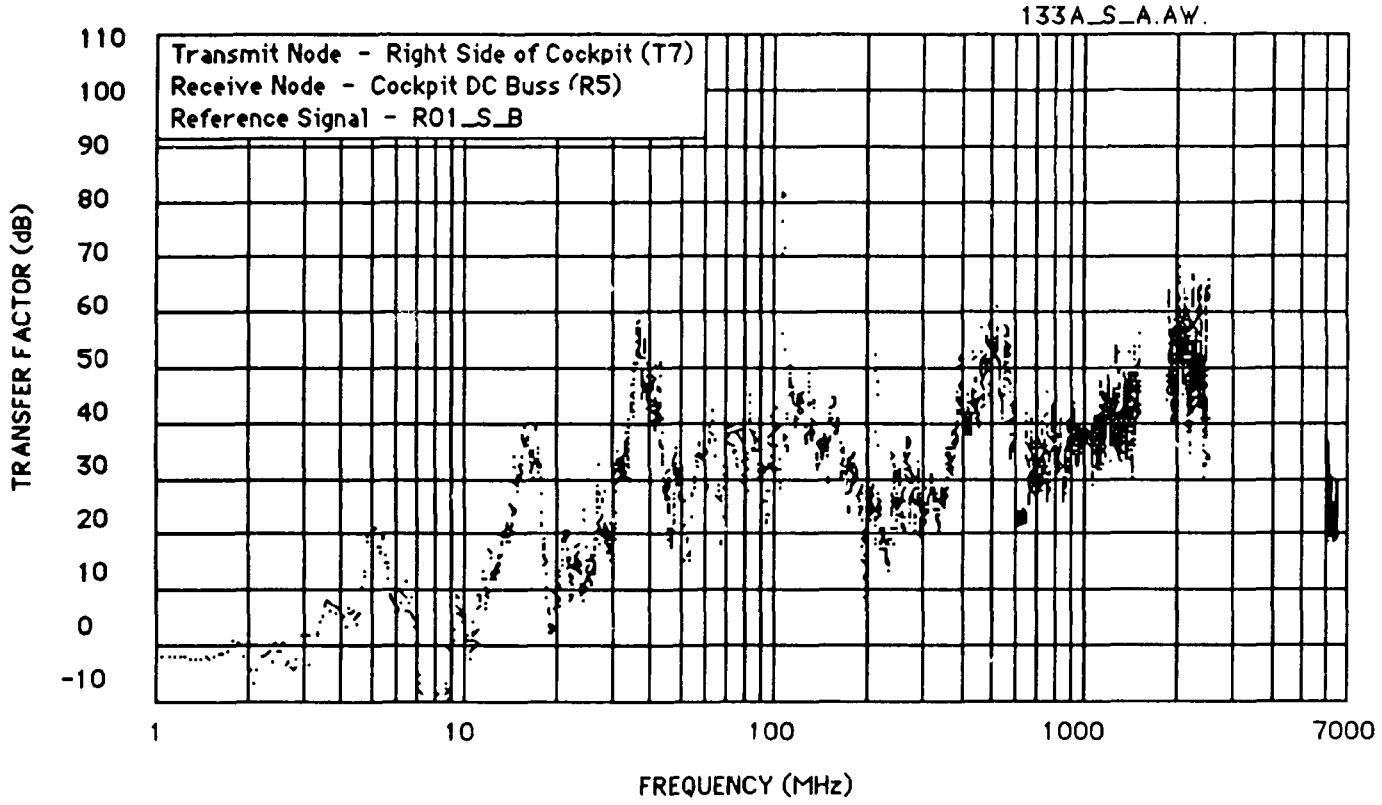

Figure E-18 Probe Transfer Factor (Test 133A)

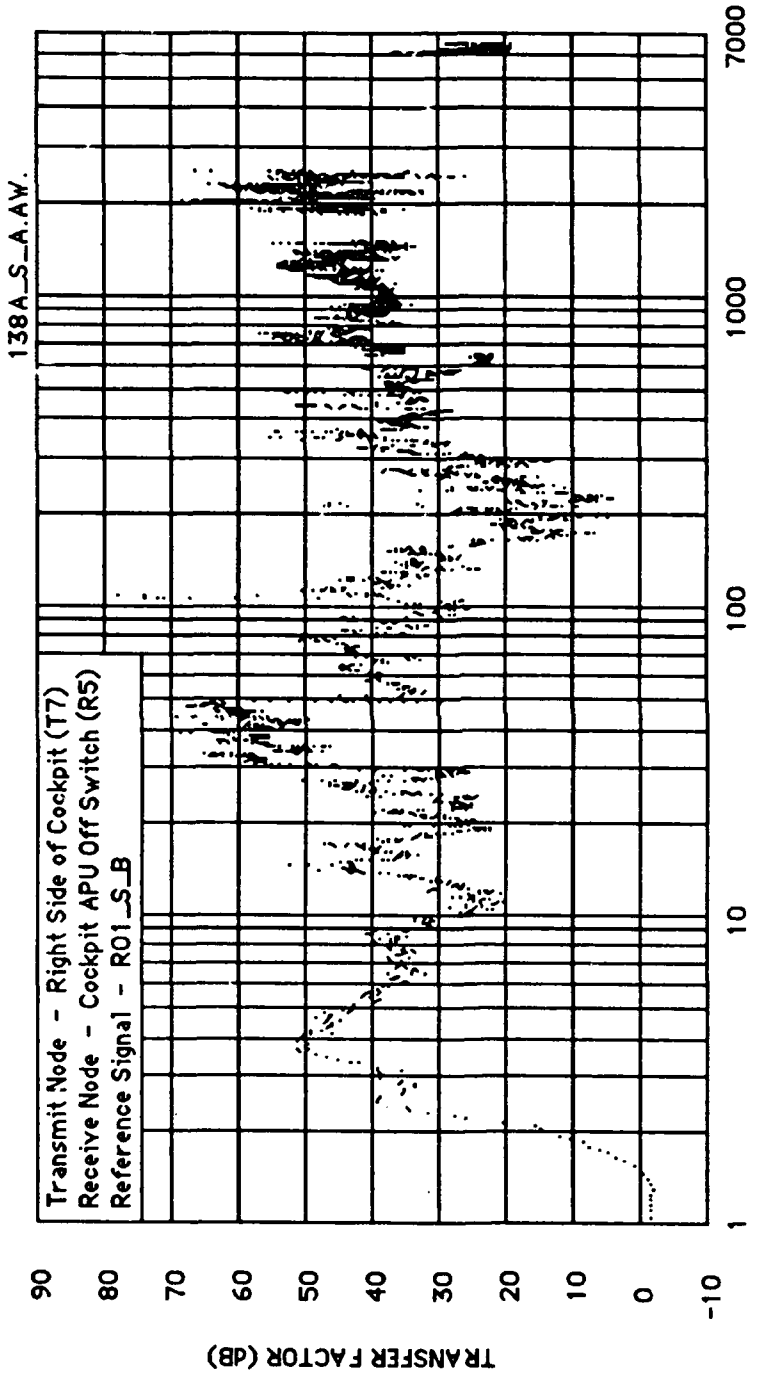

Figure E-19 Probe Transfer Factor (Test 138A)

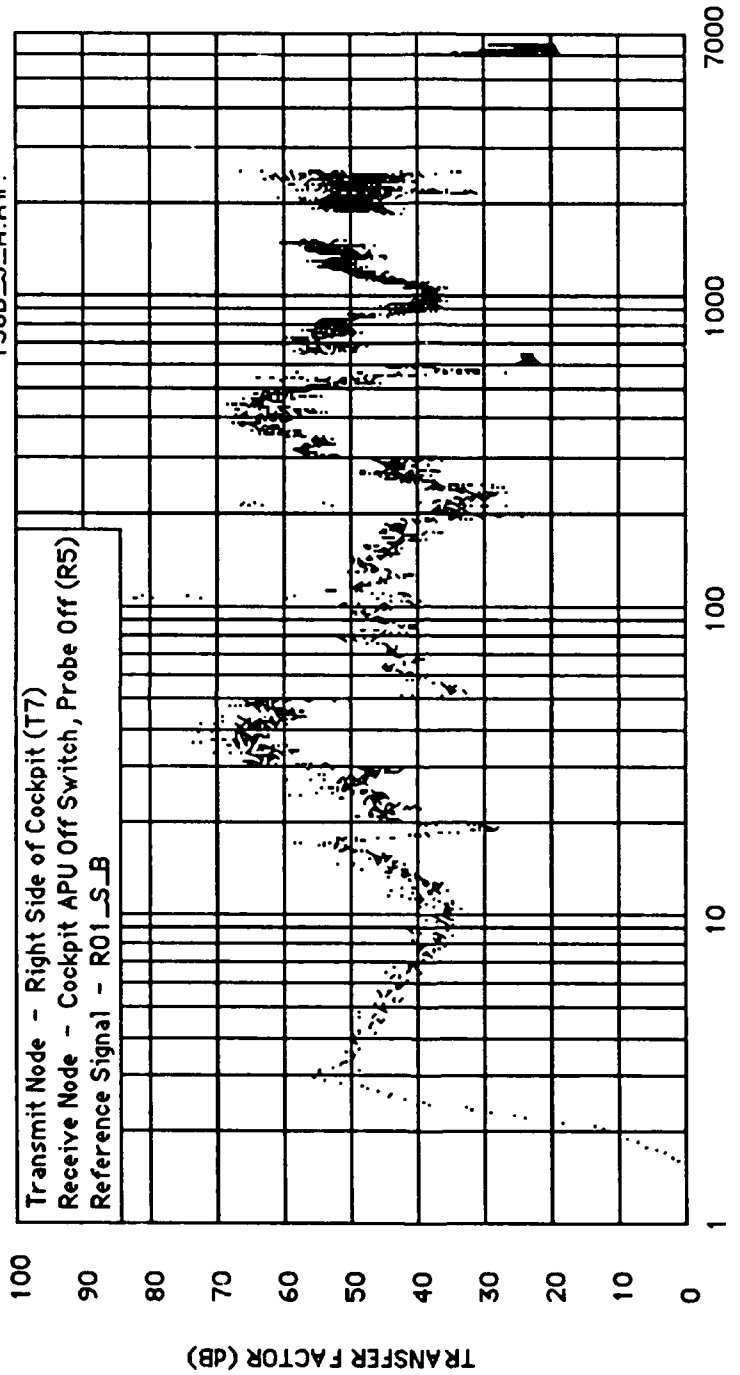

Figure E-20 Probe Transfer Factor (Test 138B)

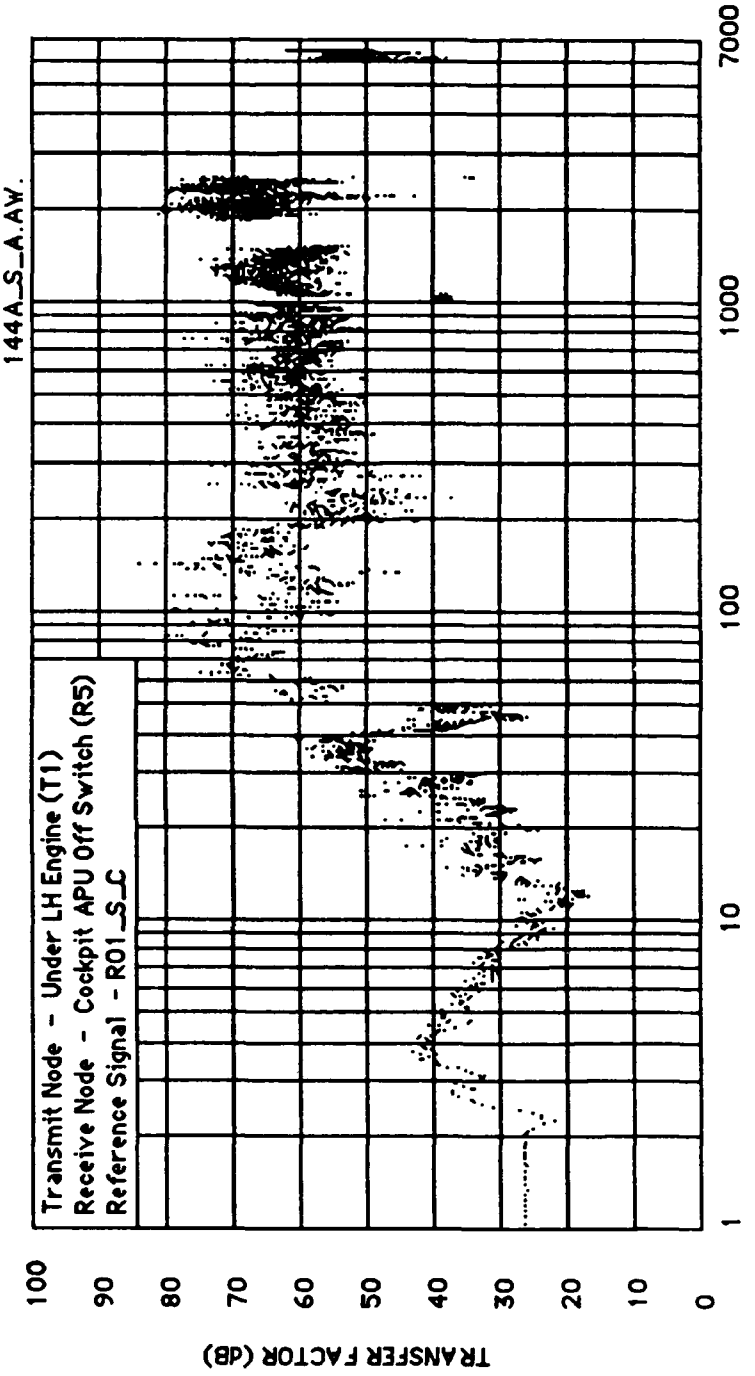

Figure E-21 Probe Transfer Factor (Test 144A)

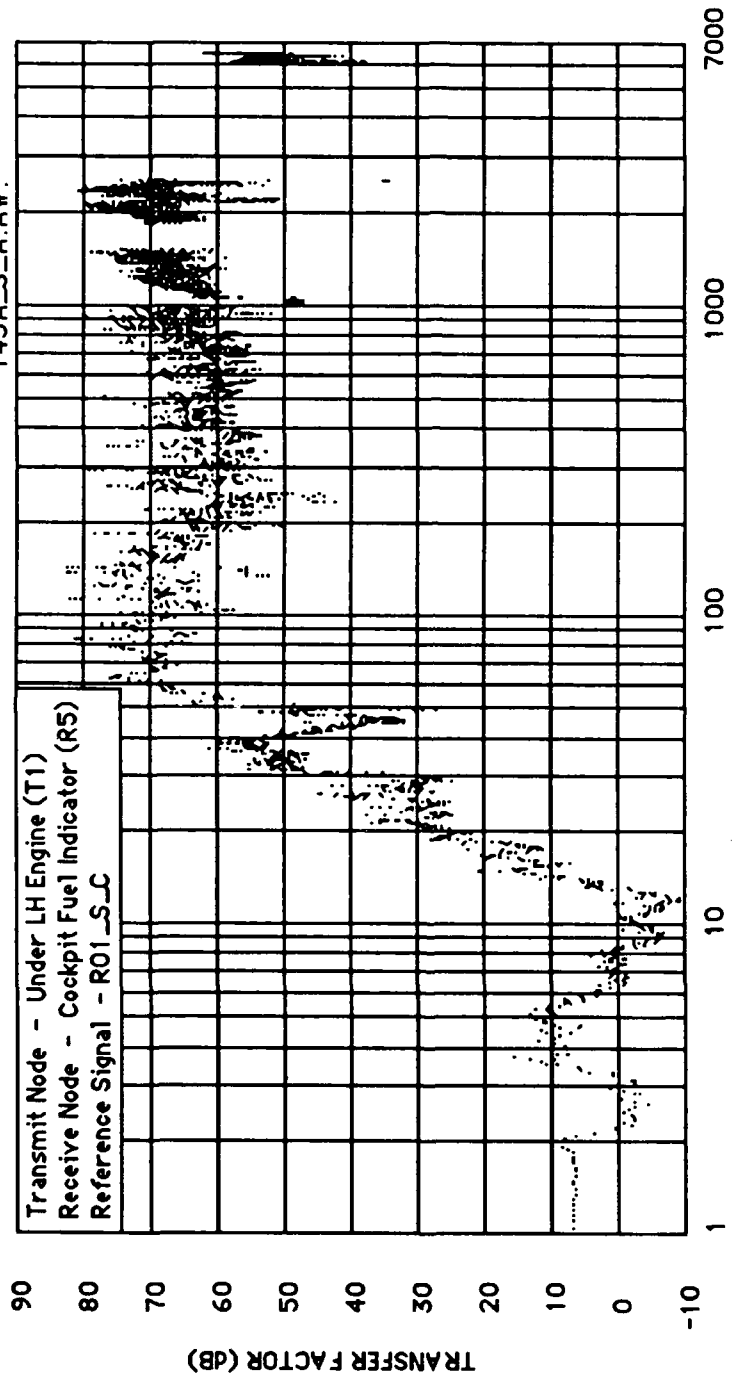

Figure E-22 Probe Transfer Factor (Test 145A)

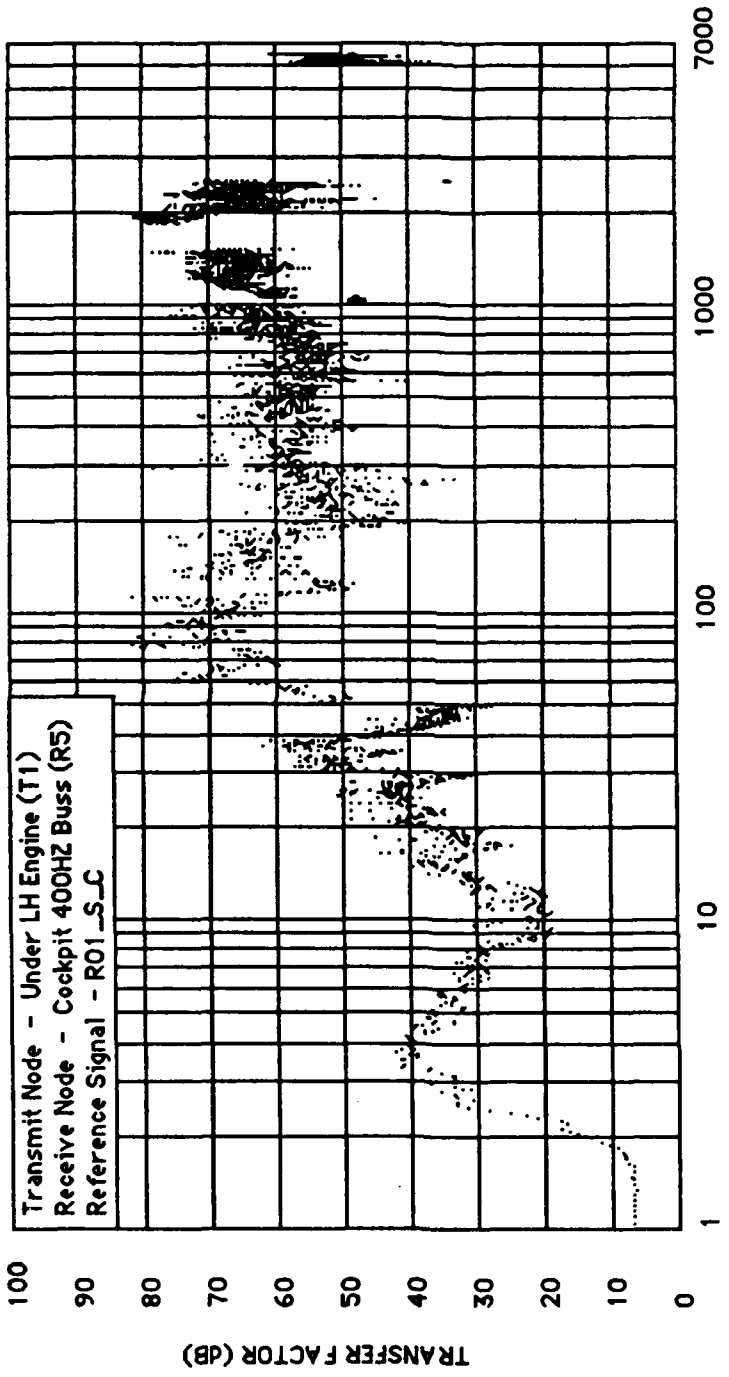

Figure E-23 Probe Transfer Factor (Test 147A)

AIR-TO-AIR DATA

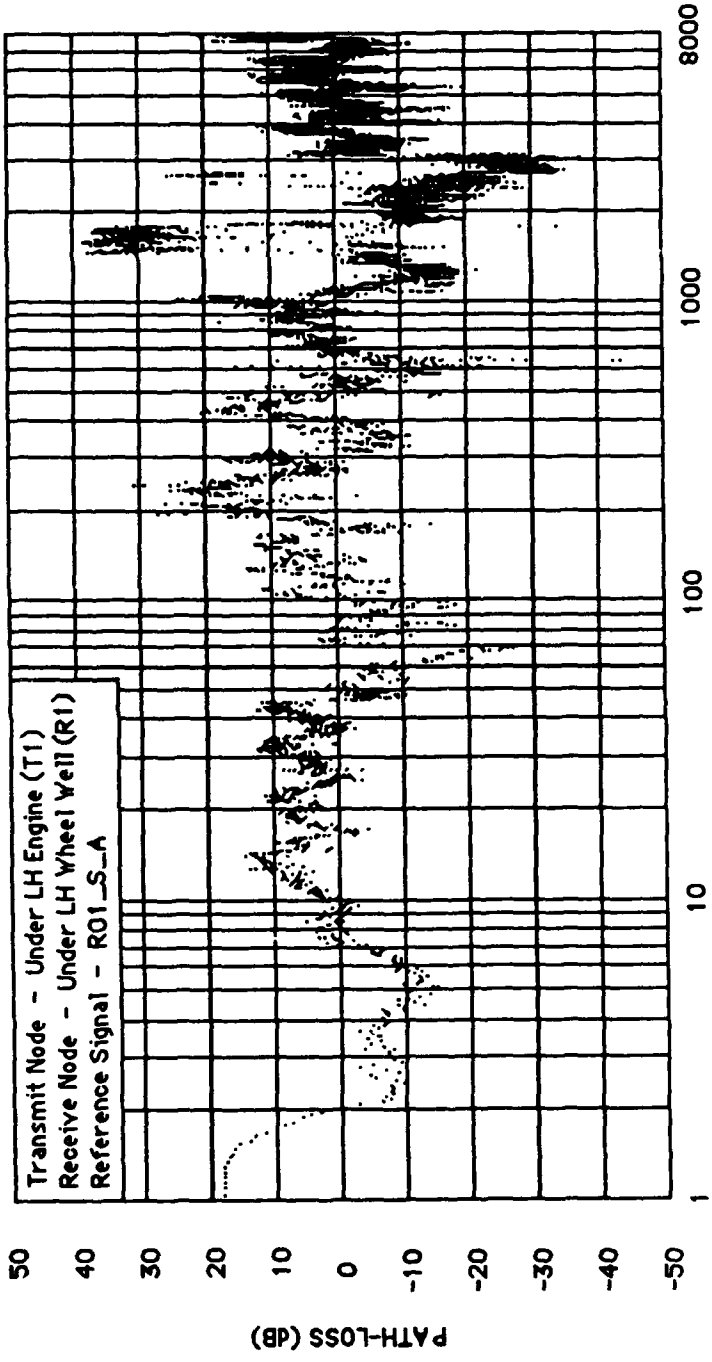

Figure E-24 Antenn Path-Loss Function (Test 001A)

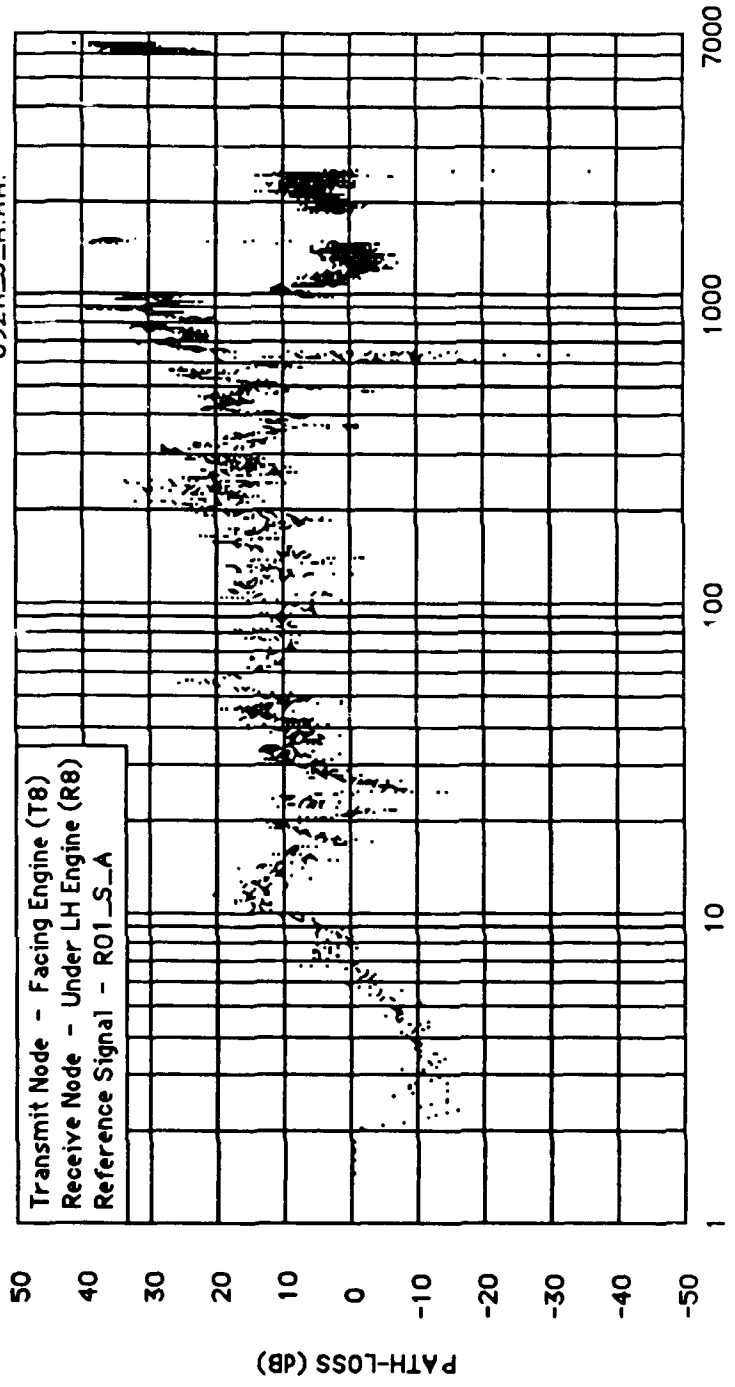

Figure E-25 Antenn Path-Loss Function (Test 092A)

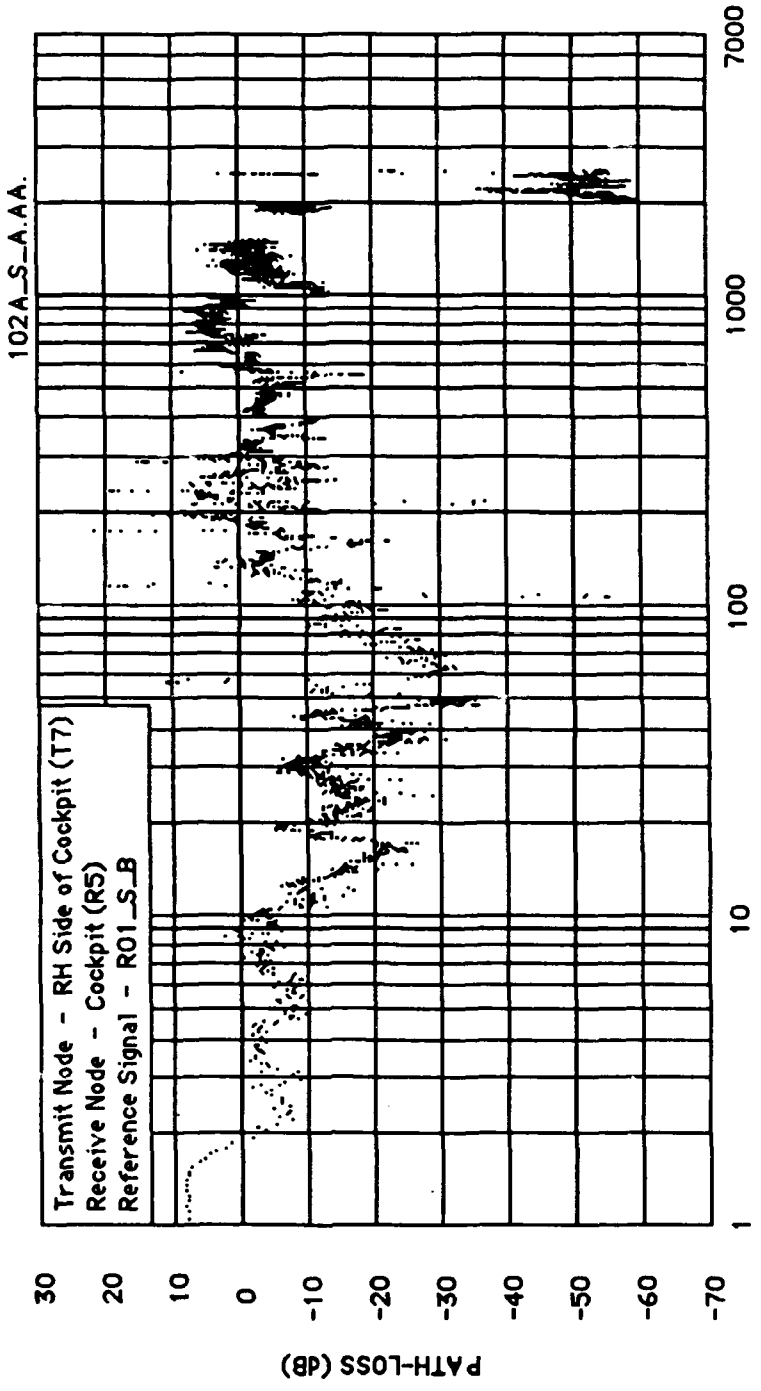

Figure E-26 Antenn Path-Loss Function (Test 102A)

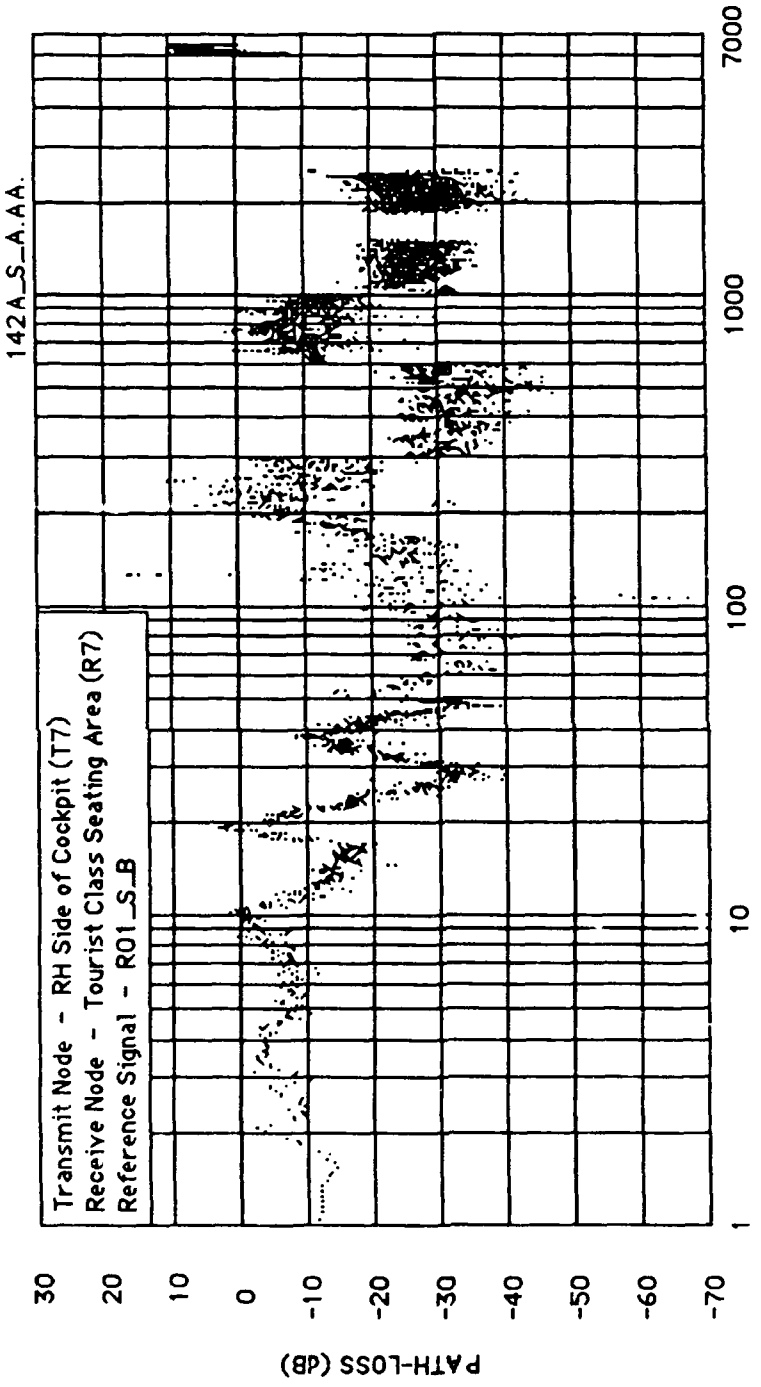

Figure E-27 Antenn Path-Loss Function (Test 142A)

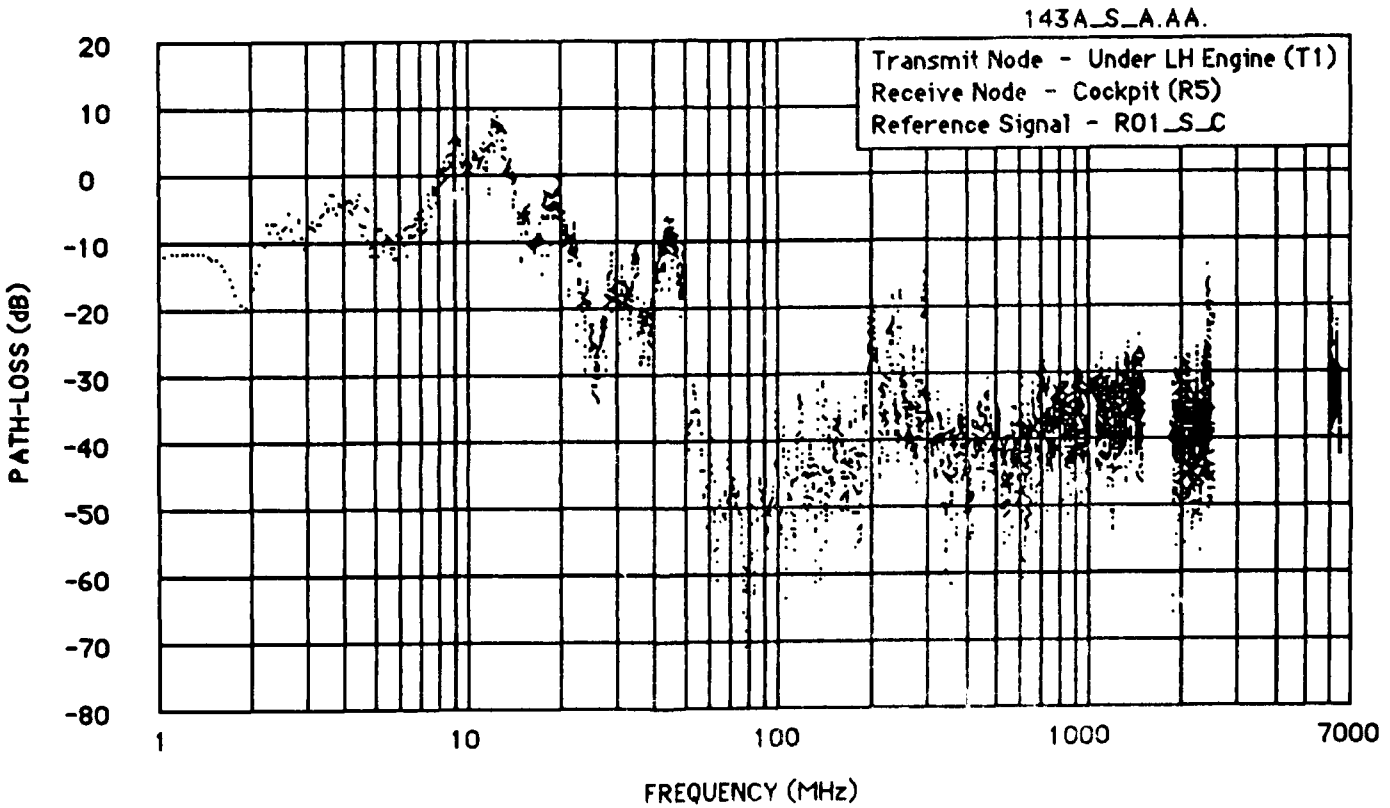

Figure E-28 Antenn Path-Loss Function (Test 143A)

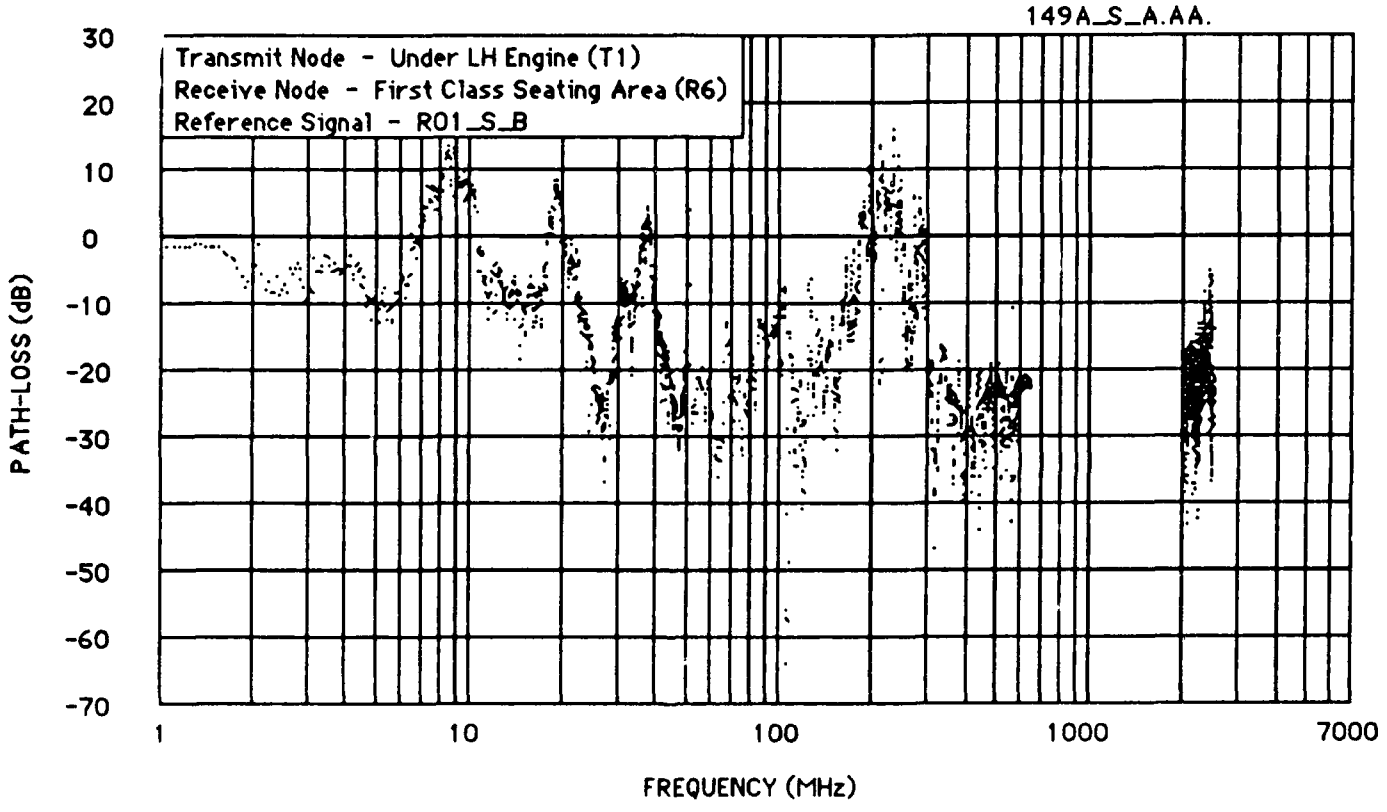

Figure E-29 Antenn Path-Loss Function (Test 149A)

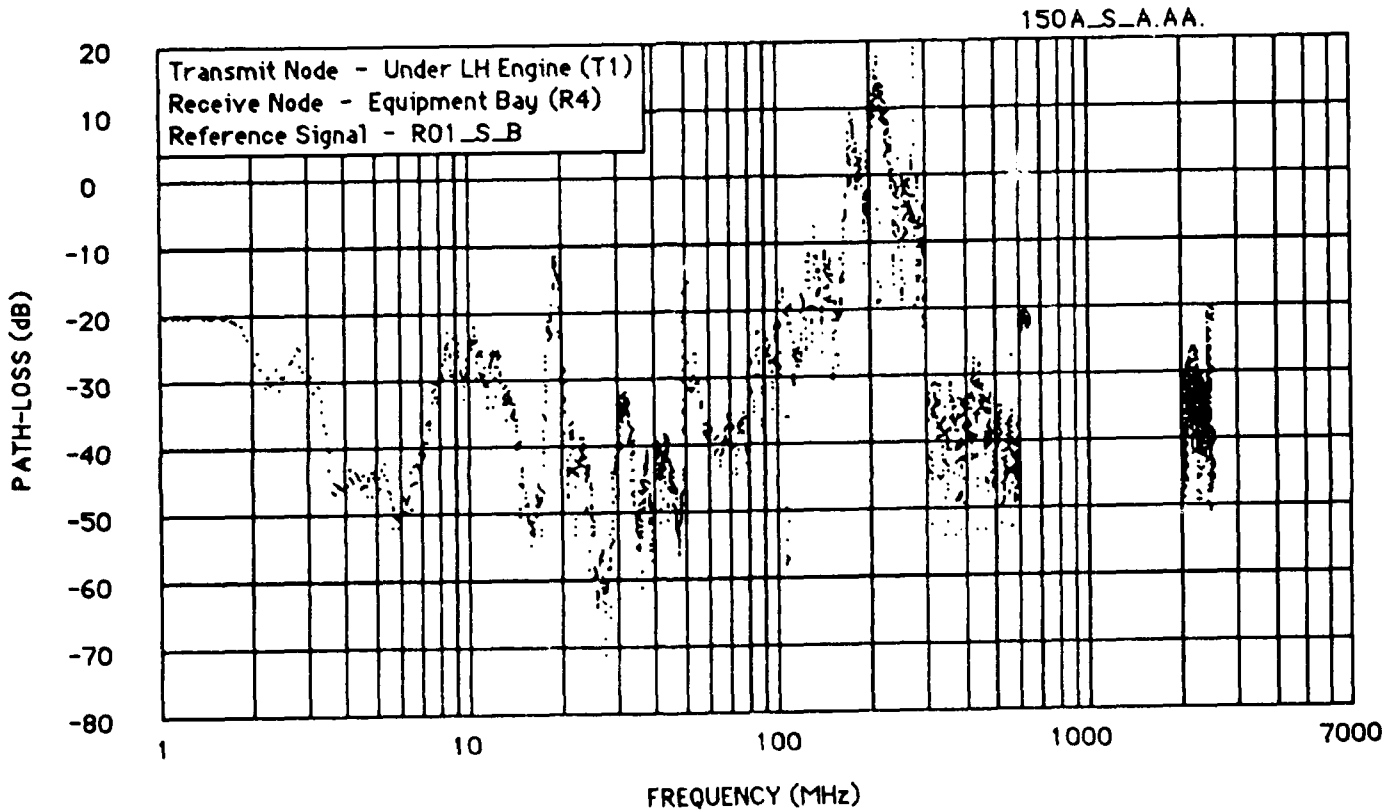

Figure E-30 Antenn Path-Loss Function (Test 150A)

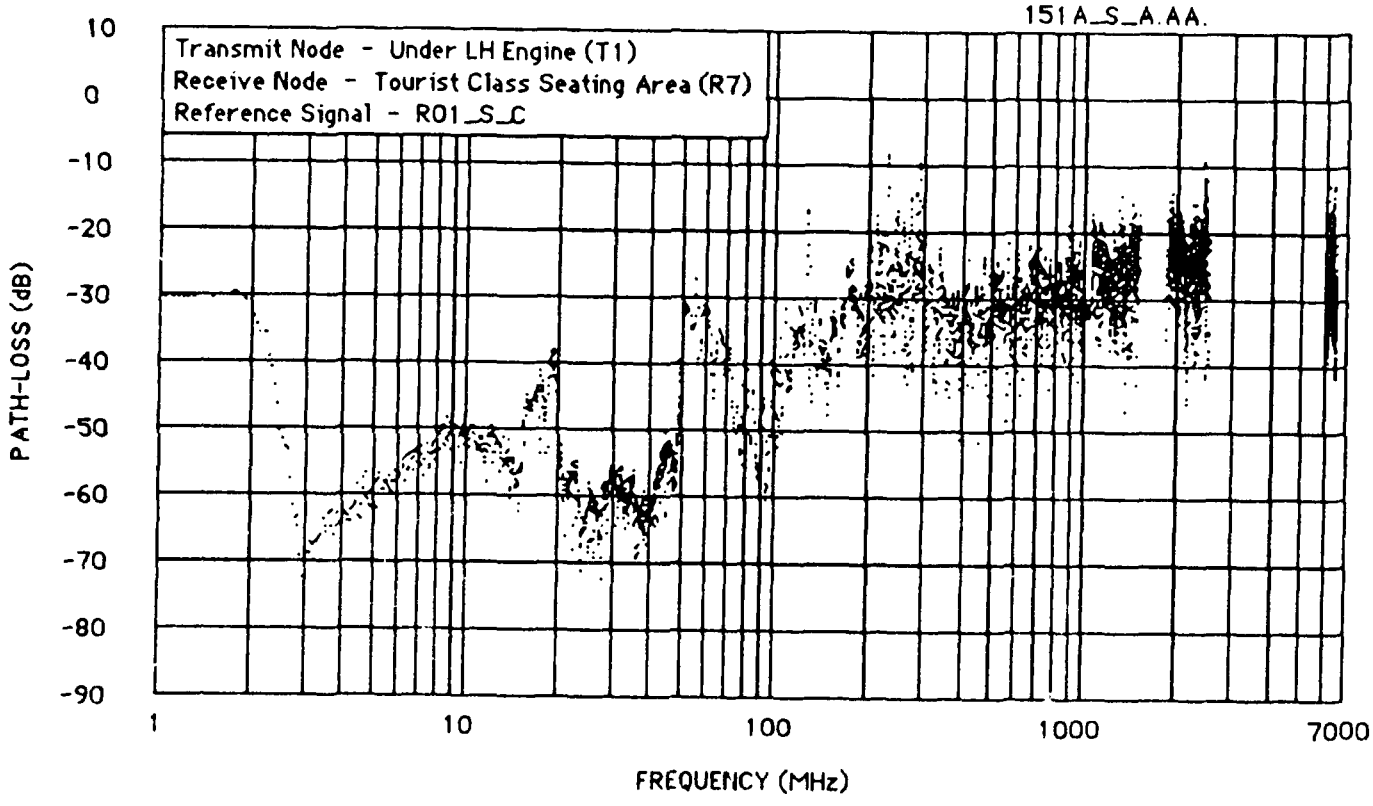

Figure E-31 Antenn Path-Loss Function (Test 151A)

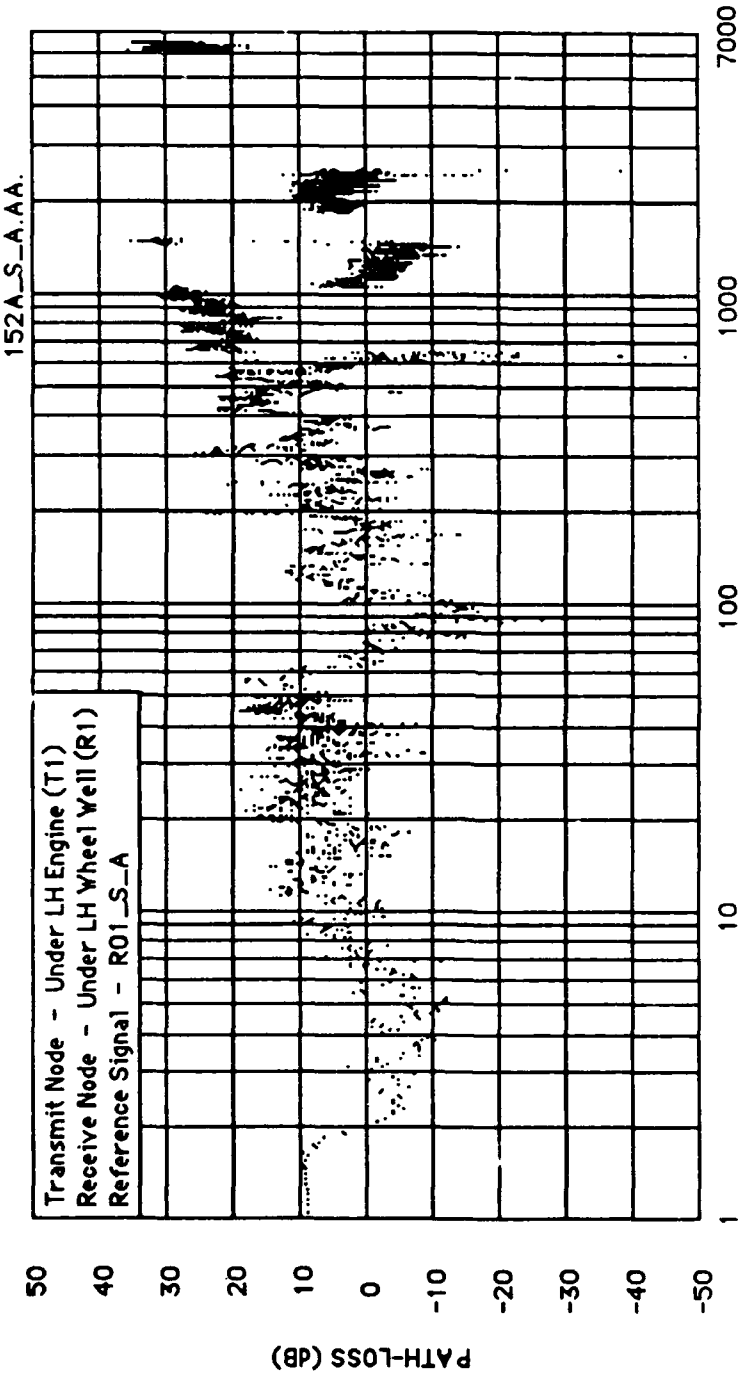

Figure E-32 Antenn Path-Loss Function (Test 152A)

APPENDIX F
DERIVATION OF INDUCED VOLTAGE

Using equation (3) of section 7.1.2:

$$dB\mu V_w + TF = dB\mu V/meter \qquad \text{(F-1)}$$

and converting from dBV to volts:

$$20\ Log_{10}\left(\frac{V_w}{10^{-6}}\right) + TF = 20\ Log_{10}\left(\frac{V/M}{10^{-6}}\right) \qquad \text{(F-2)}$$

$$Log_{10}\left(\frac{V_w}{10^{-6}}\right) = Log_{10}\left(\frac{V/M}{10^{-6}}\right) - \frac{TF}{20} Log_{10}(10) \qquad \text{(F-3)}$$

$$Log_{10}\left(\frac{V_w}{10^{-6}}\right) = Log_{10}\left[\frac{\left(\frac{V/M}{10^{-6}}\right)}{10^{TF/20}}\right] \qquad \text{(F-4)}$$

$$\frac{V_w}{10^{-6}} = \left[\frac{\left(\frac{V/M}{10^{-6}}\right)}{10^{TF/20}}\right] \qquad \text{(F-5)}$$

$$V_w = \frac{V/M}{10^{TF/20}}\ (volts) \qquad \text{(F-6)}$$

PREDICTED
MAXIMUM INDUCED VOLTAGE
DATA PLOTS

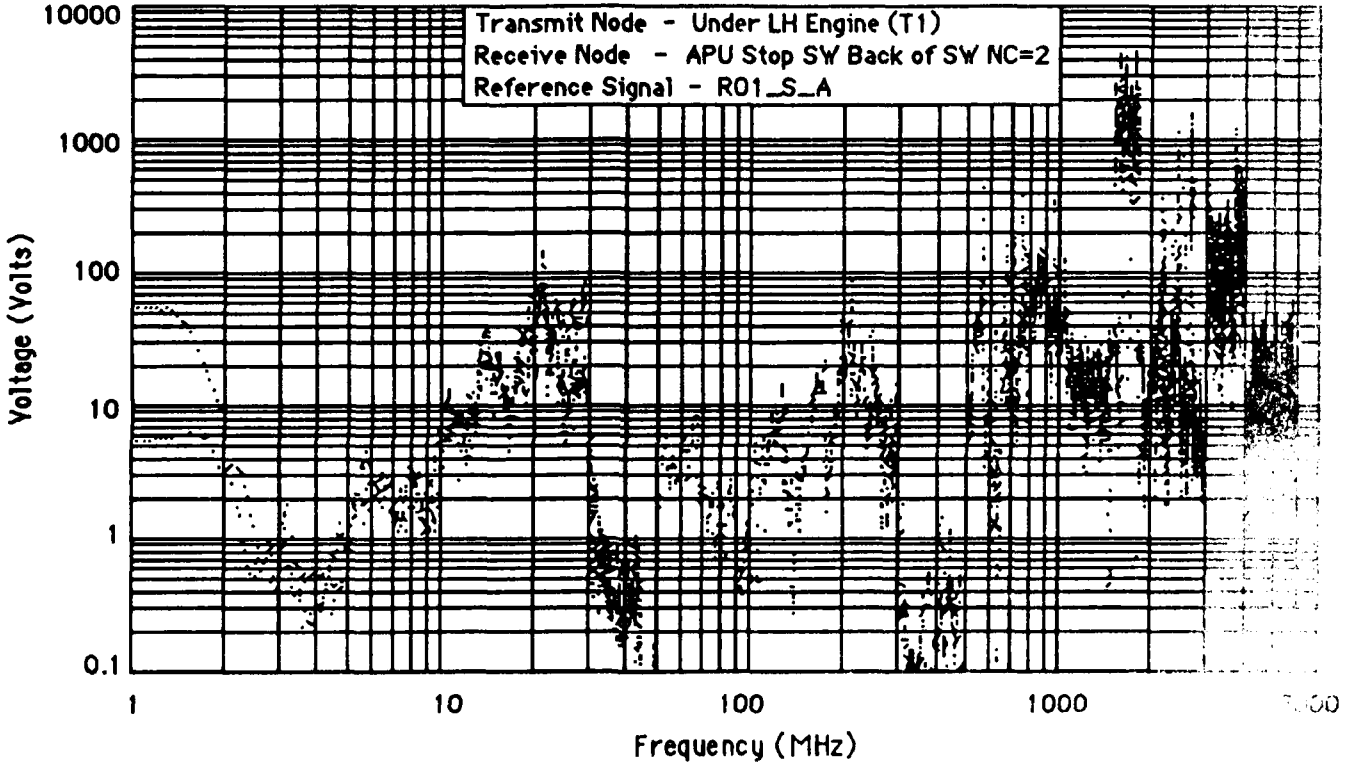

Figure F-1 Maximum Induced Voltage (002A)

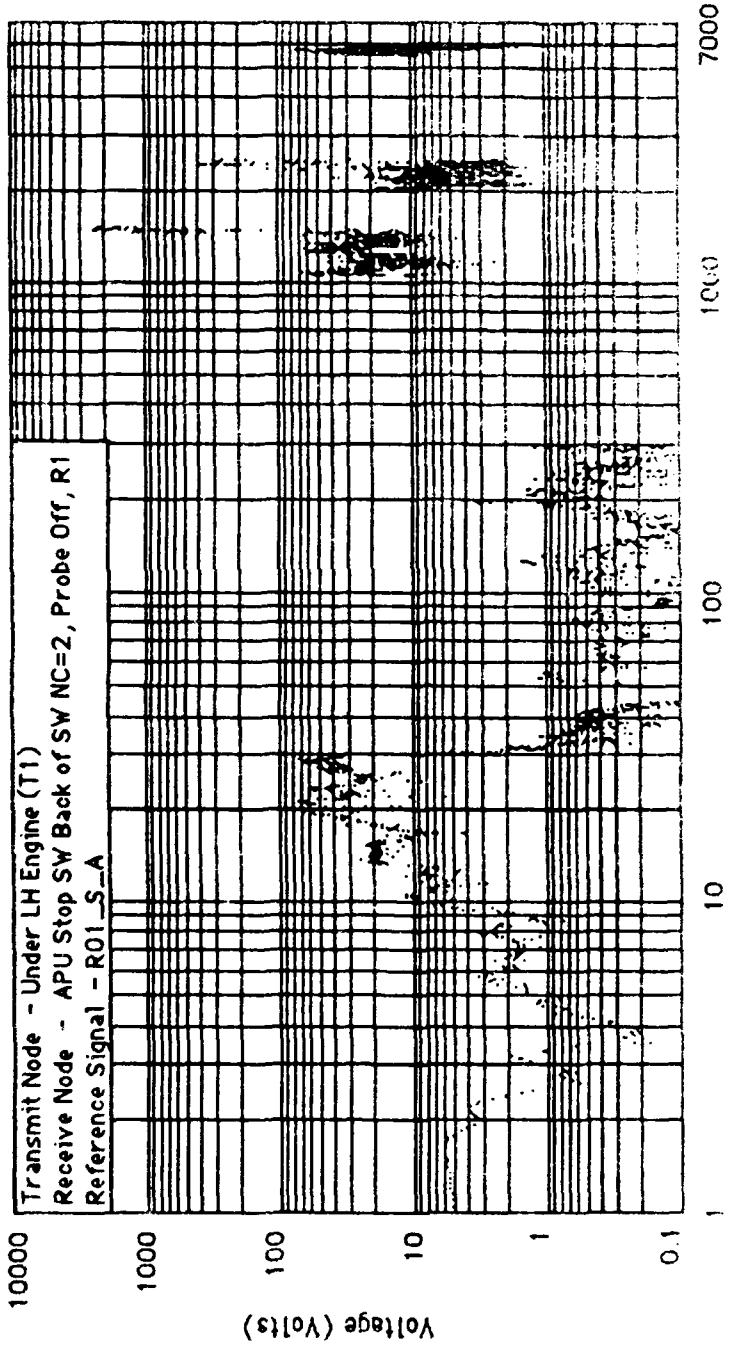

Figure F-2 Maximum Induced Voltage (002B)

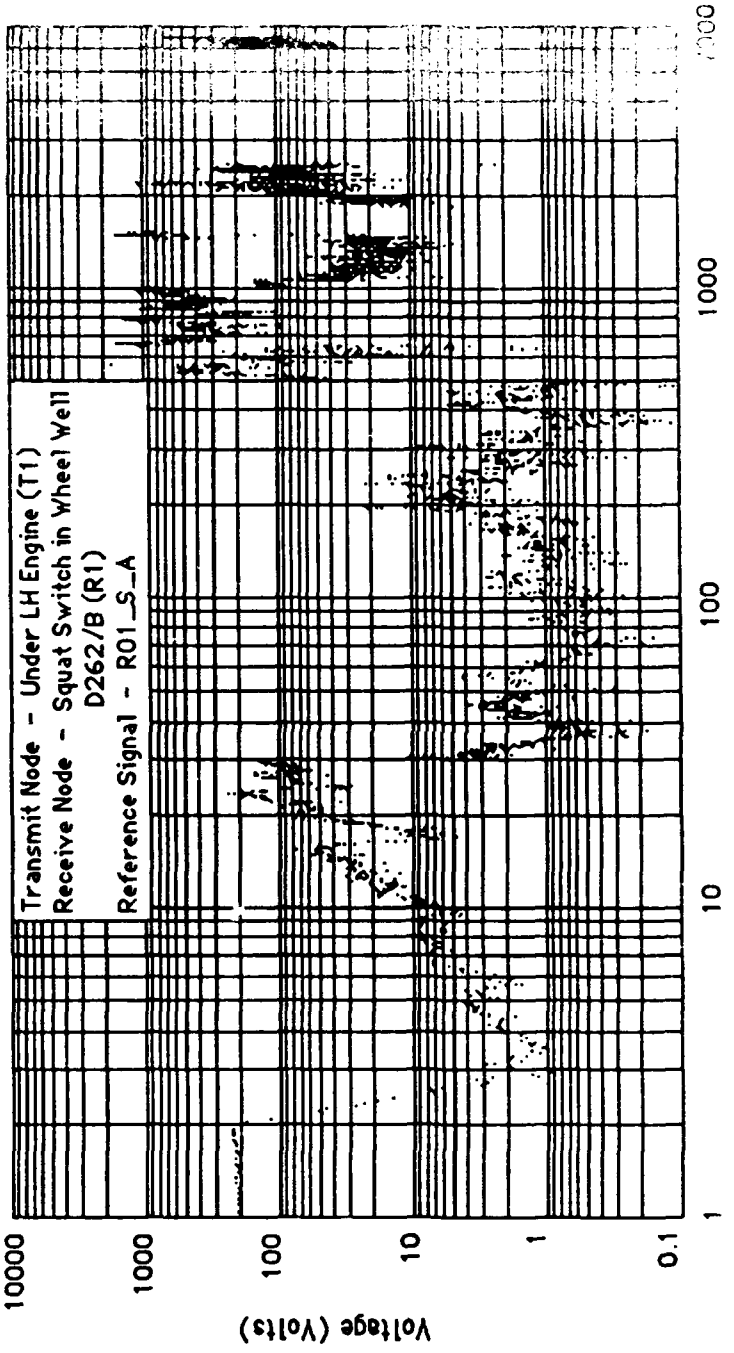

Figure F-3 Maximum Induced Voltage (013A)

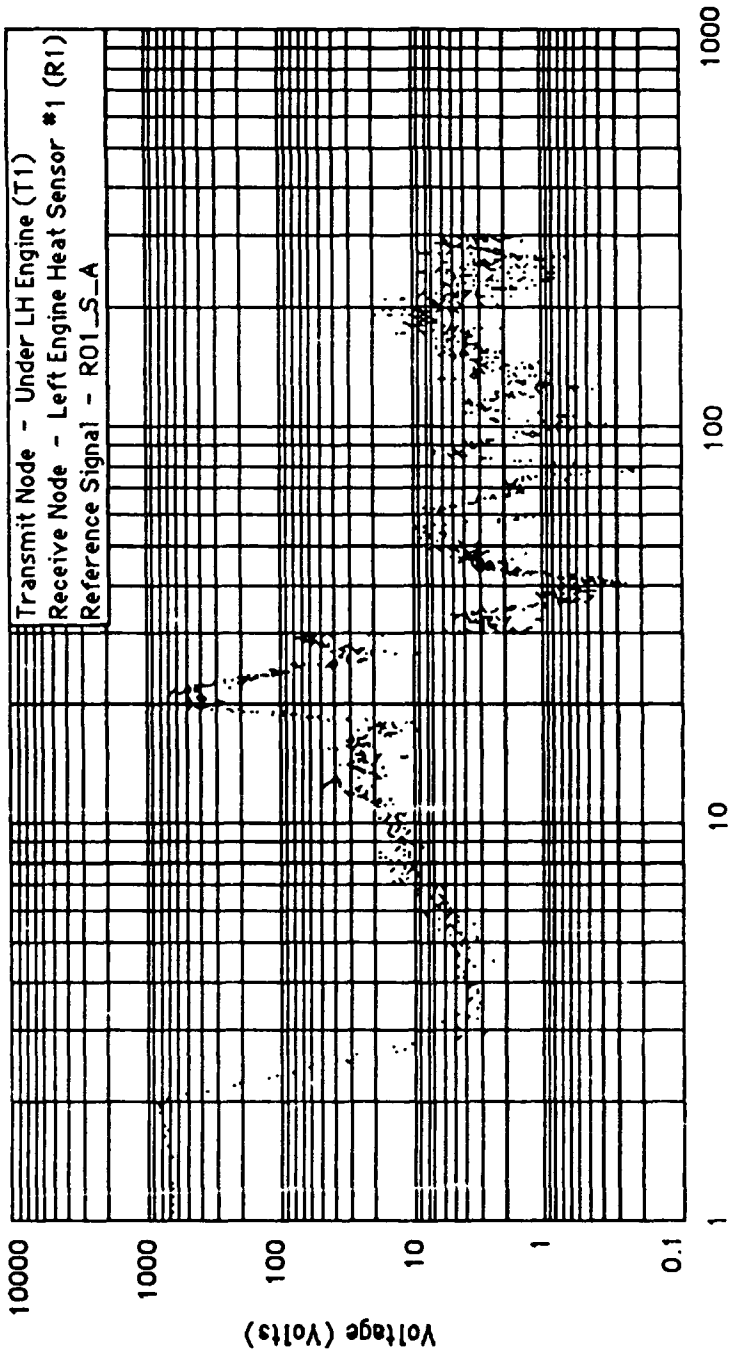

Figure F-4 Maximum Induced Voltage (017A)

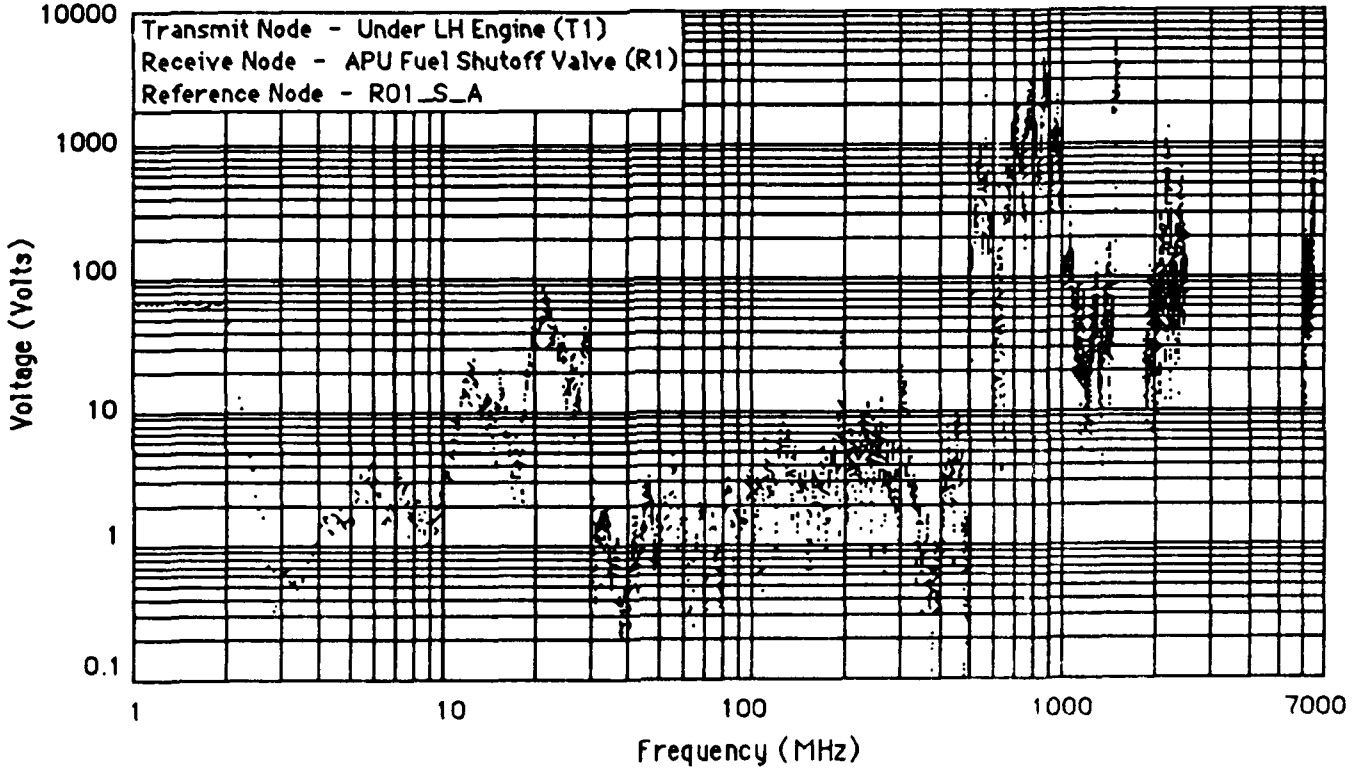

Figure F-5 Maximum Induced Voltage (022A)

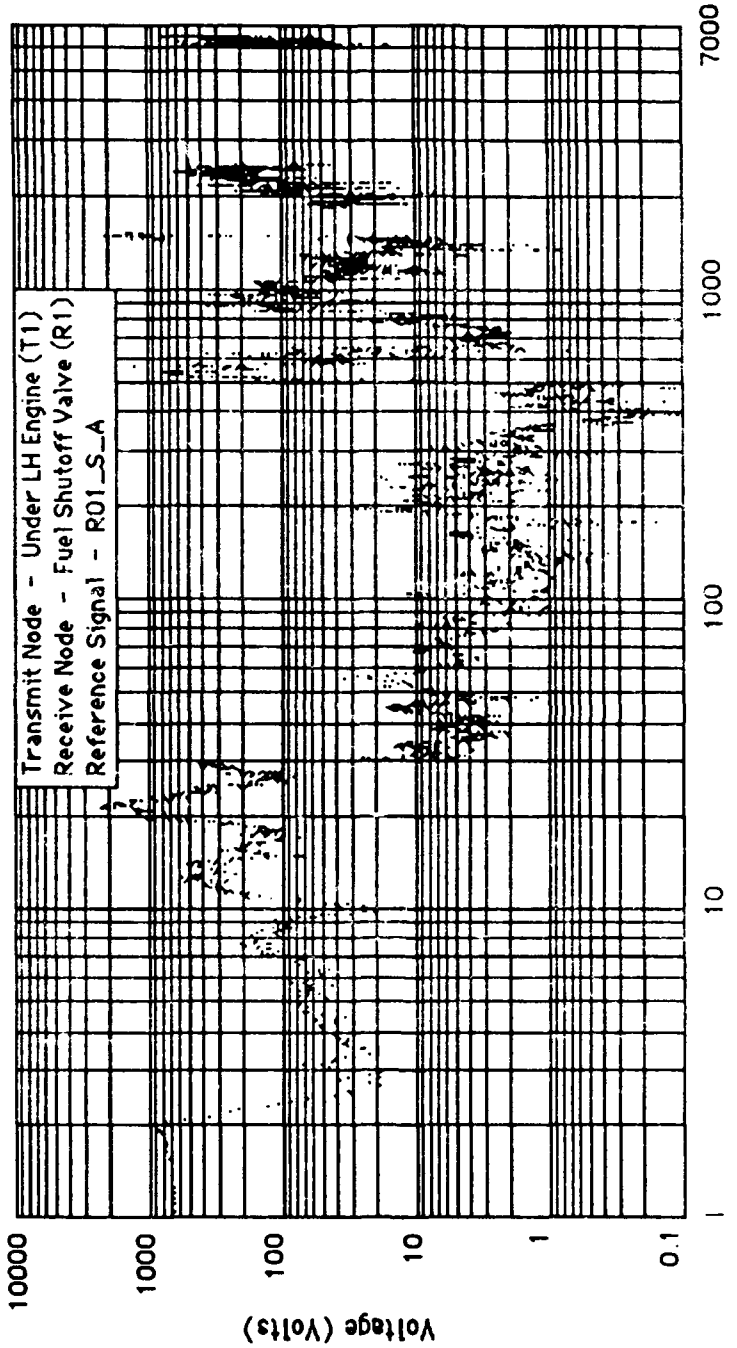

Figure F-6 Maximum Induced Voltage (024A)

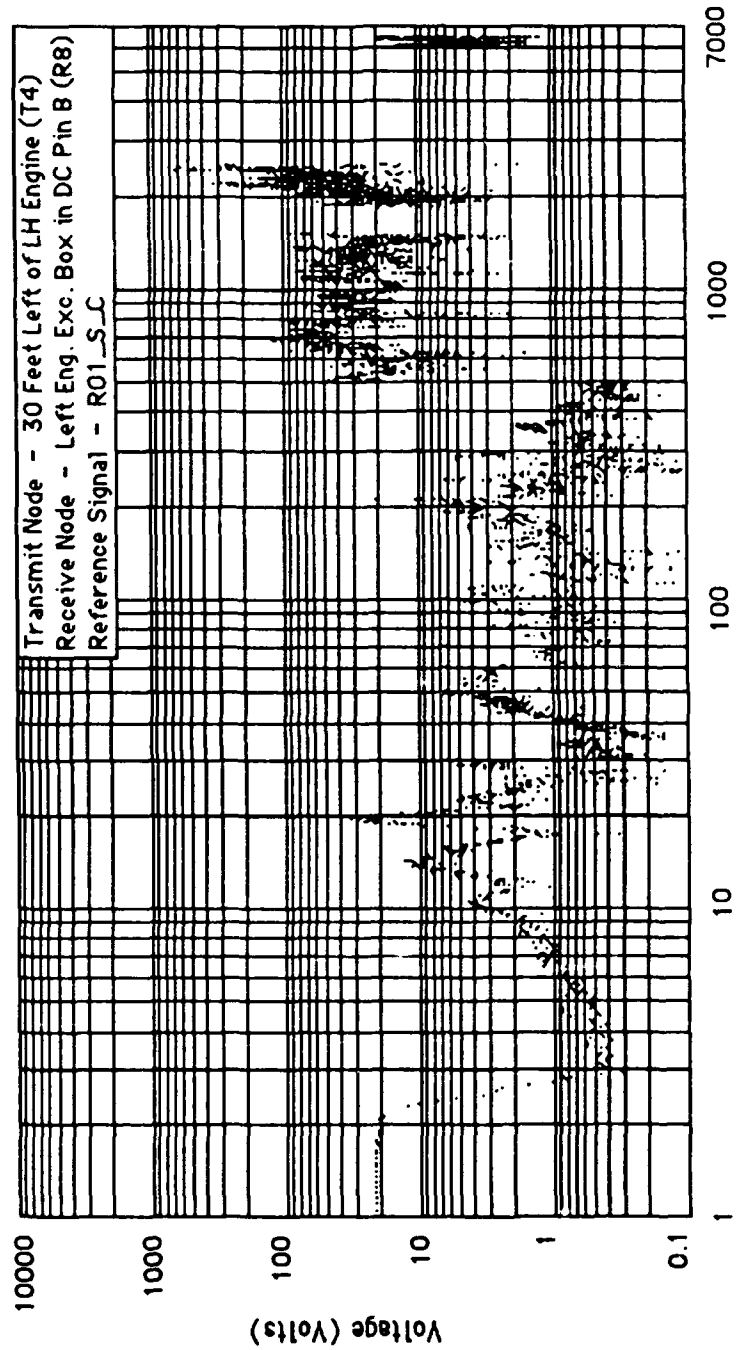

Figure F-7 Maximum Induced Voltage (093A)

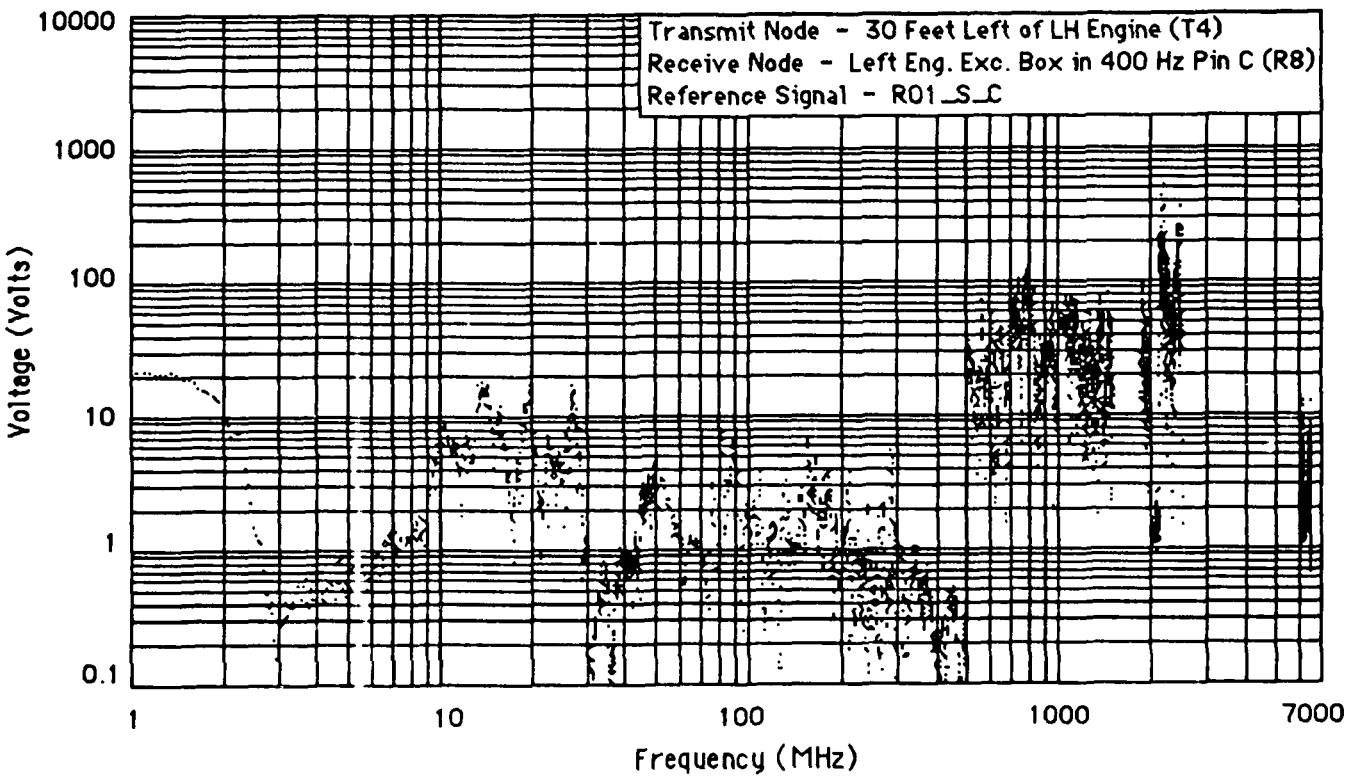

Figure F-8 Maximum Induced Voltage (093AA)

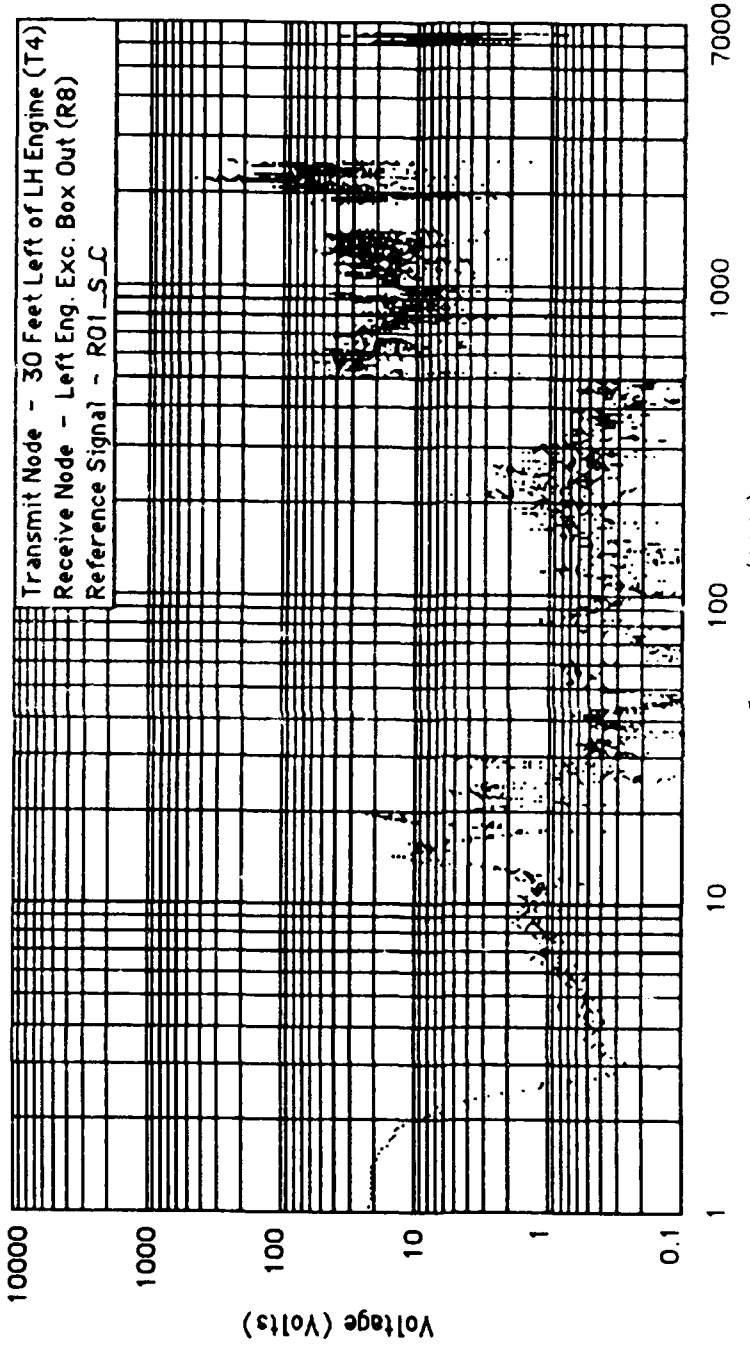

Figure F-9 Maximum Induced Voltage (094A)

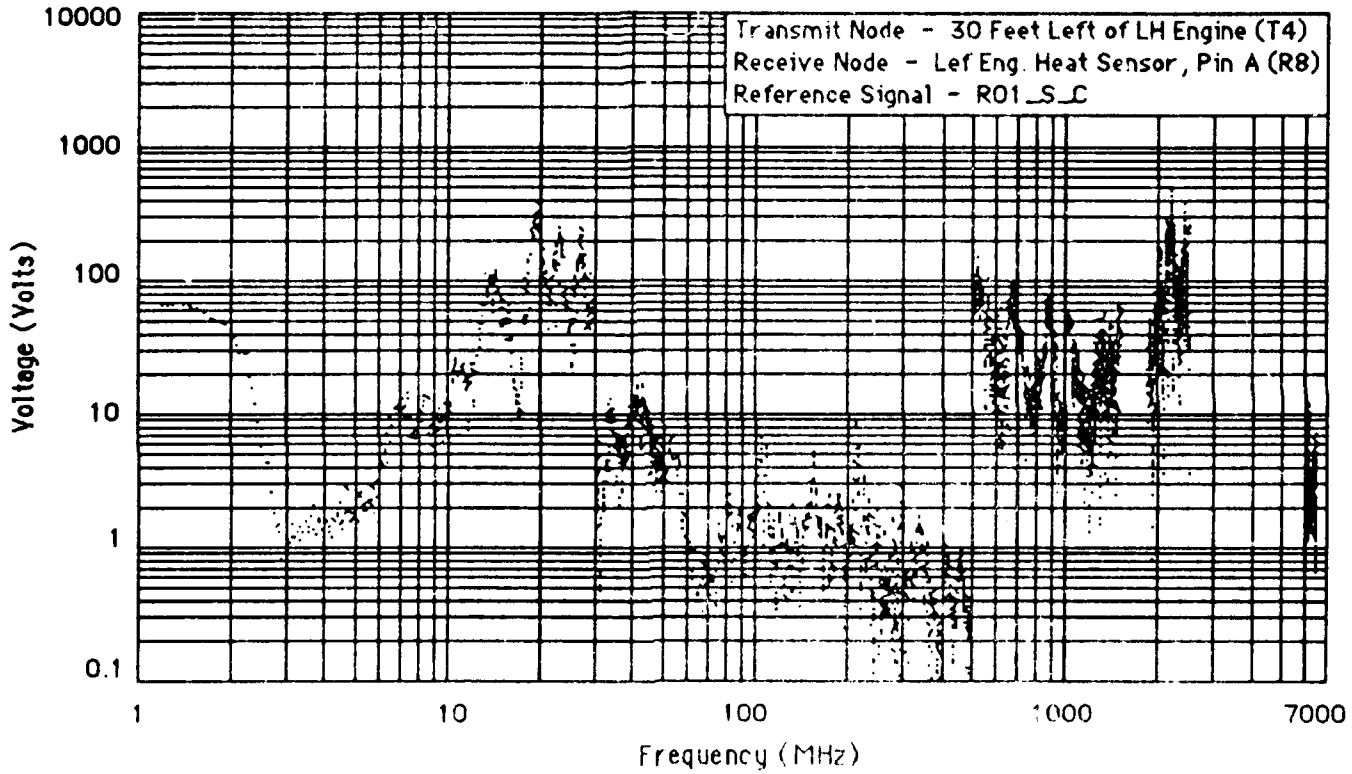

Figure F-10 Maximum Induced Voltage (095A)

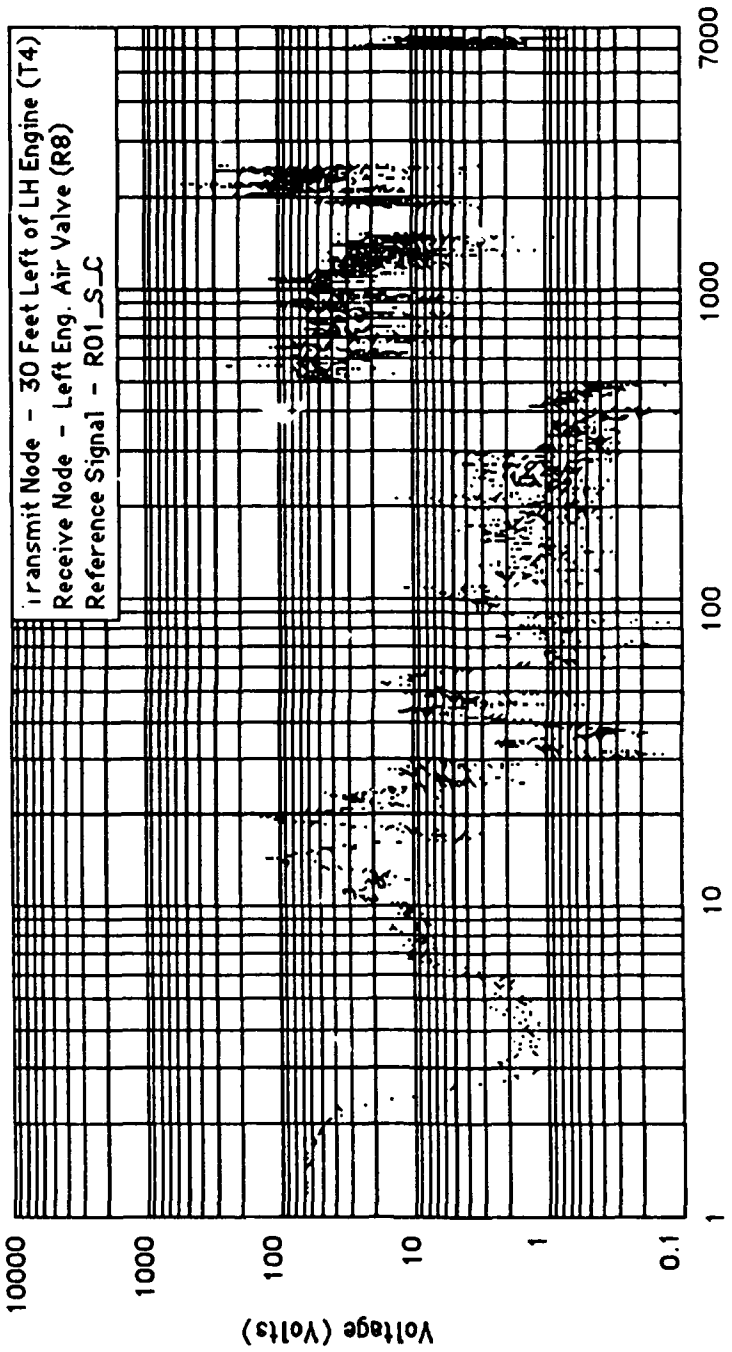

Figure F-11 Maximum Induced Voltage (095AA)

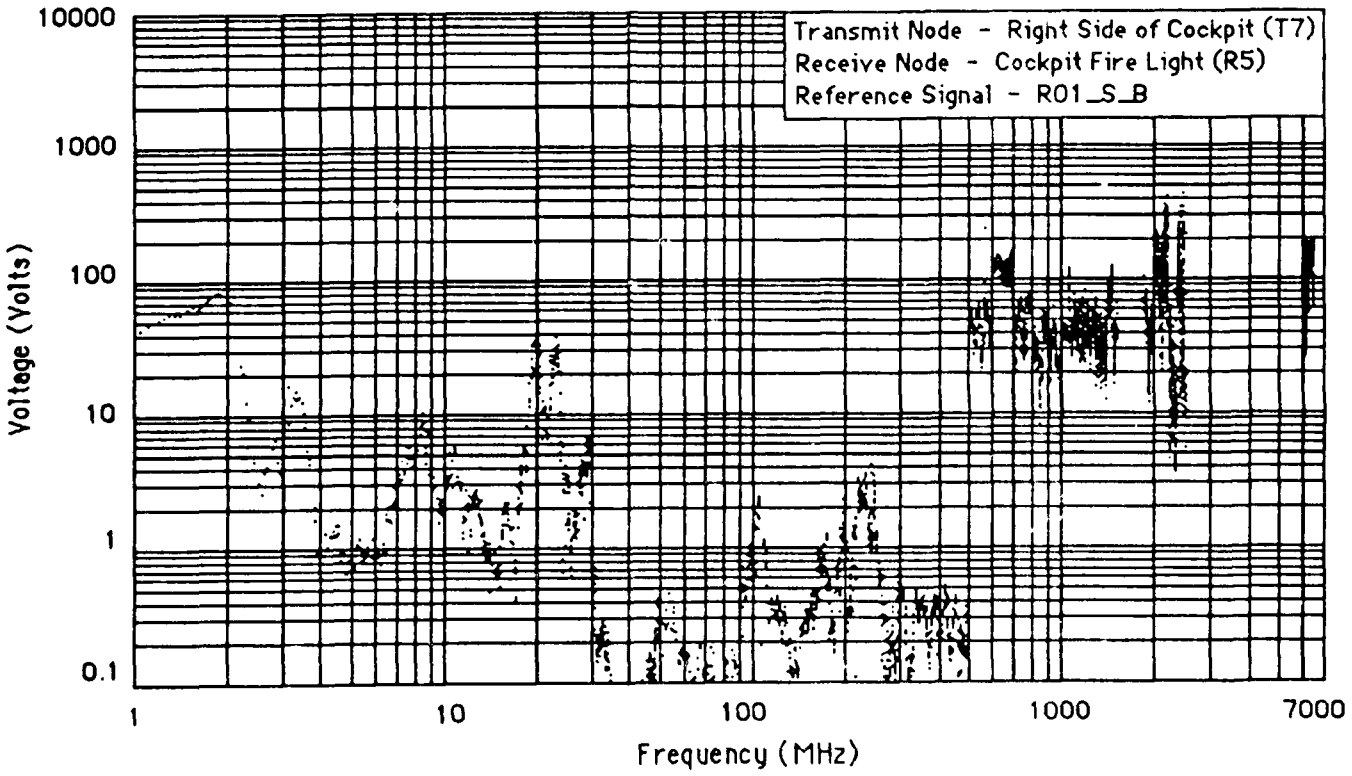

Figure F-12 Maximum Induced Voltage (126A)

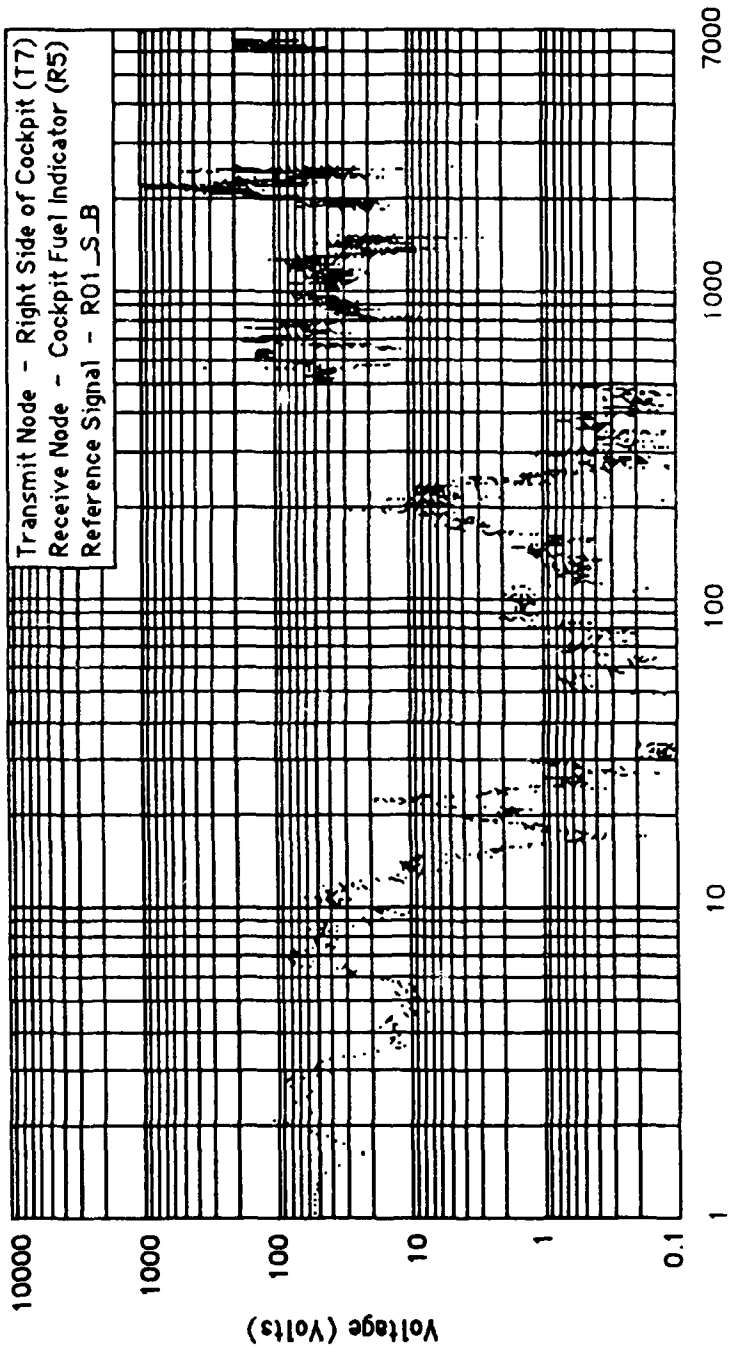

Figure F-13 Maximum Induced Voltage (128A)

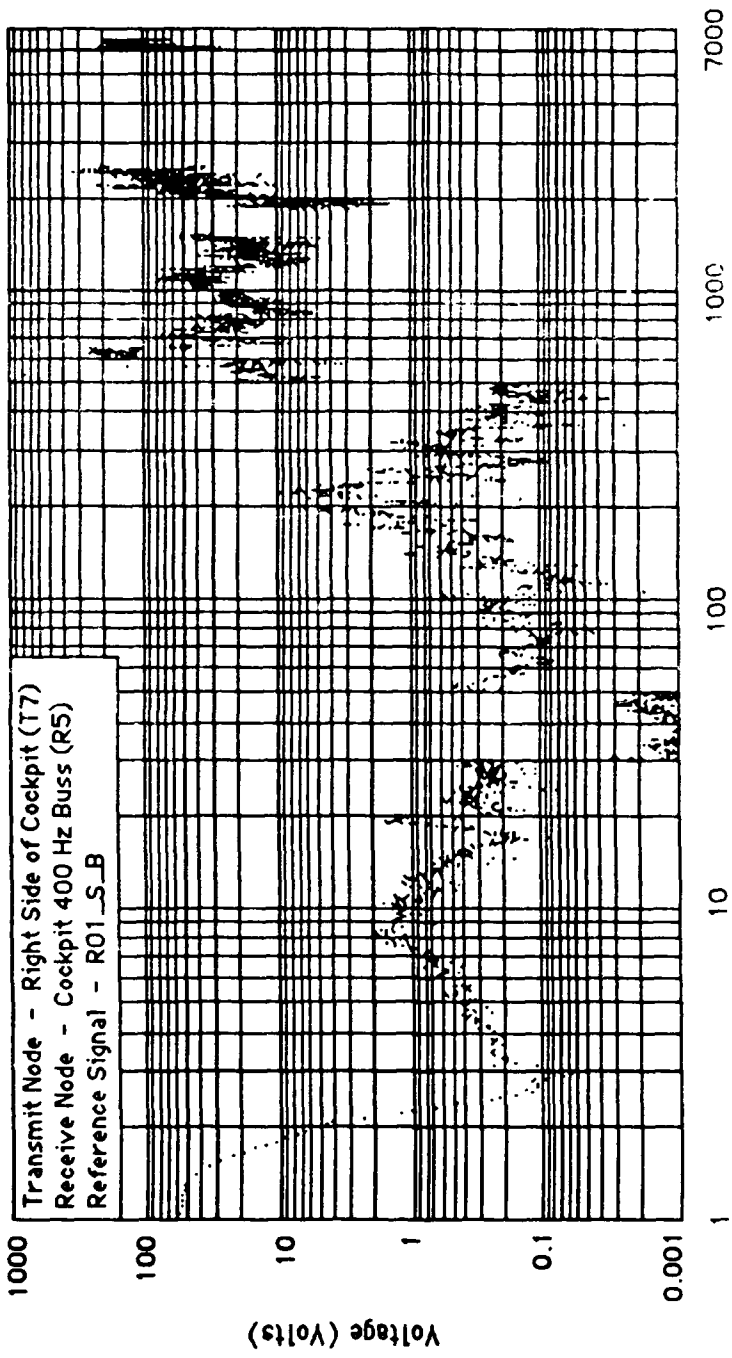

Figure F-14 Maximum Induced Voltage (132A)

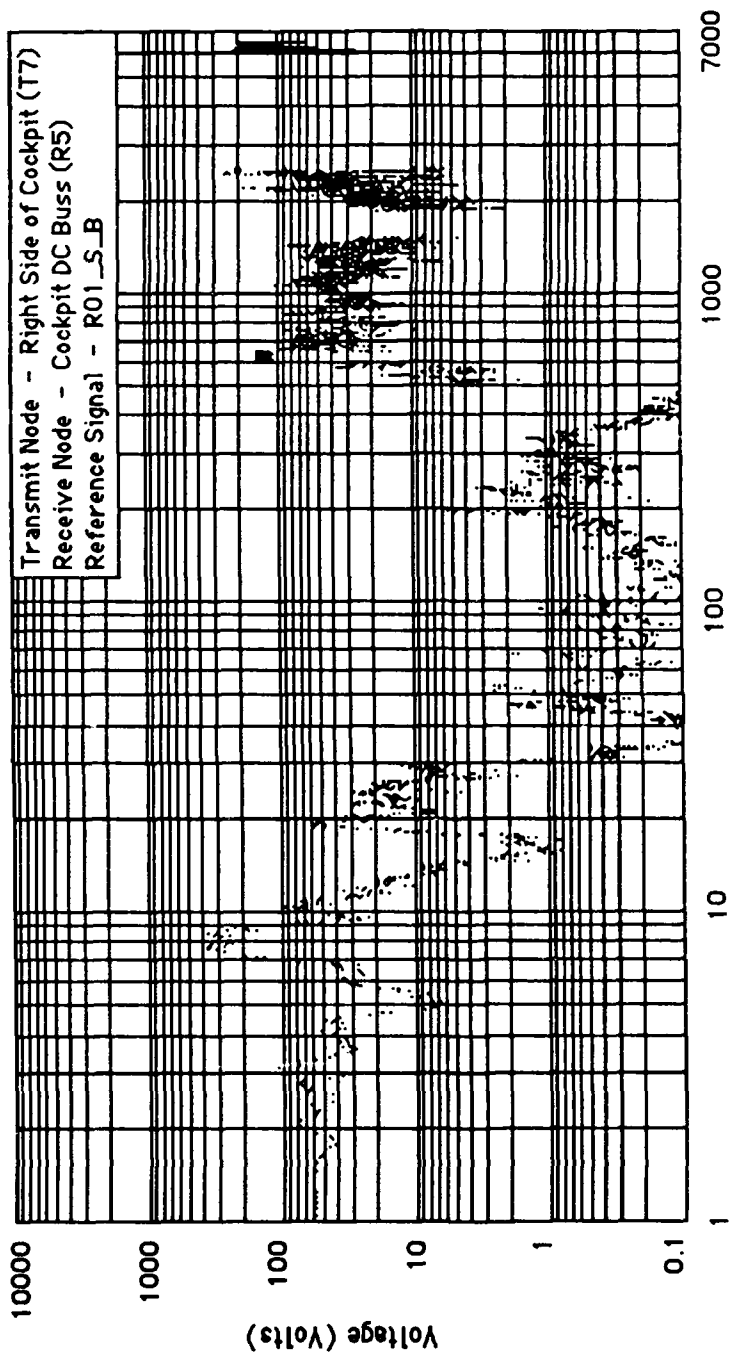

Figure F-15 Maximum Induced Voltage (133A)

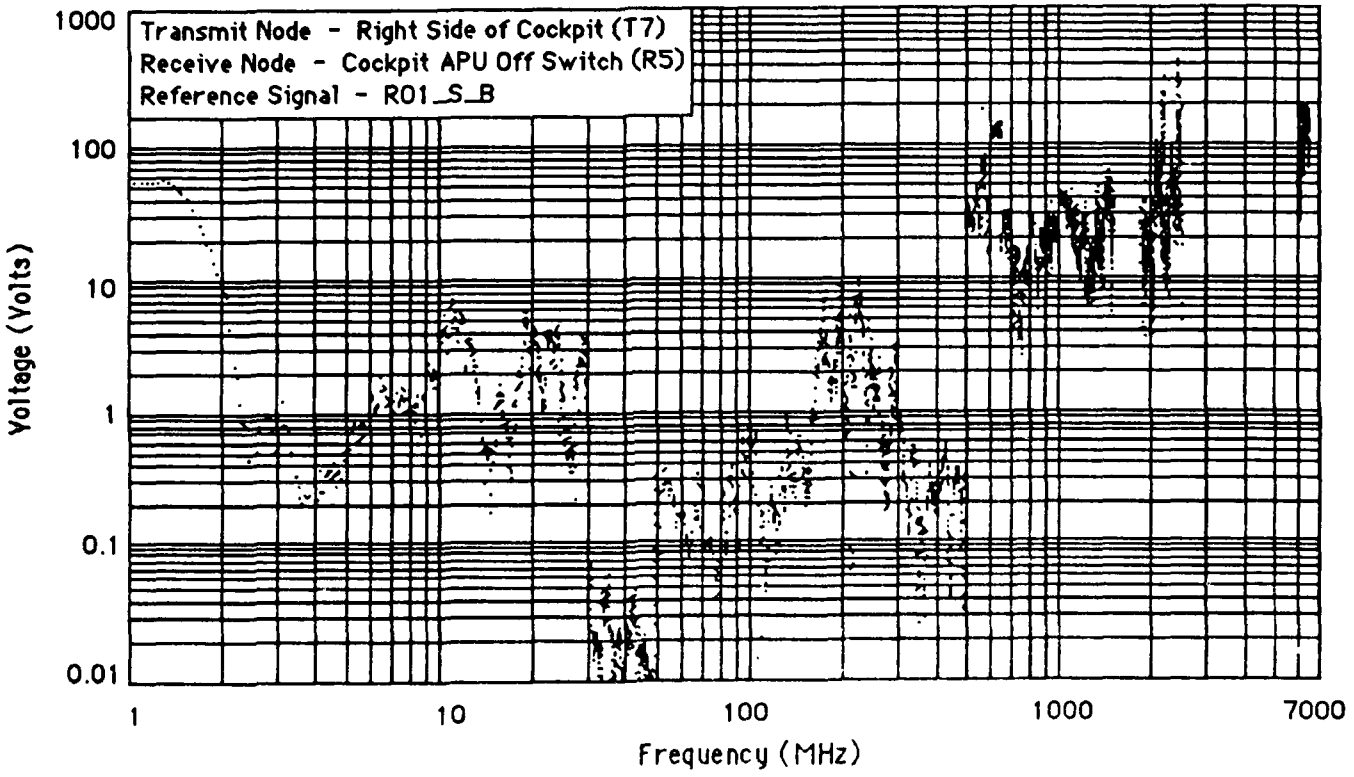

Figure F-16 Maximum Induced Voltage (138A)

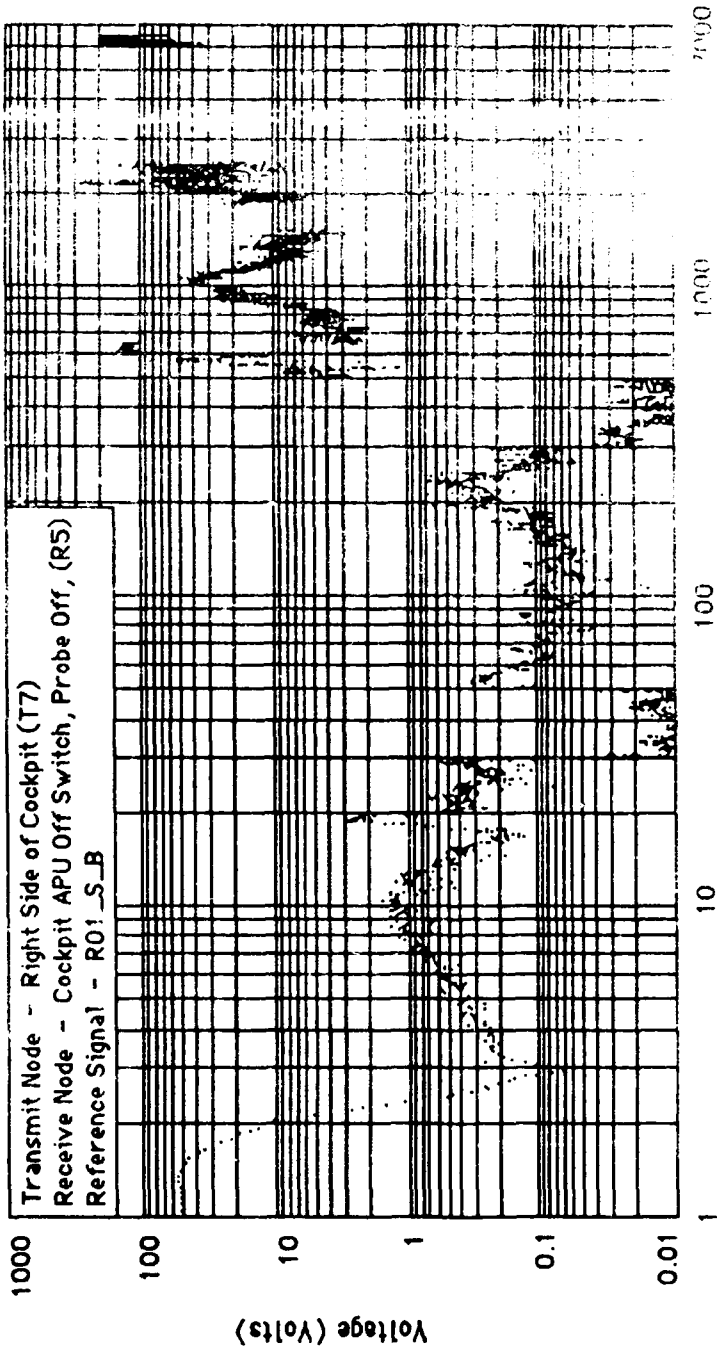

Figure F-17 Maximum Induced Voltage (1 88F)

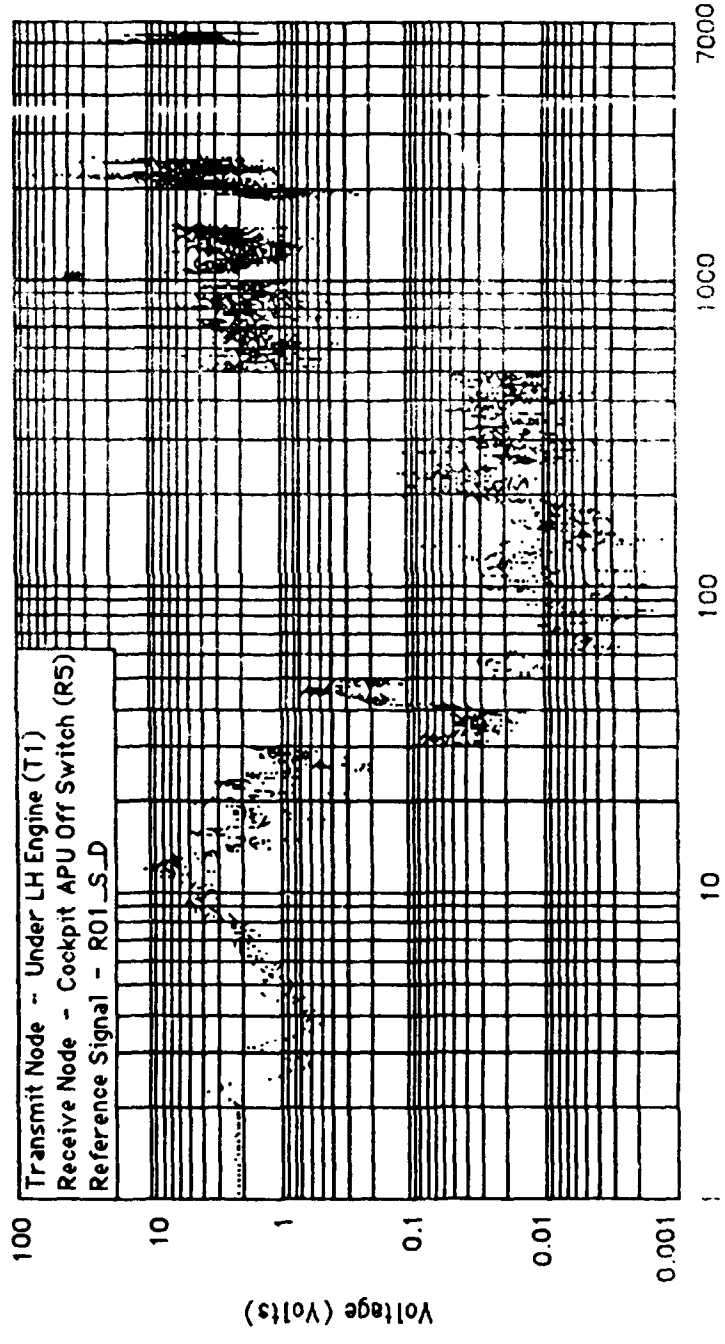

Figure F-18 Maximum Induced Voltage (144A)

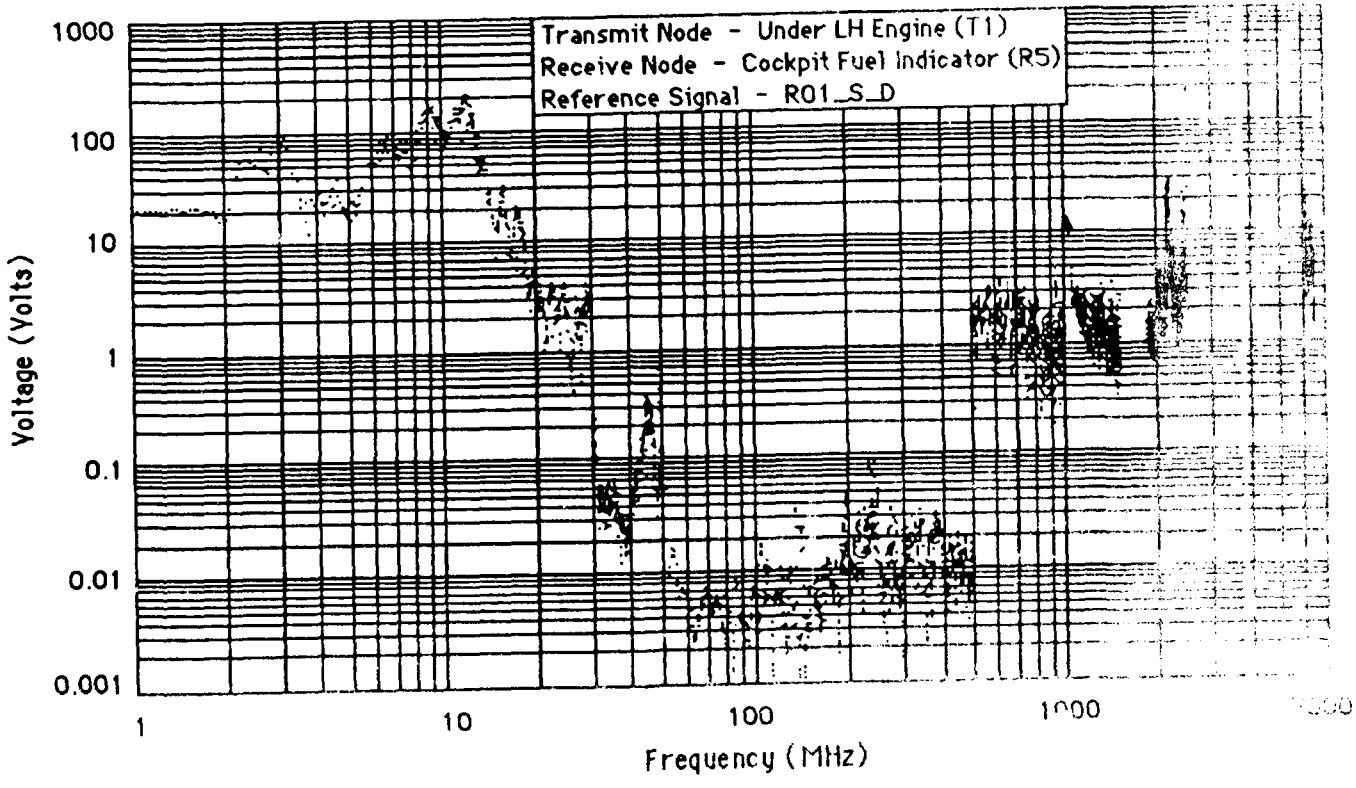

Figure F-19 Maximum Induced Voltage (145A)

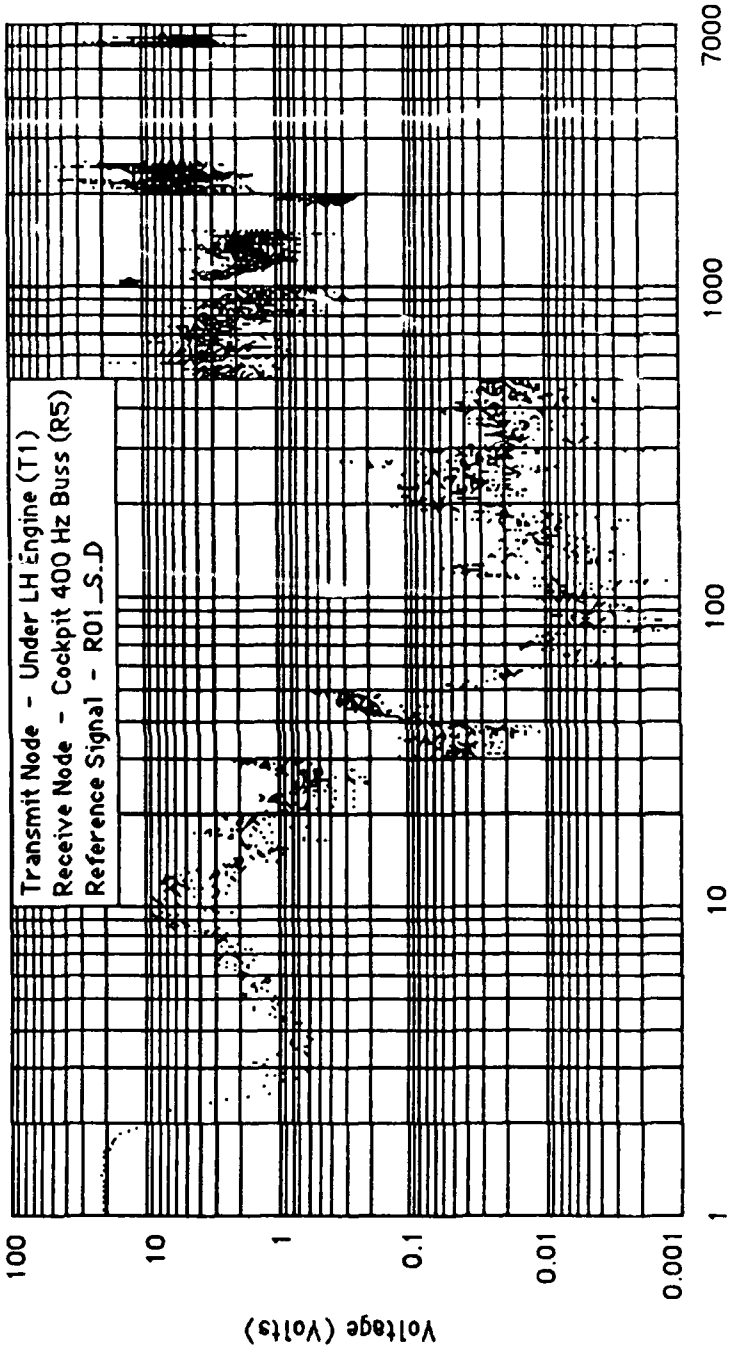

Figure F-20 Maximum Induced Voltage (147A)

APPENDIX G
PEAK RF FIELD STRENGTH AT VARIOUS INTERNATIONAL AIRPORTS

AIRCRAFT EME - RESULTS
PREDICTED MAXIMUM PEAK FIELDS STRENGTH LEVELS
COMPOSITE OF INTERNATIONAL ENVIRONMENTS*

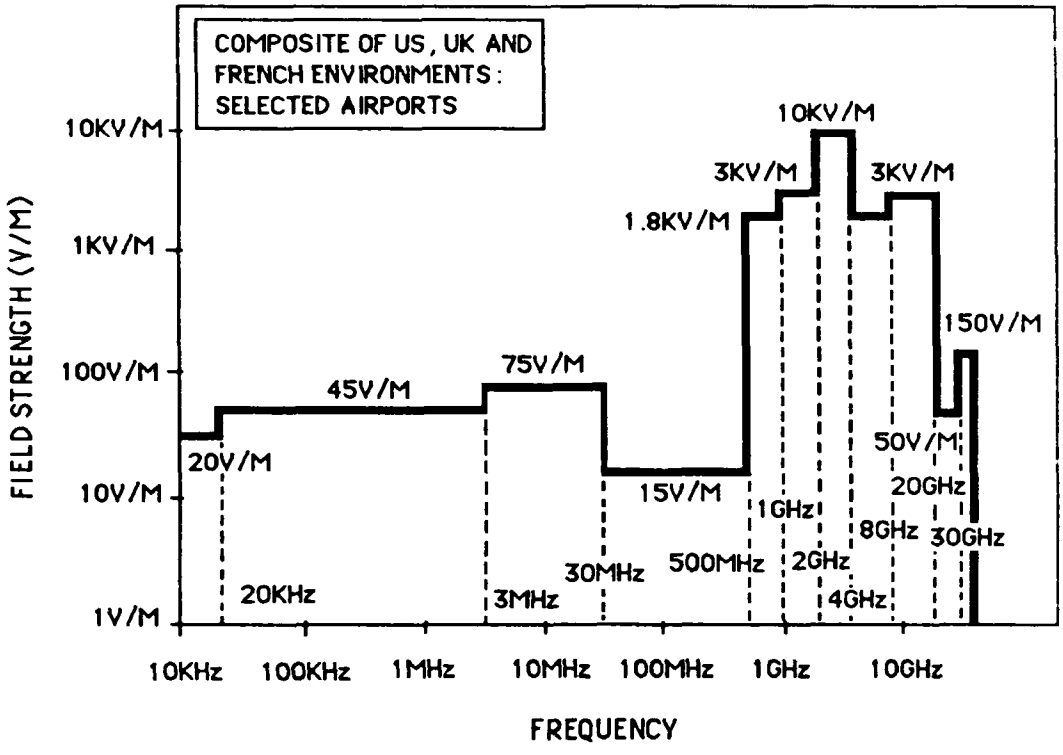

Figure G-1 Peak Field Strength of Selected Take-off/Landing Environment Within US, UK and France

* By Alexander Gross of the DOD Electromagnetic Compatibility Analysis Center